January 2016

Studies of nicotinic acetylcholine receptors containing α4 and α6 subunits in nicotine-induced synaptic plasticity in brain reward areas

Staci Engle
Purdue University

Graduate School Form
30 Updated 12/26/2015

PURDUE UNIVERSITY
GRADUATE SCHOOL
Thesis/Dissertation Acceptance

This is to certify that the thesis/dissertation prepared

By Staci E. Engle

Entitled

STUDIES OF NICOTINIC ACETYLCHOLINE RECEPTORS CONTAINING α4 AND α6 SUBUNITS IN NICOTINE-INDUCED SYNAPTIC PLASTICITY IN BRAIN REWARD AREAS

For the degree of Doctor of Philosophy

Is approved by the final examining committee:

Ryan Drenan
Chair

Val J. Watts

Greg Hockerman

Edward Bartlett

To the best of my knowledge and as understood by the student in the Thesis/Dissertation Agreement, Publication Delay, and Certification Disclaimer (Graduate School Form 32), this thesis/dissertation adheres to the provisions of Purdue University's "Policy of Integrity in Research" and the use of copyright material.

Approved by Major Professor(s): Ryan Drenan

Approved by: Chris Rochet 2/15/2016

Head of the Departmental Graduate Program Date

STUDIES OF NICOTINIC ACETYLCHOLINE RECEPTORS CONTAINING α4 AND α6 SUBUNITS IN NICOTINE-INDUCED SYNAPTIC PLASTICITY IN BRAIN REWARD AREAS

A Dissertation

Submitted to the Faculty

of

Purdue University

by

Staci E. Engle

In Partial Fulfillment of the

Requirements for the Degree

of

Doctor of Philosophy

May 2016

Purdue University

West Lafayette, Indiana

ACKNOWLEDGEMENTS

First and foremost I would like to express my sincere gratitude to my major professor, Dr. Ryan Drenan. It has been an honor to be your first Ph.D. student. I would like to thank you for the opportunity to work in your laboratory and for your motivation, patience, support, and guidance, all of which have helped me to grow as a scientist. I am also thankful for the support and guidance provided by the members of my dissertation committee, Dr. Edward Bartlett, Dr. Gregory Hockerman, and Dr. Val Watts.

I am grateful for the past and present members of the Drenan Lab, including Hilary Broderick, Dr. Pei-Yu Shih, Dr. Jennifer Berry, and Matthew Arvin who have provided encouragement, insightful conversations, and assistance with experiments. I have indicated in the figure legends where these individuals have contributed to the data collected in that figure.

Last but not least, I would like to thank my family and friends because without their support, encouragement, and love, I would not have made it to where I am today.

TABLE OF CONTENTS

Page

Page

Page

LIST OF ABBREVIATIONS

AAV	adeno-associated virus
α-BuTX	α-bungarotoxin
αCtxMII	α-conotoxin MII
ACh	acetylcholine
AMPA	2-amino-3-(3-hydroxy-5-methyl-isoxazol-4-yl) propanoic acid
AMPAR	AMPA receptor
AP-5	D-2-amino-5-phosphonopentanoic acid
BAC	bacterial artificial chromosome
CaMKII	calcium/calmodulin-dependent protein kinase II
cKO	conditional knockout
CNQX	6-cyano-7-nitroquinoxaline-2,3-dione
DA	dopamine
DHβE	dihydro-β-erythroidine
EPSC	excitatory postsynaptic current
EtOH	ethanol
GABA	gamma-aminobutyric acid
GAD	glutamic acid decarboxylase
GAPDH	glyceraldehyde-3-phosphate dehydrogenase
GFP	green fluorescent protein
GluR	glutamate receptor
HSV	herpes simplex virus
i.p.	intraperitoneal
IPSC	inhibitory postsynaptic current

ISI	interspike interval
KO	knockout
LDTg	lateral dorsal tegmental nucleus
LTD	long-term depression
LTP	long-term potentiation
MEC	mecamylamine
MLA	methyllycaconitine
NAc	nucleus accumbens
nAChRs	nicotinic acetylcholine receptors
NIC	nicotine
NMDA	N-methyl-D-aspartate
NMDAR	NMDA receptor
NMDG	N-methyl-D-glucamine
non-Tg	non-transgenic
PBS	phosphate-buffered saline
PCR	polymerase chain reaction
PFC	prefrontal cortex
PPTg	pedunculopontine tegmental nucleus
RMTg	rostromedial tegmental nucleus
RT-PCR	reverse transcription-PCR
TBS	Tris-buffered saline
TEA	tetraethylammonium
TH	tyrosine hydroxylase
TM	transmembrane
TTL	transistor-transistor logic
TTX	tetrodotoxin
VAR	varenicline
vMB	ventral midbrain

VTA	ventral tegmental area
WT	wild-type

ABSTRACT

Engle, Staci E. Ph.D., Purdue University, May 2016. Studies of nicotinic acetylcholine receptors containing α4 and α6 subunits in nicotine-induced synaptic plasticity in brain reward areas. Major Professor: Ryan Drenan.

Tobacco addiction is a serious threat to public health in the United States and abroad, and development of new therapeutic approaches is a major priority. Nicotine, the primary psychoactive compound in tobacco smoke, activates and/or desensitizes nicotinic acetylcholine receptors (nAChRs) throughout the brain. nAChRs in ventral tegmental area (VTA) dopamine (DA) neurons are crucial for the rewarding and reinforcing properties of nicotine. Nicotine causes cellular changes in VTA DA neurons, including the enhancement of AMPA receptor (AMPAR) function. This enhancement sensitizes the VTA to excitatory input and promotes drug seeking in animal models. However, which nAChR subtype(s) are responsible for initiating these cellular changes is poorly understood. nAChRs containing the α6 subunit (α6* nAChRs) are highly and selectively expressed in DA neurons in the VTA. Therefore, we hypothesized that activation of α6* nAChRs is sufficient to enhance AMPAR function on the surface of VTA DA neurons. To test this, we studied mice expressing hypersensitive, gain-of-function α6 nAChRs (α6L9S mice). We found that low concentrations of nicotine could act selectively through α6* nAChRs to enhance the function of AMPARs on the surface of VTA DA neurons. Through

pretreatment with pharmacological inhibitors, we found that NMDA receptors, as well as Ca^{2+}/calmodulin dependent protein kinase II, are also required for this effect. We subsequently expanded these studies to include alcohol because of the high rate of tobacco and alcohol co-abuse. Just as with nicotine, we found that low concentrations of ethanol were sufficient to enhance AMPAR function on VTA DA neurons of α6L9S mice. Because ethanol and nicotine both modulate AMPAR function in a manner involving α6* nAChRs, we tested the hypothesis that low concentrations of ethanol and nicotine combine to modulate AMPAR function. Remarkably, co-incubation of α6L9S brain slices in concentrations of ethanol and nicotine that are sub-threshold when incubated alone resulted in robust enhancement of AMPAR function. Within the VTA, α6 nAChR subunits form nAChRs with and without the α4 nAChR subunit. Therefore, we studied the contribution of α4 nAChR subunits to nicotine-elicited changes in VTA synaptic plasticity. To address this, we removed α4 nAChR subunits from the VTA of adult mice by injecting viral vectors directing expression of Cre recombinase into the VTA of mice with loxP sites flanking the α4 subunit gene. We found that nicotine no longer increases AMPAR function when α4 nAChR subunits are removed from the VTA, indicating a role of nAChRs that contain both α4 and α6 nAChR subunits in VTA synaptic plasticity. Interestingly, we also saw that removing α4 subunits from the VTA of adult mice increases the excitability of VTA DA neurons. We hypothesized that removal of α4* nAChRs from GABAergic neurons in the VTA results in less tonic inhibition of VTA DA neurons. To test this we measured spontaneous inhibitory postsynaptic currents (IPSCs) on VTA DA neurons. Indeed, we saw that the instantaneous frequency of IPSCs was significantly reduced when α4 nAChR

subunits are removed from the VTA. Overall, these studies highlight the importance of α4α6* nAChRs in the initiation of cellular changes that play a role in addiction to nicotine, suggesting α4α6* nAChRs may be a promising target for future smoking cessation pharmacotherapies.

PUBLICATIONS

PUBLICATIONS

Engle, S.E., Shih, P.Y., McIntosh, J.M., and Drenan, R.M. (2013) α4α6β2* nAChR activation on VTA DA neurons is sufficient to stimulate a depolarizing conductance and enhance surface AMPA receptor function. *Mol. Pharmacol*. 84(3): 393-406.

Berry, J.N., Engle, S.E., McIntosh, J.M., and Drenan, R.M. (2015) α6-containing nicotinic acetylcholine receptors in midbrain dopamine neurons are poised to govern dopamine-mediated behaviors and synaptic plasticity. *Neuroscience* 304:161-175.

Engle, S.E., McIntosh, J.M., and Drenan, R.M. (2015) Nicotine and ethanol cooperate to enhance ventral tegmental area AMPA receptor function via α6-containing nicotinic receptors. *Neuropharmacology* 91:13-22.

CHAPTER 1. INTRODUCTION

1.1 Tobacco Addiction

Tobacco use is a major health problem in the United States. It results in numerous health complications including lung cancer, ischemic heart disease, and chronic obstructive pulmonary disease, among others. Tobacco use is the leading cause of preventable death (NCCD 2014). It results in nearly 6 million deaths per year worldwide and is predicted to cause over 8 million deaths per year by 2030 (Mathers & Loncar 2006). Even though there are numerous health benefits to quitting tobacco use, nicotine, an addictive compound in tobacco, makes quitting difficult. Nearly 70% of smokers have the desire to quit, yet over 95% of attempts to quit fail within the first year of abstinence (CDC 1993, CDC 2002). Many people relapse quickly because of nicotine withdrawal symptoms, just a few of which include tobacco cravings, irritability, anxiety, insomnia, and nausea (West et al 2006). People also relapse in times of stress and to prevent the weight gain that sometimes occurs when smokers quit (McKee et al 2011, Mineur et al 2011).

While nearly 20% of the general population are smokers, an even higher percentage of people with mental illnesses smoke cigarettes. Around 50% of people with depression smoke cigarettes (Pratt & Brody 2010) and greater than 60% of schizophrenics smoke cigarettes. This increase may be explained by the possibility that smoking helps them to

overcome cognitive deficits as well as alleviate extrapyramidal symptoms caused by their medication (Sagud et al 2009).

For all of the reasons above, development of effective smoking cessation pharmacotherapies is a major priority. Current options include over-the-counter nicotine replacement therapies and prescription medications. One of the most successfully used drugs is Chantix, or varenicline. However, only 23% of people prescribed Chantix are still abstinent 1 year after quitting (Knight et al 2010). It also has the potential to cause several side effects ranging from mild to severe (Ebbert et al 2010, Hays et al 2008). Therefore, the overarching goal of our research is to better understand the mechanisms through which nicotine acts in order to identify targets for more specific and efficacious smoking cessation pharmacotherapies.

1.2 Nicotinic Acetylcholine Receptors

Nicotine is a tertiary amine alkaloid. It exerts its addictive properties through its actions on nicotinic acetylcholine receptors (nAChRs) (Laviolette & van der Kooy 2004). The endogenous ligand of nAChRs is acetylcholine (ACh). They are a member of the cys-loop family of ligand-gated ion channels that also includes gamma-aminobutyric acid (GABA), serotonin, and glycine receptors. nAChRs are composed of five subunits arranged to form a central, ion-conducting pore. Each subunit consists of four transmembrane segments, two intracellular loops, and extracellular N- and C-terminal domains (Dani & Bertrand 2007). The N-terminal domain contains the two cysteine residues of the cys-loop. Neuronal nAChRs are composed of α and β subunits and can be either homomeric or

heteromeric. Homomeric nAChRs are composed of all α subunits while heteromeric nAChRs are composed of both α and β subunits. Heteromeric receptors may contain either 3 α and 2 β subunits or 2 α and 3 β subunits (Itier & Bertrand 2001). Currently, 11 different neuronal nAChR subunits have been identified in mammals: α2-α7, α9, α10, and β2-β4. The α8 nAChR subunit is found in avian species but not mammals. α7 nAChR subunits can form homomeric nAChRs while α2-α6 and β2-β4 nAChR subunits combine to form functional heteromeric nAChRs (Le Novere et al 2002, Millar & Gotti 2009). However, α5 and β3 nAChR subunits are considered auxiliary subunits because while they are able modulate channel function, they do not form binding sites (Cui et al 2003, Drenan et al 2008b, Fowler et al 2011). This leads to a diverse array of possible nAChR subtypes. Different subunits combine to form nAChR subtypes with differing pharmacological properties (Le Novere et al 2002). α4β2* (* indicates the possibility of other subunits present in the pentamer) and α7 nAChRs are the most abundant subtypes and are expressed widely throughout the brain (Millar & Gotti 2009).

nAChRs have three conformational states: open, closed, and desensitized. In the absence of a ligand, nAChRs remain in the closed state. Upon ligand binding, channels open. The orthosteric binding site is formed at the interface of the N-termini of two adjacent α subunits in homomeric nAChRs or between that of a α and β subunit in heteromeric nAChRs. Therefore, homomeric nAChRs contain five binding sites while heteromeric nAChRs have just two. Na^+, K^+, and Ca^{2+} can flow through nAChRs in the open state. The degree of Ca^{2+} permeability varies depending on the nAChR subtype. The M2

transmembrane domain from each of the 5 subunits line the pore and help to determine ion selectivity (Corringer et al 2000). nAChRs can be found both presynaptically on terminals and postsynaptically on cell bodies. Therefore, nAChR activation can result in cell depolarization and neurotransmitter release (Dani & Bertrand 2007). nAChRs that are desensitized are in a non-conducting state (Picciotto et al 2008).

1.3 Mesolimbic Reward Pathway

Most important to tobacco addiction, several nAChR subtypes are expressed in the mesolimbic reward pathway. The mesolimbic reward pathway consists of dopamine (DA) neurons located in the ventral tegmental area (VTA) and their projections to the nucleus accumbens (NAc) (Laviolette & van der Kooy 2004)(Figure 1). Drugs of abuse, including nicotine, result in a rise in DA release in the NAc (Di Chiara & Imperato 1988). Lesions of the mesolimbic DA system, as well as DA receptor antagonists, reduce nicotine self-administration in rats (Corrigall & Coen 1991, Corrigall et al 1992). More specifically, nAChRs within the VTA are responsible for the reinforcing properties of nicotine, as shown by reduced self-administration following intra-VTA infusion of nAChR antagonists (Corrigall et al 1994). The VTA is located in the ventral midbrain. In addition to the mesolimbic pathway, the VTA is also part of the mesocortical pathway. VTA DA neurons in this pathway send projections to the prefrontal cortex (PFC) (Laviolette & van der Kooy 2004)(Figure 1). Along with DA neurons, there are also GABAergic interneurons in the VTA which provide inhibitory input to DA neurons (Figure 1). Glutamatergic terminals that provide excitatory neurotransmission in the VTA arise primarily from the PFC, bed nucleus of the stria terminalis, amygdala, pedunculopontine tegmental nucleus (PPTg),

and the lateral dorsal tegmental nucleus (LDTg) (Mao & McGehee 2010)(Figure 1). Additionally, the VTA receives cholinergic and GABAergic input from the PPTg and LDTg (Mao & McGehee 2010) (Figure 1). These cholinergic inputs help regulate burst firing of VTA DA neurons (Lanca et al 2000). In addition to modulating reward, the cholinergic system is also thought to play a role in regulating sleep cycles and memory formation (Mark et al 2011, McKinney & Jacksonville 2005).

The VTA is emerging as a heterogeneous structure. DA neurons within different regions of the VTA have different electrophysiological properties and project to different regions of the brain. For example, DAergic neurons in the lateral VTA project to the NAc shell while those in the medial VTA project to the NAc core and PFC (Lammel et al 2014). In addition, systemically administered nicotine preferentially activates DA neurons in the posterior VTA (bregma: −3.28 to −3.80 mm) over the anterior or tail VTA (Zhao-Shea et al 2011).

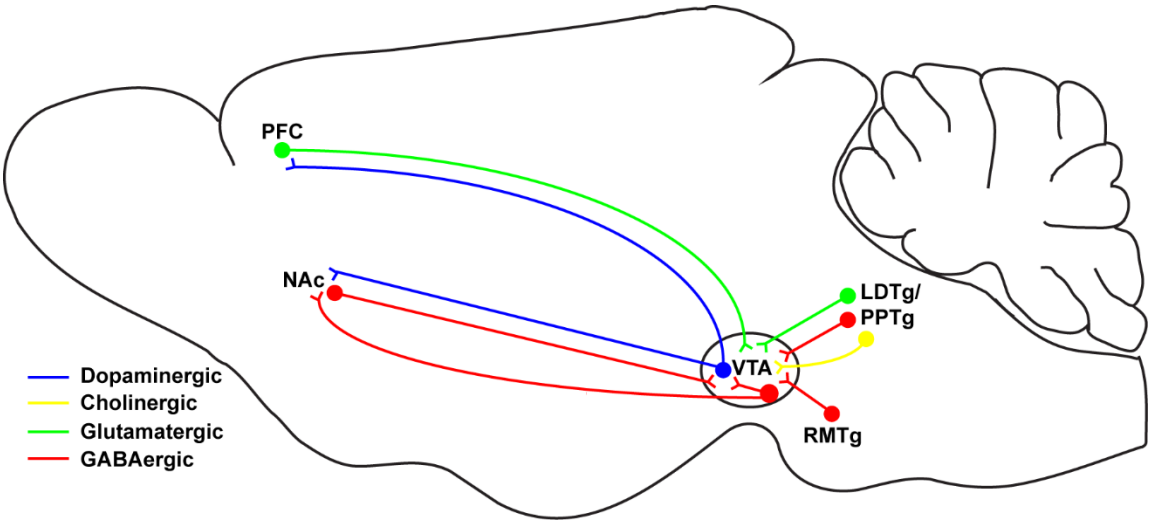

Figure 1. Simplified illustration of dopaminergic, cholinergic, glutamatergic, and GABAergic circuity projecting to and from the VTA within the mouse brain.

1.4 nAChRs in the VTA

Physiologically relevant concentrations of nicotine (around 100-500 nM) activate and/or desensitize nAChRs (Picciotto et al 2008, Pidoplichko et al 1997). Nicotine acts through nAChRs to enhance firing of VTA DA neurons (Calabresi et al 1989) and increase DA release in the NAc (Di Chiara & Imperato 1988). Within the VTA, nAChRs are located on several cell types. nAChRs are expressed on DA cell bodies, glutamatergic terminals, and GABAergic interneurons (Marubio et al 2003). DA cell bodies express heteromeric nAChRs and a subset also express homomeric α7 nAChRs (Azam et al 2002). nAChRs containing the α6 nAChR subunit are selectively expressed on DA neurons in the VTA (Drenan et al 2008a, Le Novere et al 1996, Mackey et al 2012). GABA interneurons provide inhibitory inputs onto VTA DA neurons and express mainly α4β2* nAChRs (Klink et al 2001, Mansvelder et al 2002, Nashmi et al 2007). However, nicotine only briefly activates these receptors before desensitization occurs. Therefore, after a transient increase, inhibitory neurotransmission to VTA DA neurons in ultimately decreased (Mansvelder et al 2002). Glutamatergic terminals that synapse onto VTA DA neurons express homomeric α7 nAChRs (Jones & Wonnacott 2004). Nicotine activates nAChRs on glutamatergic terminals and therefore enhances excitatory neurotransmission to VTA DA neurons (Mansvelder & McGehee 2000).

While there are several possible heteromeric nAChR subtypes in the VTA, it is important to understand which particular subtype(s) are necessary and/or sufficient for nicotine reinforcement and reward. β2* nAChRs are crucial for nicotine's reinforcing properties

(Picciotto et al 1998). Nicotine does not result in an increase in DA release in β2 knockout (KO) mice and β2KO mice do not self-administer nicotine (Picciotto et al 1998, Pons et al 2008). Furthermore, in electrophysiology studies done in brain slices from β2KO mice, DA neurons do not respond to puff application of nicotine. This can be explained by radioligand binding studies which reveal that high affinity nicotine binding sites are completely absent in β2KO mice (Picciotto et al 1995, Zoli et al 1998).

The main high-sensitivity nAChRs in the VTA include those containing α4 and/or α6 subunits (Salminen et al 2007, Salminen et al 2004). Like the β2 nAChR subunit, α4 and α6 nAChR subunits are also necessary for nicotine self-administration (Pons et al 2008). Selective re-expression of these subunits into the VTA shows that α4, α6, and β2 nAChR subunit expression specifically within the VTA drives nicotine reinforcement (Maskos et al 2005, Pons et al 2008). Because nAChR function in VTA DA neurons is absent in β2KO mice, α4 and α6 subunits must co-assemble with the β2 subunit to form functional receptors (Picciotto et al 1998). Further studies have concluded that VTA DA neurons express nAChRs with the following compositions: $(\alpha4)_3(\beta2)_2$, $(\alpha4)_2(\beta2)_3$, α4α5β2, α2α4β2, α4β2β3, α6β2, α6β2β3, α6α4β2, and α4α6β2β3 (Gotti et al 2010, Gotti et al 2005, Salminen et al 2007). α4α6β2β3 nAChRs have the highest affinity to nicotine with an EC_{50} of around 230 nM (Salminen et al 2007) and make up approximately 20% of the β2* nAChR binding sites in VTA DA neurons (Gotti et al 2010). α-conotoxin MII (αCtxMII) is a competitive antagonist selective for α6* nAChRs (Cartier et al 1996, Champtiaux et al 2002) and dihydro-β-erythroidine (DHβE) is a competitive antagonist moderately

selective for α4* nAChRs (Harvey et al 1996). Nevertheless, there are currently no antagonists that distinguish between α4α6*, (non-α6)α4*, and (non-α4)α6* nAChRs, making their differential effects difficult to study. In addition to the roles of α4* and α6* nAChRs in the reinforcing and rewarding properties of nicotine discussed below, there is evidence for the involvement of α4α6* nAChRs as well (Drenan et al 2010, Liu et al 2012, Zhao-Shea et al 2011).

The involvement of α4* nAChRs in the reinforcing properties of nicotine is not only demonstrated by the absence of nicotine self-administration in α4KO mice (Pons et al 2008), but also by wild-type (WT) mice that fail to self-administer nicotine after given an intra-VTA infusion of DHβE to block α4β2* nAChRs in the VTA (Corrigall et al 1994). α4 nAChRs contribute to the rewarding properties of nicotine as well. Selectively activating α4* nAChRs will condition a place preference to nicotine (Tapper et al 2004) and α4KO mice do not show a place preference to nicotine (Sanjakdar et al 2015). Moreover, α4 nAChRs specifically on DA neurons are necessary for nicotine reward (McGranahan et al 2011). At the cellular level, nicotine does not significantly activate VTA DA neurons in α4KO mice as compared to WT mice (Liu et al 2012, Zhao-Shea et al 2011).

α6* nAChRs are unique in that they are expressed in a limited number of brain regions, unlike α4 and β2 subunits that are widely expressed throughout the brain (Champtiaux et al 2003, Marubio et al 2003, Nashmi et al 2007, Ross et al 2000). They are mainly found in catecholaminergic neurons, and most notably in the VTA, substantia nigra pars compacta, locus coeruleus, retinal ganglion cells, and their projection areas (Champtiaux

et al 2002, Cox et al 2008, Gotti et al 2005, Hill et al 1993, Le Novere et al 1996, Lena et al 1999, Mackey et al 2012, Whiteaker et al 2000). As discussed above, α6KO mice do not self-administer nicotine (Pons et al 2008). In addition, in WT mice, intra-VTA αCtxMII infusions block nicotine self-administration, as well as DA release in the NAc (Gotti et al 2010). α6KO mice do not find nicotine rewarding at a dose that is sufficient to condition a place preference in WT mice (Sanjakdar et al 2015). αCtxMII infusions further support a role for α6* nAChRs in nicotine reward, because it dose-dependently decreases nicotine place preference in WT mice (Sanjakdar et al 2015). Likewise, selectively activating α6* nAChRs can condition a place preference to nicotine (Drenan et al 2012). Their restricted expression and their key role in the rewarding and reinforcing properties of nicotine make α6* nAChRs an attractive option to selectively target with nicotine cessation drugs.

1.5 Long-Term Potentiation

Long-term potentiation (LTP) is the strengthening of synapses for an extended period of time following stimulation. LTP is measured by a protocol that pairs presynaptic stimulation with postsynaptic depolarization. The opposite of LTP is long-term depression (LTD), or the weakening of synapses. The ability of neurons to increase and decrease the strength of synapses over time is referred to as synaptic plasticity or changes in synaptic strength (Kauer & Malenka 2007).

Both 2-amino-3-(3-hydroxy-5-methyl-isoxazol-4-yl) propanoic acid (AMPA) receptors (AMPARs) and N-methyl-D-aspartate (NMDA) receptors (NMDARs) are key players in glutamatergic synaptic plasticity. These receptors belong to the family of ionotropic

glutamate receptors, which also includes kainate receptors. AMPARs are tetramers composed of a combination of AMPA-type ionotropic glutamate receptor (GluR) 1, GluR2, GluR3, and GluR4 subunits. Glutamate receptors are activated by the binding of endogenous glutamate, or exogenous AMPA. Upon activation the pore opens and allows cations into the cell. AMPARs containing the GluR2 subunit are impermeable to Ca^{2+}. AMPARs lacking the GluR2 subunit are permeable to both Na^{+} and Ca^{2+} (Isaac et al 2007). NMDARs are also tetramers. They are composed of varying combinations of NR1, NR2A, NR2B, NR2C, NR2D, NR3A and NR3B subunits. They contain a central pore that is voltage-dependently blocked by Mg^{2+}. When cells expressing NMDARs are sufficiently depolarized, the Mg^{2+} block is relieved. NMDARs are highly Ca^{2+} permeable so once the cell is depolarized and the Mg^{2+} block is removed, binding of NDMA or glutamate results in Ca^{2+} influx into the cell (Cull-Candy et al 2001).

The most widely studied form of LTP is NMDAR-dependent LTP (Malenka & Bear 2004). This form of LTP requires the activation of NMDARs. Therefore, the postsynaptic cell must be sufficiently depolarized in order for the Mg^{2+} block to be removed. When the Mg^{2+} block is removed, glutamate released by the presynaptic cell activates NMDARs, resulting in Ca^{2+} entry into the postsynaptic cell. The rise in Ca^{2+} levels leads to intracellular signaling, including activation of calcium/calmodulin-dependent protein kinase II (CaMKII), and ultimately insertion of AMPARs into the cell membrane at the synapse on the postsynaptic cell (Kauer & Malenka 2007, Malenka & Bear 2004). Other types of LTP exist in addition to NMDAR-dependent LTP, such as presynaptic LTP (Kauer & Malenka 2007).

1.6 Synaptic Plasticity in the VTA

LTP is classically associated with learning and memory in the hippocampus (Malenka & Bear 2004). However, LTP can be induced in VTA DA neurons as well (Bonci & Malenka 1999). Excitatory synapses on VTA DA neurons, but not excitatory synapses on VTA GABA neurons, can be potentiated by a standard LTP pairing protocol (Bonci & Malenka 1999). LTP in VTA DA neurons is NMDAR-dependent and does not involve metabotropic glutamate receptors, like some other forms of LTP in the hippocampus (Bonci & Malenka 1999). LTD can also be observed on VTA DA neurons (Thomas et al 2000). These results show that stimulation of the VTA can lead to long-term alterations in the synaptic strength of synapses on DA neurons.

Increased DA release in the NAc long outlives the actions of nicotine on nAChRs on VTA DA neurons. The concentration of nicotine achieved by smokers rapidly desensitizes nAChRs on VTA DA neurons (Pidoplichko et al 1997). Nevertheless, nicotine causes increased DA levels in the NAc for an hour or more in rodent models (Di Chiara & Imperato 1988). Therefore, additional cellular changes must occur in VTA DA neurons following nicotine exposure to maintain enhanced DA release. This long-lasting enhancement of DA release is suggested to be a result of increased glutamatergic synaptic plasticity in the VTA (Kauer & Malenka 2007, Wolf et al 2004). Glutamatergic signaling in the VTA plays an important role in DA release in the NAc. Stimulating the PFC, the main source of glutamatergic inputs to the VTA, results in enhanced burst firing of VTA DA neurons and increased DA release in the NAc (Murase et al 1993). Furthermore, blocking NMDARs with an intra-VTA infusion of a NMDAR antagonist will dose-dependently decrease nicotine-

enhancement of DA release in the NAc of rats (Schilström et al 1997). Thus, strengthening of glutamatergic synapses on VTA DA neurons could support prolonged DA release.

Mansvelder and McGehee found for the first time that exposing brain slices to nicotine leads to the induction of LTP on VTA DA neurons (Mansvelder & McGehee 2000). Pairing a brief 200 second nicotine application with a postsynaptic depolarization is sufficient to increase the amplitude of evoked excitatory postsynaptic currents (EPSCs) for as long as 40 minutes. Nicotine-induced LTP was prevented by both methyllycaconitine (MLA; α7 nAChR antagonist) and D-2-amino-5-phosphonopentanoic acid (AP-5; competitive NMDAR antagonist; also commonly known as APV), indicating the mechanism is mediated by α7 nAChRs and NMDARs (Mansvelder & McGehee 2000).

Following this discovery, it was also found that *in vivo* drug exposure can induce LTP-like changes in VTA DA neurons. This was first observed with a single exposure to cocaine (Ungless et al 2001) and then generalized to other drugs of abuse, including nicotine (Saal et al 2003). Because drugs were given *in vivo*, the classical method of measuring LTP had to be altered. Therefore, to measure changes in synaptic strength, these studies compared AMPA receptor mediated currents to NMDA receptor mediated currents (AMPA/NMDA ratios) as a surrogate measure of LTP. It is important to note that AMPA/NMDA ratios are not similarly increased after exposure to psychoactive drugs that are not addictive (Saal et al 2003). These drug-induced synaptic changes are correlated with addiction-related behaviors, such as the acquisition of self-administration and

behavioral sensitization (Borgland et al 2004, Chen et al 2008, Dong et al 2004, Luscher & Malenka 2011)

1.7 Mechanisms of Nicotine-Evoked Synaptic Plasticity in the VTA

To better understand nicotine-induced increases in synaptic strength, various aspects such as the time course, which nAChR subtypes are involved, and intracellular signaling mechanisms have been studied. Changes in glutamatergic synaptic strength on VTA DA neurons have been observed after both *in vivo* nicotine exposure via nicotine injections and *ex vivo* via incubation of naïve brain slices in nicotine. The duration of nicotine exposure determines whether increases in AMPA/NMDA ratios occur and how long they last. Several studies have demonstrated that increases in AMPA/NMDA ratios are seen 24 hours after a nicotine injection (Baker et al 2013, Gao et al 2010, Placzek et al 2009, Saal et al 2003). Wu and colleagues performed further experiments to look at additional time points (Gao et al 2010). They found that waiting 10 minutes after the nicotine injection was not sufficient to see increases in AMPA/NMDA ratios. However, after a single nicotine injection, increases in AMPA/NMDA ratios are seen after one hour, and last at least 72 hours, but do not persist for as long as 5 days. Multiple nicotine injections (once daily for seven days) result in increased AMPA/NMDA ratios for as long as 8 days after the last injection (Gao et al 2010).

Studies using naïve brain slices have also found that the slices must be incubated in nicotine for a sufficient amount of time before changes in AMPA/NMDA ratios are observed (Jin et al 2011, Mao et al 2011). While one study reports that a 10 minute nicotine incubation was not sufficient to increase AMPA/NMDA ratios (Jin et al 2011),

another saw significant changes with after incubating slices in nicotine for just 15 minutes (Mao et al 2011).

Not only is the length of nicotine exposure important to consider when investigating changes in AMPAR function, but also the age of the animal at the time of nicotine exposure. Placzek *et al.* found that lower doses of nicotine could increase AMPA/NMDA ratios in young mice (postnatal days 21-35) compared to the doses required for adult mice (postnatal days 60-90) (Placzek et al 2009). This suggests that the developing brain may be more sensitive to nicotine-induced changes in glutamatergic synaptic plasticity on VTA DA neurons. This could be the result of differing nAChR expression between adolescence and adulthood. Interestingly, there are higher levels of α6 nAChR subunit mRNA expressed in the VTA of juvenile rats (Azam et al 2007). This makes α6* nAChRs an interesting target to explore when investigating which nAChR subtypes are responsible for nicotine-induced synaptic plasticity.

Understanding which nAChR subtypes nicotine acts through to increase AMPA/NMDA ratios will lead to a better understanding of the mechanism through which glutamatergic plasticity occurs in the VTA. Different studies have addressed this topic but it remains unclear which nAChR subtypes are primarily involved because of conflicting results. As in any comparison between scientific studies, differences in experimental details may account for contrasting results. Studies exposing naïve brain slices to nicotine do not agree on the involvement of α4β2* nAChRs (Jin et al 2011, Mao et al 2011). One group concluded that α4β2* nAChRs are not involved because pre-incubating brain slices from Wistar rats in DHβE, a moderately selective α4* nAChR antagonist, before nicotine

incubation did not inhibit increases in AMPA/NMDA ratios (Jin et al 2011). A similar experiment that instead used Sprague Dawley rats, however, found DHβE had the ability to block nicotine-induced increases in AMPA/NMDA ratios (Mao et al 2011). Findings on the involvement of α7 nAChRs, which are primarily found on glutamatergic terminals, are also conflicting. One study found no increases in AMPA/NMDA ratios after pre-incubating brain slices in MLA, a α7 nAChR antagonist (Jin et al 2011). Yet a second study using brain slices reports no involvement of α7 nAChRs as they found MLA pre-incubation was not able to block nicotine's ability to increase AMPA receptor function (Mao et al 2011).

An *in vivo* study concluded that increases in AMPA/NMDA ratios could proceed through activation of either α7 nAChRs or β2* nAChRs. They found that pre-injecting rats with a α7 nAChR antagonist before giving a nicotine injection did not block increases in AMPA/NMDA ratios, but neither did a β2 nAChR antagonist. However, increases were prevented when both antagonists were injected together (Gao et al 2010).

In addition to studies relying on pharmacological inhibitors, genetically modified mice have also been used as a tool to measure changes in glutamatergic synaptic plasticity. In agreement with the results from *in vivo* antagonist pre-injection, nicotine injections still resulted in increased AMPA/NMDA ratios in both α7KO and β2KO mice (Gao et al 2010). However, a study done by Jin *et al* found no increases in AMPA/NMDA ratios in α7KO mice, more in agreement with their MLA slice incubation procedure (Jin et al 2011).

No previous studies have looked at the role of α6* nAChRs in increased AMPA/NMDA ratios. A study by *Brown et al* leads us to believe these receptors may of interest. They showed that using optogenetics to selectively activate DA neurons via light stimulation is

sufficient for enhancement of AMPA/NMDA ratios in the VTA (Brown et al 2010). Because α6* nAChRs are selectively expressed on DA neurons in the VTA (Drenan et al 2008a, Mackey et al 2012), their activation may be sufficient to increase AMPA/NMDA ratios as well.

In addition to determining which nAChR subtype nicotine acts through, it is also important to understand what circuit and molecular events downstream of nAChR activation are involved in the enhancement of excitatory synapses on VTA DA neurons. Enhanced AMPA/NMDA ratios could be mediated by changes in the distribution and/or composition of AMPARs expressed on the surface of VTA DA neurons. An increase in the number of AMPARs expressed at glutamatergic synapses would result in an increase in AMPAR function (Kauer & Malenka 2007). Alternatively, an exchange of Ca^{2+} impermeable AMPARs for Ca^{2+} permeable AMPARs would also enhance the AMPA mediated component of AMPA/NMDA ratios (Luscher & Malenka 2011). AMPARs lacking the GluR2 subunit are Ca^{2+} permeable. Inward rectification is a hallmark of GluR2-lacking AMPARs (Isaac et al 2007, Liu & Zukin 2007). There are some studies suggesting the presence of inwardly-rectifying AMPARs on VTA DA neurons after nicotine exposure (Brown et al 2010, Gao et al 2010) as well as another report that there are not (Baker et al 2013). These contrasting results indicate that nicotine may either cause an increase in sensitivity and/or an increase in the number of AMPARs expressed on VTA DA neurons. More work is needed to uncover what changes are occurring at the AMPAR level following nicotine exposure.

There is no debate, however, on the necessity of NMDAR activation in the mechanism of nicotine-evoked increases in AMPA/NMDA ratios. Whether it be pre-injection with MK-801, a selective and non-competitive NMDAR antagonist, (Gao et al 2010) or pre-incubating slices in AP-5 (Mansvelder & McGehee 2000, Mao et al 2011), all studies show NMDAR antagonists inhibit increases in glutamatergic synaptic strength.

In order for NMDARs to be activated, the neuron first must be sufficiently depolarized to relieve the Mg^{2+} block present in NMDARs (Cull-Candy et al 2001). Nicotine itself leads to depolarization of DAergic neurons (Liu et al 2012, Pidoplichko et al 1997). This may be sufficient to remove the Mg^{2+} block or it may initiate other signaling events that further contribute to DA neuron depolarization or NMDAR activation. Nicotine results in somatodendritic DA release (Rahman et al 2003). DA released in this manner could then activate D5 DA receptors in the VTA, resulting in the initiation of changes in AMPA and/or NMDA receptors, possibly through altered glutamate release (Mao et al 2011, Schilstrom et al 2006). Several studies have investigated this through the use of D1/D5 DA receptor antagonists. While the antagonists do not differentiate between D1 and D5 DA receptors, the involvement of the D5 DA receptor is more likely as D1 DA receptors have not been found in VTA DA neurons (Schilstrom et al 2006). Mao *et al* found that pre-incubating slices in the D1/D5 DA receptor antagonist SCH-23390 before nicotine exposure could abolish increases in AMPA/NMDA ratios. Further, they also found that incubating slices in SKF 81297 (a D1/D5 DA receptor agonist) alone was sufficient to increase AMPA/NMDA ratios (Mao et al 2011). Brown *et al* found a similar effect *in vivo*. Intra-VTA infusion of SCH-23390 before light stimulation of VTA DA neurons blocked increases in AMPA/NMDA

ratios (Brown et al 2010). However, another *in vivo* study was not consistent with those discussed above. Gao *et al* found that pre-injection of a solution of SCH-23390 and haloperidol did not block nicotine-mediated increases in AMPA/NMDA ratios (Gao et al 2010).

Because NDMAR activity is required, it is highly likely that calcium signaling plays a role in enhanced AMPA/NMDA ratios. Therefore, calcium dependent protein kinases or phosphatases could be required for changes in nicotine-mediated glutamatergic synaptic plasticity. When activated, calcineurin, a serine/threonine phosphatase, dephosphorylates AMPARs and NMDARs among other targets. Its activity is necessary in the VTA for nicotine-mediated locomotor sensitization (Addy et al 2007). However, Gao *et al*. found that calcineurin involvement in not necessary for nicotine-mediated increases in AMPA/NMDA ratios, as they found that pre-injection of cyclosporine, a calcineurin inhibitor, had no effect on increases in AMPA/NMDA ratios (Gao et al 2010). Additional work on other calcium dependent kinases and phosphatases, such as CaMKII, will reveal more about the role of calcium signaling in nicotine-induced increases in glutamatergic synaptic strength in VTA DA neurons.

1.8 Nicotine and Ethanol Co-Abuse

Tobacco and alcohol co-abuse is extremely common (Bobo 1992, DiFranza & Guerrera 1990, Falk et al 2006, Grant et al 2004, Miller & Gold 1998). Alcohol consumption increases the amount of cigarettes smoked, cigarette cravings, and the rewarding effects experienced from smoking (Friedman et al 1991, Harrison et al 2009, Mitchell et al 1995, Rose et al 2004). Likewise, nicotine increases the amount of alcohol consumed (Barrett et

al 2006). The high prevalence of tobacco and alcohol co-abuse suggests that nicotine and ethanol may have common molecular targets in the brain mediating their rewarding effects.

1.9 Ethanol and nAChRs

Ethanol has the ability to modulate several types of ionotropic receptors including $GABA_A$, NMDA, and serotonin receptors (Dopico & Lovinger 2009). It is now starting to be appreciated that ethanol modulates nAChRs as well. Several studies using heterologous expression systems or cultured neurons suggest that ethanol potentiates or inhibits ACh-evoked currents depending on the subtype of nAChR expressed. In *Xenopus* oocytes expressing human nAChR subunits, ethanol potentiated ACh-evoked currents from $\alpha4\beta2$, $\alpha4\beta4$, $\alpha2\beta2$, $\alpha2\beta4$ nAChRs but inhibited $\alpha7$ nAChRs. The same study found ethanol did not alter currents from $\alpha3\beta2$ or $\alpha3\beta4$ nAChRs (Cardoso et al 1999). In rat cultured cortical neurons, α-bungarotoxin (α-BuTX) was used to distinguish $\alpha7$ nAChRs from heteromeric nAChRs (α-BuTX sensitive and α-BuTX insensitive, respectively). As in *Xenopus* oocytes, $\alpha7$ nAChRs are inhibited by ethanol and heteromeric nAChRs are potentiated by ethanol (Aistrup et al 1999).

nAChRs *in vivo* also indicate ethanol modulates nAChRs. Mice given mecamylamine (MEC), a non-competitive nAChR antagonist, consumed less ethanol (Hendrickson 2009) and do not acquire a place preference when administered ethanol (Bhutada et al 2012). nAChRs specifically within the VTA are also implicated in ethanol's mechanism of action.

Intra-VTA infusions of MEC reduced ethanol-induced DA release into the NAc (Blomqvist et al 1996).

More specifically, α4* and α6* nAChRs play an important role in the rewarding properties of ethanol. α4 nAChR subunits are necessary for ethanol to condition a place preference in mice (Liu et al 2013a). α6* nAChR activity, specifically within the VTA, is necessary for both ethanol consumption and reinforcement (Larsson et al 2004) (Lof et al 2007). Furthermore, enhanced α6* and α4* nAChR activity increases ethanol reward-like behavior (Liu et al 2013a, Powers et al 2013).

These data indicate that ethanol can modulate nAChRs and nAChRs within the VTA contribute to the rewarding properties of ethanol. Future studies need to be conducted to better understand the mechanism of action.

1.10 Effects of Combined Nicotine and Ethanol Administration

Studies utilizing simultaneous nicotine and ethanol co-exposure indicate that the two drugs have synergistic or additive properties. Results from VTA-containing brain slices demonstrate ethanol and nicotine have synergistic effects on action potential firing. A subthreshold concentration of nicotine co-applied with ethanol was able to increase the firing rate of VTA DA neurons when perfused over brain slices. (Clark & Little 2004). Similarly, in acute brain slices, ethanol can potentiate ACh-induced increases in the firing rate of VTA DA neurons, which requires both α4 and α6 nAChR subunits. (Liu et al 2013a, Liu et al 2013b). Results *in vivo* show similar trends. In microdialysis experiments in awake rats, subthreshold intraperitoneal ethanol injections paired with subthreshold intra-VTA nicotine injections resulted in increased DA release in the NAc (Tizabi et al 2002).

1.11 Ethanol-Mediated Changes in Synaptic Plasticity

Early work done *in vitro* provided evidence that glutamatergic signaling may be altered by ethanol. AMPAR and NMDAR subunit levels were increased in rat primary neuronal cultures exposed to ethanol (Chandler et al 1999). While not as widely studied as nicotine or other drugs of abuse, a single ethanol exposure also increases AMPA/NMDA ratios in VTA DA neurons (Heikkinen et al 2009, Saal et al 2003). Additionally, AMPA/NMDA ratios are increased after voluntary ethanol self-administration (Stuber et al 2008). To our knowledge, the role of nAChRs in ethanol-mediated increases in AMPA/NMDA ratios has not been previously studied.

1.12 Objectives

The overarching goal of these studies is to better understand the role of α6* nAChRs in addiction. We began by studying their ability to activate VTA DA neurons, moved onto their role in glutamatergic synaptic plasticity on VTA DA neurons in response to both nicotine and ethanol exposure, and finally looked into the contribution of α4 nAChR subunits to α6* nAChR activity.

CHAPTER 2. METHODS

Portions of this chapter (pgs 23-38) are reprinted from:

Molecular Pharmacology 2013 Sept; 84(3):393-406, doi: 10.1124/mol.113.087346 with permission of the American Society for Pharmacology and Experimental Therapeutics. All Rights Reserved.

Neuropharmacology 2015 Apr; 91:13-22, doi:10.1016/j.neuropharm.2014.11.014 and *Neuroscience* 2015 Sept 24; 304:161-75, doi: 10.1016/j.neuroscience.2015.07.052 with permission from Elsevier. All Rights Reserved.

2.1 Materials

(-) Nicotine hydrogen tartrate salt was obtained from Glentham Life Sciences (Wiltshire, United Kingdom). Nicotine doses are reported as freebase. 6-cyano-7-nitroquinoxaline-2,3-dione (CNQX), D-2-amino-5-phosphonopentanoic acid (AP-5), KN-93, and tetrodotoxin (TTX) were purchased from Tocris Biosciences (Ellisville, MO). α-Conotoxin MII (αCtxMII) was synthesized as previously described (Azam et al 2010). All other chemicals without a specified supplier were obtained from Sigma (St. Louis, MO).

2.2 Mice

All experiments were conducted in accordance with the guidelines for the care and use of animals provided by the National Institutes of Health Office of Laboratory Animal Welfare, and protocols were approved by the Institutional Animal Care and Use Committee at Purdue University. All efforts were made to minimize animal suffering, to reduce the number of animals used, and to utilize alternatives to *in vivo* techniques when available. Mice were kept on a standard 12-hour light/dark cycle at 22°C and given food and water ad libitum. Mice were weaned and group housed with same sex littermates on postnatal day 21. Tail biopsies were collected 21–28 days after birth and used to determine the genotype of the mice via polymerase chain reaction (PCR) analysis as previously described (Drenan et al 2008a). Male and female α6L9S mice and their non-transgenic (non-Tg) littermates were 8–16 weeks old at the time experiments were conducted. No differences were noted between results obtained from male versus female mice, so results were pooled.

α6L9S mice were generated as described (Drenan et al 2008a). Briefly, a mouse bacterial artificial chromosome (BAC) containing the *Chrna6* gene was obtained and an L9'S mutation was introduced by codon replacement using a BAC recombineering approach. Mutant BAC DNA was introduced into FVB/N embryos, which were then implanted into pseudopregnant Swiss-Webster surrogates. The BAC insertion site in the mouse genome is unknown. Founder animals were isolated and have been continuously back-crossed to C57BL/6 for >12 generations. Over 90% of the α6L9S strain genome is expected to contain C57BL/6 alleles, but FVB/N allelic DNA close to the insertion site is likely to remain in place

in this strain. α6L9S mice are thus transgenic and express mutant (L9'S) and wild-type (WT) α6 nAChR subunits (Cohen et al 2012). α6* nAChR function is sensitized in these mice, producing a 10- to 100-fold leftward shift in concentration-response relationships involving α6* nAChRs, depending on the assay being used (Cohen et al 2012, Drenan et al 2010, Drenan et al 2008a). We previously confirmed that α6* nAChRs in α6L9S mice are not overexpressed or misexpressed in ectopic brain locations (Drenan et al 2010, Drenan et al 2008a).

α6L9S mice lacking α4 nAChR subunits were generated as previously described (Drenan et al 2010). α4 knockout (KO) mice were a generous gift of Dr. Michael Marks (University of Colorado, Boulder, CO), and were produced by mating mice heterozygous for the α4KO allele. Briefly, α6L9S mice, in which the mutant allele is maintained in a heterozygous fashion, were crossed to homozygous α4KO mice to produce mice that are heterozygous for both the α6L9S allele and the α4KO allele. These mice were subsequently crossed to homozygous α4KO mice to produce mice heterozygous for the α6L9S allele and homozygous for the α4KO allele.

α6 green fluorescent protein (GFP) mice were generated as previously described (Mackey et al 2012). To create α6GFP mice lacking α4 subunits, α4KO mice were crossed to α6GFP mice, generating α6GFP mice heterozygous for the α4KO allele. These mice were crossed again to mice homozygous for the α4KO allele, yielding α6GFP mice that were also homozygous for the α4KO allele.

Chrna4 loxP/loxP mouse embryos were a generous gift from Dr. Stephen Heinemann (Salk Institute for Biological Studies, La Jolla, CA). They were generated as previously described

(McGranahan et al 2011). Homologous recombination was used to insert loxP sequences into intronic regions flanking exon V of the α4 gene. *Chrna*4 loxP/loxP mice were crossed with α6L9S mice to generate mice with hypersensitive α6* nAChRs and floxed α4 subunit genes. α4 subunits were removed from *Chrna4* loxP/loxP mice by injecting viral vectors driving the expression of Cre into the brain region of interest as described below. The virus also drives the expression of GFP. Therefore, *Chrna*4 loxP/loxP mice that received intra-VTA Cre virus injections are referred to as *Chrna*4 ventral midbrain conditional KO mice (*Chrna*4 vMB cKO). Control *Chrna4 loxP/loxP* were injected with a virus that only drives the expression of GFP. Not every cell is infected with the virus thus when referring to data from individual neurons, Cre(+) and Cre(-) is indicated. Cre(+) refers to cells that are from *Chrna*4 vMB cKO mice that also express the Cre virus (identified by the presence of GFP). Cre(-) refers to cells from *Chrna*4 loxP/loxP mice given control GFP virus injections.

2.3 Stereotaxic Surgery

Adult mice (at least 8 weeks of age) were anesthetized with a ketamine/xylazine cocktail (α6L9S: 100 mg/kg ketamine, 10 mg/kg xylazine; non-Tg and *Chrna*4 loxP/loxP: 120 mg/kg ketamine, 16 mg/kg xylazine; intraperitoneal (i.p.) injection). The surgical area was shaved and cleansed via three applications of alternating iodide ointment and 70% ethanol. Mice were then placed into a stereotaxic frame (Kopf; Tujunga, CA, USA) and a small incision was made to expose the skull. The skull was leveled in the coronal and sagittal planes using the coordinates for the bregma and lambda as landmarks. Bilateral

holes were drilled in the skull according to adjusted coordinates from the third edition of the Franklin and Paxinos mouse brain atlas (for VTA: M/L: ±0.5 mm from bregma, A/P: −3.2 mm from bregma; for NAc: M/L: ±0.6 mm from bregma, A/P: +1.5 mm from bregma). The A/P coordinate was adjusted for each animal to accommodate individual variations in size; the distance between the bregma and lambda was measured for each mouse and divided by the published distance in this species (4.21 mm), and this ratio was then multiplied by the proper A/P coordinate from the atlas to determine the proper A/P coordinates for each animal. At this point mice were either implanted with guide cannulae or given intra-VTA or intra-NAc viral injections.

Guide cannulae 3.0 mm in length (Plastics One; Roanoke, VA, USA) along with a dummy cannula (also 3.0 mm in length; Plastics One) were slowly lowered into position and secured using Geristore cement (Den-Mat; Lompoc, CA, USA). Animals remained in the stereotaxic apparatus until the cement fully dried. Once removed from the stereotaxic apparatus, a dust cap was screwed onto the dorsal portion of the guide cannula to keep the dummy cannula in place and to prevent contamination of the guide cannula.

Chrna4 loxP/loxP mice and α6L9S/*Chrna4* loxP/loxP were injected with viruses that drive the expression of Cre recombinase in order to remove α4 nAChR subunits. A syringe loaded with the virus was slowly lowered to D/V coordinates of -4.5 mm from bregma for intra-VTA injections or -4.4 mm from bregma for intra-NAc injections. For the AAV-GFP and AAV-GFP-Cre viruses (AAV2.CMV.PI.eGFP.WPRE.bGH and AAV2.CMV.HI.eGFP-Cre.WPRE.SV40 purchased from Penn Vector Core), 250 nL of virus was infused at a rate

of 50 nL/min. The injection needle was left in place for 5 minutes after the infusion ended before slowly retracting the needle out of the brain. For the HSV-YFP and HSV-YFP-Cre retrograde viruses (hEF1-EYFP and hEF1-EYFP-IRES-cre purchased from the MIT McGovern Institute Viral Gene Transfer Core), 500 nL of virus was infused at a rate of 50 nL/min. The injected needle was left in place for 10 minutes after the infusion ended before slowly retracting the needle out of the brain. Sutures were used to close the incision.

Following surgery, mice were given ketoprofen (5 mg/kg, subcutaneous) and allowed to recover on a heating pad under close observation until ambulatory. Mice were singly housed following surgery. Mice implanted with guide cannulae were allowed to recover for at least 5 days prior to infusions. Mice given viral injections were given 2 (AAV viruses) or 3 (HSV viruses) weeks to recover and for the virus to reach peak expression.

2.4 *in vivo* Drug Administration

Prior to receiving i.p. injections, mice were gently handled once a day for three days to habituate them to handling. The next day, mice were scruffed and given a mock injection. One day prior to the experiment, mice were scruffed and given a saline injection (i.p.). On the experimental day, mice were given an i.p. injection of vehicle (0.9% saline), nicotine, or ethanol. Nicotine was administered at a dose of 0.03 mg/kg or 0.17 mg/kg. Ethanol was administered at a dose of either 0.5 or 2.0 g/kg. Immediately following the injection, mice were placed in a novel conditioning chamber for 15 minutes (nicotine) or 5 minutes (ethanol) before they were returned to their home cage. One hour after the injection mice were euthanized for brain slice preparation.

A subset of α6L9S mice received intra-VTA infusions of αCtxMII (10 pmol) or vehicle (sterile saline) immediately prior to nicotine (0.03 mg/kg, i.p.) injections. Infusions were carried out using a dual syringe pump connected to internal cannulae (extending 1.5 mm beyond guide cannulae; Plastics One) via two identical Hamilton syringes and PE50 tubing (Plastics One). Mice were anesthetized using isoflurane (5% for initiation of anesthesia; 1.8% for maintenance). While maintained on isoflurane anesthesia, the dust cap and dummy cannula were removed and the internal cannula was fully inserted into the guide cannula. Drugs were infused at a rate of 0.1 µL/min for 5 minutes for a total volume of 0.5 µL. The internal cannula was left in place for an additional 5 minutes to prevent backflow into the guide cannula. Following the infusion, the internal cannula was removed and the dummy cannula and dust cap were replaced. The animal was immediately removed from the isoflurane and allowed to recover (approximately 10 minutes) in the home cage.

2.5 Brain Slice Preparation for Electrophysiology

Mice were anesthetized with sodium pentobarbital (100 mg/kg, i.p.) followed by cardiac perfusion with oxygenated (95% O_2/5% CO_2), 4°C *N*-methyl-D-glucamine (NMDG) recovery solution containing the following: 93 mM NMDG, 2.5 mM KCl, 1.2 mM NaH_2PO_4, 30 mM $NaHCO_3$, 20 mM HEPES, 25 mM glucose, 5 mM Na^+ ascorbate, 2 mM thiourea, 3 mM Na^+ pyruvate, 10 mM $MgSO_4 \bullet 7H_2O$, and 0.5 mM $CaCl_2 \bullet 2H_2O$ (300–310 mOsm, pH 7.3–7.4). Brains were removed and retained in 4°C NMDG recovery solution for 1 minute. Coronal slices (200 µm) were cut with a microslicer (DTK-Zero 1; Ted Pella, Redding, CA).

Brain slices recovered for 12 minutes at 33°C in oxygenated NMDG recovery solution, after which they were held until recording in room temperature HEPES holding solution containing the following: 92 mM NaCl, 2.5 mM KCl, 1.2 mM NaH_2PO_4, 30 mM $NaHCO_3$, 20 mM HEPES, 25 mM glucose, 5 mM Na^+ ascorbate, 2 mM thiourea, 3 mM Na^+ pyruvate, 2 mM $MgSO_4 \bullet 7H_2O$, and 2 mM $CaCl_2 \bullet 2H_2O$ (300–310 mOsm, pH 7.3–7.4). Coordinates for recordings in the VTA were approximately −3.5 mm from bregma, 4.0–4.5 mm from the surface, and 0.5–1.0 mm from the midline. In adult C57 mice, these coordinates correspond to NAc lateral shell-projecting VTA neurons, which are expected to be approximately 96% tyrosine hydroxylase (TH)-positive (Lammel et al 2008).

2.6 Patch-Clamp Electrophysiology

A single slice was transferred to a 0.8-ml recording chamber (RC-27L bath with PH-6D heated platform; Warner Instruments, Hamden, CT), and slices were superfused throughout the experiment with standard recording artificial cerebrospinal fluid (1.5–2.0 ml/min) containing the following: 124 mM NaCl, 2.5 mM KCl, 1.2 mM NaH_2PO_4, 24 mM $NaHCO_3$, 12.5 mM glucose, 2 mM $MgSO_4 \bullet 7H_2O$, and 2 mM $CaCl_2 \bullet 2H_2O$ (300–310 mOsm, pH 7.3–7.4). Cells were visualized with an upright microscope (FN-1; Nikon Instruments, Melville, NY) using infrared or visible differential interference contrast optics. Patch electrodes were constructed from Kwik-Fil borosilicate glass capillary tubes (1B150F-4; World Precision Instruments, Inc., Sarasota, FL) using a programmable microelectrode puller (P-97; Sutter Instrument Company, Novato, CA). The electrodes had tip resistances of 4.5–8.0 MΩ when filled with internal pipette solution (pH adjusted to 7.25 with Tris base, osmolarity adjusted to 290 mOsm with sucrose). Three internal pipette solutions

were used. The following solution was used when recording nicotine- or ACh-evoked currents (bath application or puff-applied), action potential firing, and spontaneous EPSCs: 135 mM K^+ gluconate, 5 mM EGTA, 0.5 mM $CaCl_2$, 2 mM $MgCl_2$, 10 mM HEPES, 2 mM MgATP, and 0.1 mM GTP. The following solution was used when recording AMPA- or NMDA-evoked currents and AMPA/NMDA ratios: 117 mM $CsCH_3SO_3$, 20 mM HEPES, 0.4 mM EGTA, 2.8 mM NaCl, 5 mM tetraethylammonium (TEA)-Cl, 2.5 mM MgATP, and 0.25 mM GTP. When recording AMPA-evoked currents 100 μM spermine was added to this internal solution so the rectification index could be evaluated. Finally, inhibitory post synaptic current (IPSC) recordings were done using an internal solution containing (in mM): 75 K^+ gluconate, 65 KCl, 5 EGTA, 10 HEPES, 0.5 $CaCl_2$, 2 MgATP, 0.1 GTP.

Whole-cell recordings were taken at 32°C with an Axopatch 200B amplifier, a 16-bit Digidata 1440A A/D converter, and pCLAMP 10.3 software (all from Molecular Devices, Sunnyvale, CA). Data were sampled at 5 kHz and low-pass filtered at 1 kHz. The junction potential between the patch pipette and the bath solution was nulled immediately prior to gigaseal formation. Series resistance was uncompensated.

DA neurons in VTA were identified according to previously published methods (Drenan et al 2008a, Nashmi et al 2007, Wooltorton et al 2003). We avoided recording from neurons on the slice surface and neurons deep in the slice that were difficult to visualize. Briefly, DA neurons were identified via several electrophysiological characteristics: 1) broad spike width (≥2 milliseconds), 2) slow spontaneous firing (<5 Hz), and 3) expression of hyperpolarization-activated cation current (I_h).

To examine the function of somatic ligand-gated ion channels, agonists were locally applied using a Picospritzer III (General Valve, Fairfield, NJ). Atropine (1 μM) was present in the bath solution when administering ACh to avoid activation of muscarinic receptors. During AMPA- and NMDA-evoked current recordings, picrotoxin (a $GABA_A$ receptor antagonist; 75 μM) and TTX (a selective sodium channel blocker; 0.5 μM) were added to the recording solution to isolate the recorded DA neuron. A drug-filled micropipette, identical to a typical recording pipette, was mounted onto a single-dimension piezoelectric translator (PA-100/12; Piezosystem Jena, Inc., Hopedale, MA), which was fixed to a micromanipulator (Sutter Instrument Company). Between drug applications, the drug-filled pipette was maintained ≥100 μm from the recorded cell. To apply drugs to the recorded cell, pClamp software triggered the piezoelectric translator to advance the drug-filled pipette to a predetermined position adjacent to the recorded cell (20–40 μm from the cell), drug was applied to the cell using a 250-millisecond pressure (12 psi) ejection, and the piezoelectric translator subsequently retracted the drug-filled pipette. This setup allowed for better reproducibility and reduced receptor desensitization compared with manual control of the drug-filled pipette. The first application to a cell was typically with the drug-filled tip approximately 40 μm from the cell, and we subsequently moved the position of the drug-filled pipette closer to the cell to achieve a more rapid response. Responses to AMPA were deemed acceptable based on two criteria: 1) the pressure application caused slight to modest cell movement, and 2) the seal parameters remained stable for multiple responses. Under these conditions, the 10–90% rise time for

AMPA application was 222 ± 17 milliseconds. Faster rise times and excessive cell movement were commonly associated with loss of a stable seal. Responses were much slower (10–90% rise time was 546 ± 75 milliseconds) when the cell did not move during the application.

AMPA to NMDA ratio recordings were carried out as previously described (Etherton et al 2011, Mao et al 2011), but with minor modifications. Coronal slices were used (as for AMPA-evoked currents), neurons were chosen as described above, and whole-cell recordings were established. Picrotoxin (75 μM) was added to the recording solution. A concentric bipolar stimulating electrode (FHC cat. #CBAPC75) was placed 100–200 μm lateral to the recorded cell, typically in/around the medial lemniscus in the ipsilateral hemisphere. Synaptic responses were stimulated (250–750 μA, 40 μsec, 0.1 Hz) such that evoked EPSCs were ∼50% of maximum amplitude. First, the cell was held at a command voltage of −70 mV, and an EPSC was evoked. Because there is little to no current through NMDA receptors at a membrane potential of −70 mV (due to Mg^{2+} block), the response at −70 mV, and therefore the time to peak, is likely to be completely mediated by AMPARs. Five sweeps were recorded at −70 mV, and the average time-to-peak was noted and subsequently used to measure AMPAR-mediated EPSCs at +40 mV. Next, cells were depolarized to a command voltage of +40 mV and membrane current was allowed to stabilize for several minutes prior to evoking EPSCs. EPSCs were again evoked, and 5 sweeps were averaged. The amplitude of the AMPA-mediated component at +40 mV was estimated to be the membrane current value at the time corresponding to when the evoked EPSCs peaked when the command voltage was −70 mV. The NMDA component

was derived by averaging the membrane current value during a 10 millisecond window that began 40 milliseconds after the time of the peak AMPAR response. Because AMPA components of evoked EPSCs decay to baseline well before 40 milliseconds, this window accurately isolates the NMDA-mediated component of the evoked EPSC. AMPA components at +40 mV and NMDA components at +40 mV were used to derive an AMPA/NMDA ratio for each cell. This method was shown to yield results congruent with those obtained using AP-5 to pharmacologically isolate NMDA and AMPA components of the evoked EPSC in recordings of nicotine-evoked plasticity from VTA DA neurons (Mao et al 2011). In a subset of cells, we verified our measured AMPA/NMDA ratios by using AP-5 to pharmacologically isolate NMDA and AMPA components. For all recordings in VTA, one or two slices per animal were used, and data were obtained from between one and six cells per slice.

A current injection protocol was used to record action potential firing and measure changes in excitability of VTA DA neurons in *Chrna4* loxP/loxP control slices versus Cre(+) VTA DA neurons in *Chrna*4 vMB cKO slices. In current clamp mode, current was injected from -40 to +80 pA in 20 pA intervals. Each step lasted 2 seconds.

Spontaneous EPSCs and IPSCs were measured while holding the cell at -60 mV in voltage clamp mode with the internal solution specified above. CNQX (10 μM), an AMPA/kainate receptor antagonist, was added to the recording solution during IPSC recordings to exclude the possibility of recording EPSCs. At the end of the recording in a subset of cells, picrotoxin (100 μM), a $GABA_A$ receptor antagonist, was bath applied to confirm the events

recorded were GABA receptor mediated IPSCs. Picrotoxin (100 μM) was added to the recording solution during EPSC recordings to exclude the possibility of recording IPSCs. At the end of the recording in a subset of cells, CNQX (10 μM), was bath applied to confirm the events recorded were AMPAR mediated EPSCs. Instantaneous frequency and amplitude were analyzed using the threshold search feature of Clampfit. First, the baseline was adjusted to zero to correct for any baseline drift before starting the threshold search. The threshold search was set to detect events between two cursors placed two minutes apart. For IPSCs, CNQX bath application was started immediately after whole-cell access was established. Therefore the time window was set to start a minimum of 8 minutes after the start of CNQX bath application. Negative going deflections were detected as events by placing the top level marker at zero and the bottom level marker below the baseline current. Any event crossing the bottom level marker was detected as an event when the threshold search was ran. At the completion of the run, the shape of event was manually examined so any noise detected as an event could be rejected. A results summary sheet was automatically generated by Clampfit. It included the instantaneous frequency and amplitude of each event. All events per cell were averaged to give the data points displayed in the figures.

2.7 Single-Cell RT-PCR

These methods for reverse transcription (RT)-PCR were adapted from (Zhao-Shea et al 2011). VTA neurons were studied using the K^+ gluconate-based internal solution listed above but made with DEPC-treated water. After whole-cell recording, the recorded cell

was aspirated into the pipette, under visual control, with gentle negative pressure. Input resistance was monitored during aspiration. Successful PCR reactions were typically only attained when a seal resistance of > 1 GΩ was maintained after aspiration. Cellular contents were expelled into 75% ethanol, and RNA was precipitated and isolated by centrifugation at 4°C. cDNA was formed from RNA via reverse transcription (Sensicript RT, Qiagen) using oligo-dT primers, and a nested PCR strategy was subsequently used to detect target mRNA species. In round #1 of nested PCR, TH and glyceraldehyde-3-phosphate dehydrogenase (GAPDH) cDNA was amplified (1 cycle: 94°C 2 minutes; 20 cycles: 94°C 1 minute, 56°C 1 minute, and 72°C 1.5 minutes; 1 cycle: 72°C 10 minutes) with the following primers: TH_F (CAGTGATGCCAAGGACAAGC), TH_R2 (GAGAAGGGGCTGGGAACTTT), GAPDH_F2 (AACTTTGGCATTGTGGAAGG), and GAPDH_R2 (CCCTGTTGCTGTAGCCGTAT23). Subsequently, TH and GAPDH signals were further amplified (1 cycle: 94°C 2 minutes; 36 cycles: 94°C 1 minute, 56°C 1 minute, 72°C 1.5 minutes; 1 cycle: 72°C 10 minutes) in round #2 with the following primers: TH_F, TH_R1 (CCT GTG GGT GGT ACC CTA TG), GAPDH_F1 (GTG TTC CTA CCC CCA ATG TG), and GAPDH_R1 (GGT CCT CAG TGT AGC CCA AG).

2.8 Immunohistochemistry and Confocal Microscopy.

Transgenic mice expressing α6* nAChR subunits fused in-frame with GFP (α6GFP mice; *n* = 3), along with α6GFP mice homozygous for the α4KO allele, were anesthetized with sodium pentobarbital (100 mg/kg i.p.) and transcardially perfused with 15 ml of heparin-containing ice-cold phosphate-buffered saline (PBS) followed by 30 ml ice-cold 4% paraformaldehyde in PBS. Brains were removed and postfixed overnight at 4°C. Coronal

sections (50 µm) were cut on a microslicer and collected into PBS. Sections were permeabilized (20 mM HEPES, pH 7.4, 0.5% Triton X-100, 50 mM NaCl, 3 mM $MgCl_2$, 300 mM sucrose) for 1 hour at 4°C, blocked [0.1% Triton X-100, 5% donkey/horse serum in Tris-buffered saline (TBS)] for 1 hour at room temperature, and incubated overnight at 4°C in solutions containing primary antibodies (diluted in 0.1% Triton X-100, 5% donkey serum in TBS). Sections were stained with rabbit anti-GFP primary antibodies (A11122; Invitrogen, Carlsbad, CA) with a final dilution of 1:500. Sections were washed three times for 10 minutes each in TBS/Tween 20 (0.1% Triton X-100 in TBS) followed by incubation at room temperature for 1 hour with goat anti-rabbit Alexa 488 secondary antibodies (A11008; Invitrogen) diluted in 0.1% Triton X-100, 5% donkey serum in TBS. Sections were then washed three times in TBS/Tween 20 for 10 minutes each. Sections were stained with Qnuclear Deep Red Stain (1:1000, Q10363; Invitrogen) in PBS for 20 minutes at room temperature followed by three 5-minute washes in PBS. All sections were mounted on slides and coverslipped with Vectashield (Vector Laboratories, Burlingame, CA), and then imaged with a Nikon A1 laser-scanning confocal microscope system (Nikon Instruments). Nikon Plan Apo 10X air and 60X oil objectives were used. Alexa 488 was excited with an argon laser at 488 nm. VTA DA neurons were imaged at 60X, and mean pixel intensity per cell was measured for >100 cells in both α6GFP and α6GFPα4KO slices.

Slices from *Chrna*4 vMB cKO mice were treated with the same staining and imaging procedure with the exception of a modified permeabilization step. Slices were alternatively permeabilized with a two minute incubation in PBS-Triton X (0.3% Triton X-100 in PBS). Sections were co-stained with sheep anti-TH (1:800) and rabbit anti-GFP

(1:500). Secondary antibodies used include anti-sheep Alexa 555 and anti-rabbit Alexa 488 with a final dilution factor of 1:500.

2.9 Statistical Analysis.

Statistical analysis was performed with GraphPad Prism 6 software (GraphPad Software, Inc., La Jolla, CA). Data are reported as the mean ± standard error of the mean (S.E.M.). To determine whether data sets were normally distributed, all data sets were subjected to a D'Agostino and Pearson omnibus normality test. Only when all data sets to be compared passed this normality test (α level = 0.05) were parametric statistical tests used. For data sets that were either not normally distributed or not large enough for a normality test, statistical significance ($P < 0.05$) was assessed with nonparametric tests. A student's *t*-test or a Mann–Whitney test was used for comparisons between two groups. One-way analysis of variance (ANOVA) or a Kruskal–Wallis (nonparametric one-way analysis of variance) test followed by a Dunn's post hoc test was used for comparisons between three or more groups. Concentration-response curve data were fitted to the Hill equation. Error bars for plotted EC_{50} values indicate 95% confidence intervals.

CHAPTER 3. α4α6β2* nAChR ACTIVATION ON VTA DA NEURONS IS SUFFICIENT TO STIMULATE A DEPOLARIZING CONDUCTANCE AND ENHANCE SURFACE AMPA RECEPTOR FUNCTION

3.1 Electrophysiological Identification of VTA DA Neurons

To study VTA DA neurons in adult mice (aged ≥60 days), we prepared coronal slices and recorded from VTA cells residing in the lateral aspect of the VTA. Although the VTA is emerging as a heterogeneous structure (Lammel et al 2011), 96.3% of neurons in this area test positive for TH expression in adult C57 mice, and these cells exhibit I_h currents (Lammel et al 2011). VTA neurons in this study typically fired spontaneous (Figure 3.1 A), wide action potentials (with a width of approximately 2–5 milliseconds; Figure 3.1 B).

Hyperpolarizing current injections induced “sag” responses in the transmembrane voltage record (I = 120 pA; Figure 3.1 A), and these cells exhibited inward currents in response to hyperpolarizing voltage steps (I_h currents; Figure 3.1 C). To provide further confirmation that these neurons are DAergic, we conducted single-cell RT-PCR reactions from a subset of recorded neurons. All recorded neurons (n = 5) in lateral VTA with a PCR signal for GAPDH were also positive for TH mRNA (Figure 3.1 D), and all of these TH(+) cells exhibited electrophysiological features as shown above (Figure 3.1 A–C). On the basis of these results and supporting studies in the literature (Lammel et al 2008, Lammel et al 2011, Zhang et al 2010) we proceeded with reasonable confidence that cells with these characteristics, and in the lateral part of the VTA, were DAergic neurons.

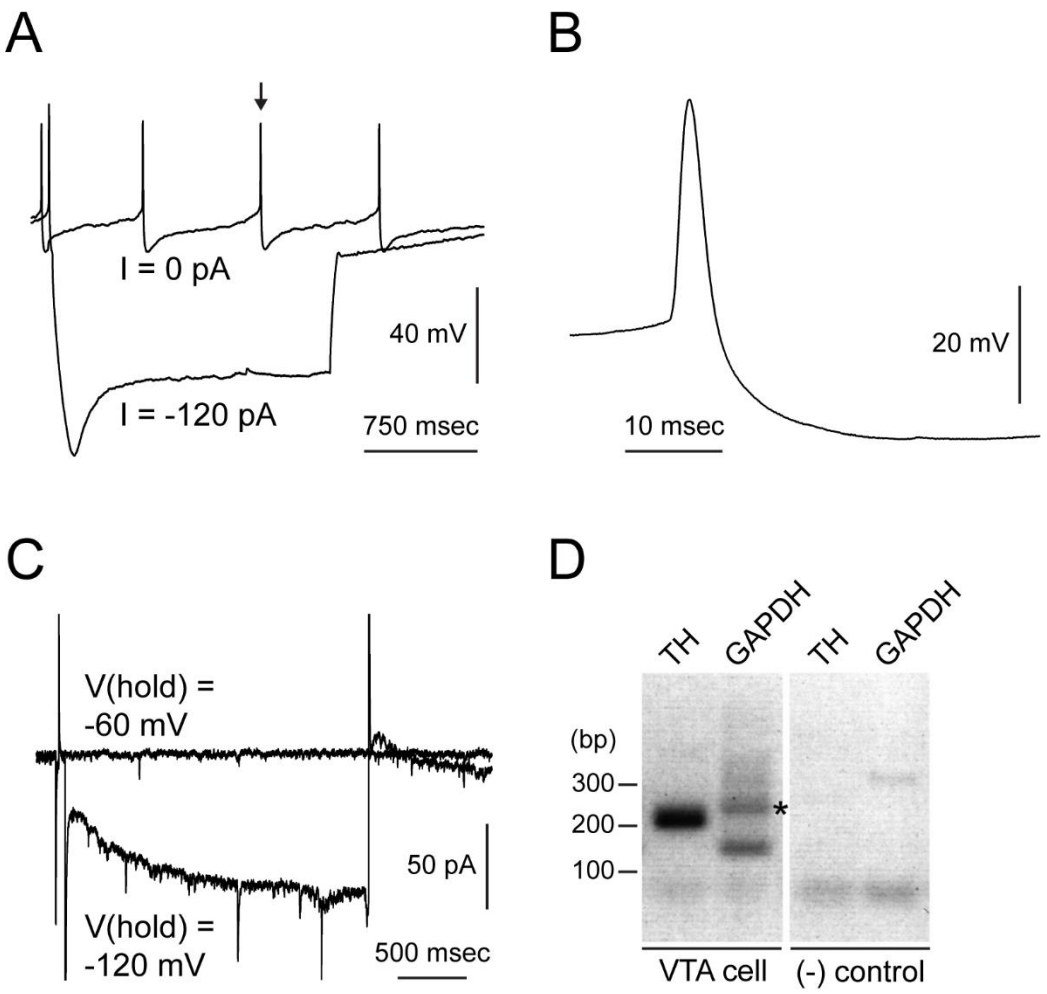

Figure 3.1 Electrophysiological identification of VTA DA neurons. **(A)** Whole-cell current-clamp recordings of VTA DA neurons show spontaneous (*I* = 0 pA), pacemaker firing (1–5 Hz), and "sag" responses in the membrane potential in response to hyperpolarizing (*I* = -120 pA) current injections. **(B)** VTA DA neurons have wide action potentials. The neuron in (A) indicated with an arrow is shown on an expanded time scale to better view the action potential width (typically 2–5 milliseconds) seen in the neurons under study. **(C)** I_h currents in VTA DA neurons. VTA cells were held at -60 mV in voltage-clamp mode and membrane current was recorded at baseline and during a voltage step to -120 mV. **(D)** Single-cell RT-PCR (done by Dr. Pei-Yu Shih). VTA DA neurons recorded in whole-cell mode were aspirated into the recording pipette, followed by RT of RNA and subsequent PCR reactions to detect TH and GAPDH (positive control) expression. Expected band sizes are as follows: TH = 207 bp and GAPDH = 138 bp (the asterisk indicates a spurious PCR reaction, possibly generated from external primer pairs). As a negative control, a pipette was lowered into the slice and mild negative pressure was applied. The pipette was removed from the slice and assayed with RT-PCR as for a recorded cell.

3.2 Hypersensitive α6* nAChRs in α6L9S mice

In these experiments we used transgenic α6L9S mice to study the selective activation of α6* nAChRs. In these mice, the leucine at the nine prime position is mutated to a serine (L9'S) in the second transmembrane domain (TM2) of α6 nAChR subunits. This mutation results in hypersensitive α6* nAChRs. They are 10- to 100- fold more sensitive than non-α6* nAChRs (Cohen et al 2012, Drenan et al 2010, Drenan et al 2008a). Therefore, low concentrations of agonists such as ACh and nicotine can be used to selectively activate α6* nAChRs (Figure 3.2). The leucine residue where the mutation is made is highly conserved among nAChR subunits and is found in the channel pore. Mutating this leucine residue to a polar amino acid, such as serine or threonine, has successfully increased the sensitivity of several different nAChR subunits (Drenan & Lester 2012). It was first demonstrated with α7 nAChRs in 1991 (Revah et al 1991). Drenan *et al* first generated gain-of-function α6L9S transgenic mice in 2008 and carried out studies showing low doses/concentrations of nicotine act selectively through α6* nAChRs to enhance locomotor activity, stimulate DA release in striatal synaptosomes, and increase VTA DA neuron action potential firing rate (Drenan et al 2008a). Here, we use α6L9S mice to test the hypothesis that α6* nAChR activation in VTA DA neurons is sufficient to elicit prolonged inward currents and to enhance AMPAR function.

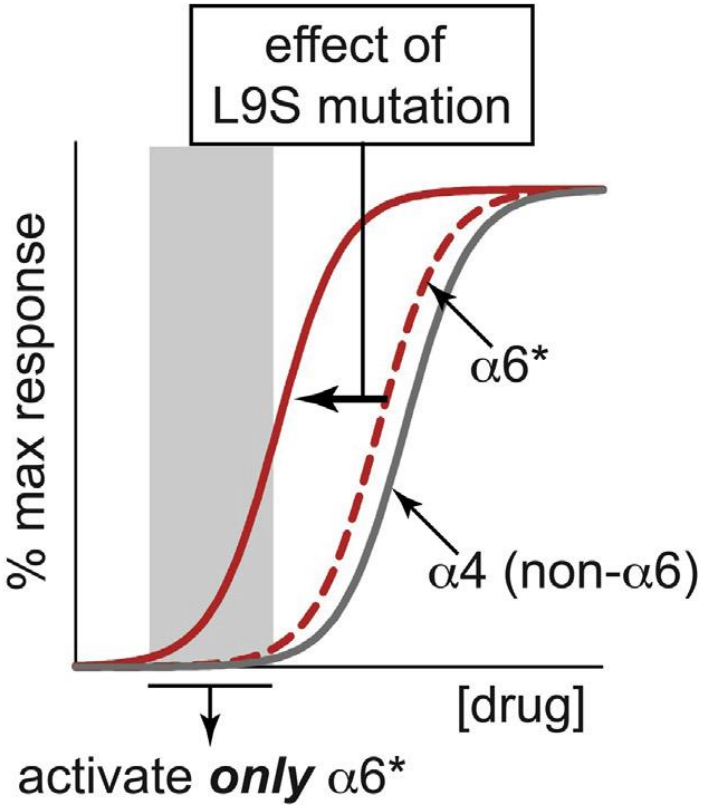

Figure 3.2 Effect of L9S mutation in α6L9S mice. In α6L9S mice, a Leu to Ser mutation was introduced at the 9' position within transmembrane domain 2 of the α6 nAChR subunit protein. This mutation increases the sensitivity of the population of channels containing the mutant α6 subunit, allowing ligands such as ACh and nicotine to selectively activate these channels when low concentrations are used. The theoretical concentration response curve for most responses involving α6 containing receptors is left-shifted.

3.3 A Low Concentration of Nicotine is Sufficient to Increase Inward Currents in VTA DA Neurons

First, we tested the hypothesis that activation of α6* nAChRs is sufficient to elicit inward currents in VTA DA neurons by recording from VTA DA neurons from adult α6L9S and non-Tg littermate mice. Whole-cell voltage-clamp recordings from VTA DA neurons were established using a K^+ gluconate-based internal recording solution, and an inhibitor cocktail containing CNQX (10 μM), picrotoxin (75 μM), and TTX (0.5 μM) was bath-applied to the cell to eliminate most external influences on membrane potential. We measured inward currents in response to a 10-minute bath exposure to nicotine. We previously reported that brief (250 milliseconds) puff-application of 100 nM nicotine elicited small (approximately 10 pA) inward currents (Drenan et al 2008a). We reasoned that sustained exposure of VTA DA neurons to 100 nM nicotine could be sufficient to provide prolonged activation of these cells. Nicotine (100 nM) elicited a significant inward current in α6L9S VTA DA neurons (mean change in holding current value relative to prenicotine baseline = -18.0 ± 3.0 pA; Figure 3.3 A, B, and E). Coapplication of αCtxMII (100 nM) with nicotine (100 nM) eliminated these inward currents (mean change in holding current value relative to prenicotine baseline = –2.7 ± 4.1 pA; Mann–Whitney test, $P < 0.05$; Figure 3.3 A, B, and E), suggesting that α6* nAChRs mediate inward currents in response to 100 nM nicotine. To determine whether responses to 100 nM nicotine were selective for α6* nAChRs in α6L9S slices, 100 nM nicotine was applied to VTA DA neurons from non-Tg littermate slices. Nicotine (100 nM) only slightly increased inward currents in non-Tg littermate VTA

DA neurons in this assay (mean change in holding current value relative to prenicotine baseline = -3.1 ± 0.8 pA; Figure 3.3 C and E), but the same concentration of nicotine significantly increased inward currents in α6L9S neurons (Mann–Whitney test, $P < 0.05$; Figure 3.3 E). αCtxMII did not alter this response in non-Tg littermate cells (Figure 3.3 C and E). As a positive control, we applied 300 nM nicotine to non-Tg VTA DA neurons. This concentration was sufficient to moderately increase inward currents in these cells (mean change in holding current value relative to prenicotine baseline = -8.7 ± 2.2 pA; Figure 3.3 D and E), consistent with a previous report (Liu et al 2012). αCtxMII did not block these responses (mean change in holding current value relative to prenicotine baseline = -7.0 ± 1.0 pA; Figure 3.3 D and E), presumably because responses in non-Tg cells are mediated by both α6* and non-α6* (α4β2) nAChRs. Together, these results demonstrate that selective activation of α6* nAChRs is sufficient to increase inward currents in VTA DA neurons. Application of 100 nM nicotine to α6L9S slices was used in subsequent experiments to study the effects of selectively activating α6* nAChRs.

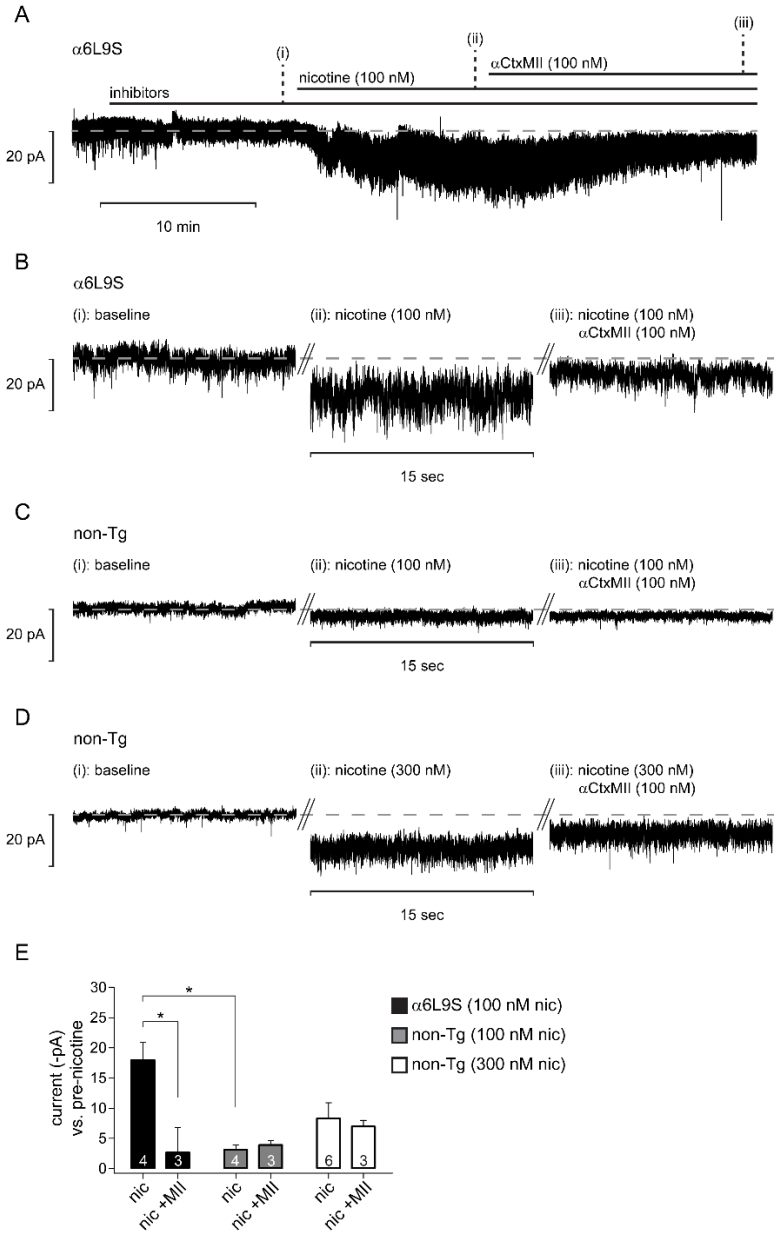

Figure 3.3 A low concentration of nicotine is sufficient to increase inward currents in VTA DA neurons. **(A)** α6L9S or non-Tg control neurons were voltage clamped in whole-cell mode. Inhibitor cocktail [10 μM CNQX, 75 μM picrotoxin, 0.5 μM TTX] was superfused, followed by nicotine (100 nM) and then αCtxMII (100 nM). A representative experiment from a α6L9S neuron is shown. Expanded recordings from time points (i), (ii), and (iii) are shown in B–D. **(B–D)** Voltage-clamp recording segments from α6L9S (B; 100 nM nicotine), non-Tg (C; 100 nM nicotine), and non-Tg (D; 300 nM nicotine) VTA DA neurons at (i) baseline with inhibitor cocktail present, (ii) inhibitor cocktail plus nicotine, and (iii) inhibitor cocktail/ nicotine plus αCtxMII. **(E)** Summary showing mean holding current (-pA) change from baseline in response to nicotine (nic), and nicotine plus αCtxMII in the indicated mouse strain (α6L9S and non-Tg littermate). **P* < 0.05.

3.4 AMPA-Evoked Current Methodology

The initial exposure of brain cells to smoking-relevant concentrations of nicotine results in activation of high-sensitivity nAChRs, including those on VTA DA neurons (Calabresi et al 1989). This exposure to nicotine leads to upregulation of AMPA receptor (AMPAR) function in these cells (Saal et al 2003), which could support behavioral changes that lead to nicotine dependence. Because high-sensitivity nAChRs are expressed on VTA DA neurons, terminals from GABA neurons that synapse onto VTA DA neurons, and other glutamatergic fibers, it is not known whether activation of nAChRs specifically on VTA DA neurons can lead to increased AMPAR function. We previously demonstrated that α6* nAChRs are expressed only in DA neurons in VTA (Mackey et al 2012). We hypothesized that selective activation of α6* nAChRs in VTA, which should stimulate DAergic neurons but not other VTA nAChRs (such as those on GABA or glutamatergic terminals)(Drenan et al 2008a), is sufficient to enhance AMPAR function in these cells.

To measure AMPAR function on the cell surface, we applied AMPA to VTA DA neurons using a drug-filled pipette (Kobayashi et al 2009, Li et al 2008, Sanchez et al 2010) that was positioned using a piezoelectric translator. A cell was voltage clamped and a stable recording was established. The drug-filled pipette remained stationary above/outside the slice until our recording software delivered an analog signal to the piezoelectric translator, triggering movement of the pipette to a predetermined position approximately 20–40 μm from the recorded cell. A digital transistor–transistor logic (TTL) pulse (5 V, 250-millisecond duration) activated the Picospritzer, resulting in drug delivery to the recorded

cell. After the TTL pulse, the piezoelectric translator withdrew the drug-filled pipette. This procedure is summarized in schematic form in Figure 3.4 A. Figure 3.4 B shows a representative record of the movement of the piezoelectric translator, the TTL pulse, and a response to 100 μM AMPA in a VTA DA neuron.

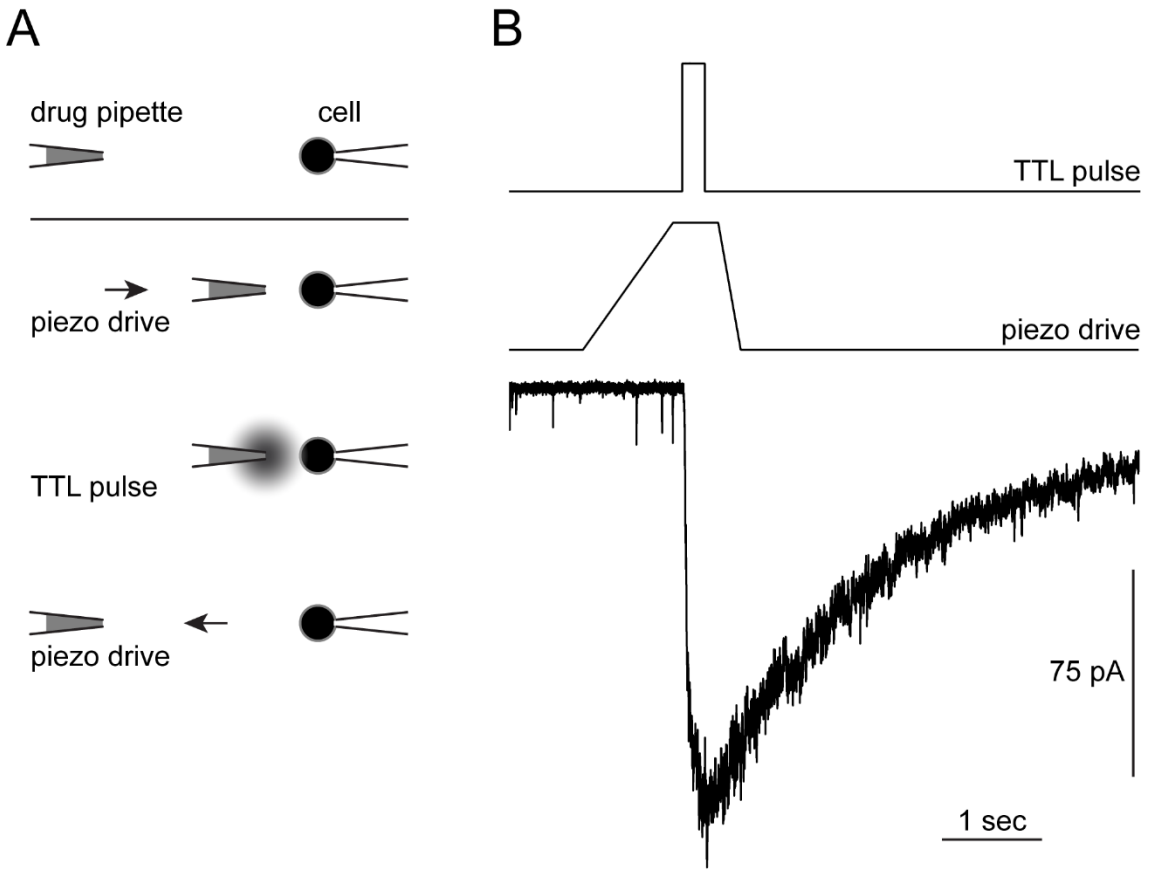

Figure 3.4 AMPA-evoked current methodology. **(A)** A drug-filled pipette is positioned above/next to the cell being recorded. A piezoelectric translator brings the pipette close (20–40 μm) to the cell, a TTL pulse triggers a pressure ejection that dispenses drug (AMPA) onto the cell, and the piezoelectric translator withdraws the pipette away from the cell. **(B)** Representative recording showing the timing of the TTL pulse, piezo drive movement, and resulting inward current elicited by application of 100 μM AMPA to a VTA DA neuron.

3.5 Activation of α6* nAChRs is Sufficient to Enhance AMPAR Function on the Surface of VTA DA Neurons

To test the hypothesis that selective activation of α6* nAChRs is sufficient to enhance AMPAR function, we prepared coronal slices from α6L9S mice and their non-Tg littermates. Slices were cut and allowed to recover for 60 minutes, followed by exposure of the slices to 100 nM nicotine (or a control solution containing no nicotine) for 60 minutes similar to previous studies (Jin et al 2011, Mao et al 2011) (Figure 3.5 A). After a washout period (≥60 minutes), whole-cell recordings were established in VTA DA neurons using a Cs-methanesulfonate–based internal solution. AMPA currents were evoked at holding potentials of -60, 0, and +40 mV. Whereas nicotine (100 nM) exposure did not alter AMPAR function in non-Tg VTA DA neurons, this treatment was sufficient to robustly increase AMPA-evoked currents in α6L9S VTA DA neurons (Figure 3.5 B). Mean AMPA-evoked current amplitude was not altered by nicotine (100 nM) at -60, 0, or +40 mV in non-Tg littermates (Figure 3.5 C). In contrast, there was a significant increase in AMPA-evoked current amplitude at -60 and +40 mV in α6L9S neurons (-60 mV: control = -173.5 ± 29.4 pA, 100 nM nicotine = -358.4 ± 48.5 pA; Mann–Whitney test, $P = 0.004$) (+40 mV: control = 82.2 ± 14.3 pA, 100 nM nicotine = 167.1 ± 23.5 pA; Mann–Whitney test, $P = 0.0045$) (Figure 3.5 D). As a positive control, we incubated non-Tg slices in a higher concentration of nicotine (500 nM). This treatment led to a significant increase in AMPA-evoked currents at a holding potential of -60 mV (control = -184.2 ± 18.3 pA and 500 nM nicotine = -283.4 ± 35.8 pA; unpaired *t* test, $P = 0.0487$) (Figure 3.5 B and C), consistent

with previously published experiments with VTA DA neurons in slices (Jin et al 2011). We next sought to determine whether enhanced AMPA-evoked currents in α6L9S slices treated with nicotine (100 nM) were due to a change in the efficacy versus the potency of AMPA. First, we constructed an AMPA concentration-response curve to confirm that changes in AMPA-evoked currents between non-Tg and α6L9S slices were not due to differences in initial AMPAR sensitivity. Multiple concentrations of AMPA were applied to α6L9S and non-Tg neurons, and the data were fitted to the Hill equation (non-Tg: R^2 = 0.9467; α6L9S: R^2 = 0.9819). There was no substantial difference in AMPA EC_{50} in α6L9S VTA DA neurons compared with non-Tg neurons (EC_{50} = 174 μM for non-Tg, and EC_{50} = 182 μM for α6L9S; Figure 3.5 E). Figure 3.5 E plots these EC_{50} values along with their respective 95% confidence intervals. Similarly, we constructed a concentration-response curve for AMPA-evoked currents in α6L9S slices exposed to nicotine. AMPA at a range of concentrations was applied to cells in slices exposed to nicotine, and the data were fitted to the Hill equation (α6L9S nicotine: R^2 = 0.9942). The EC_{50} for AMPA-evoked currents in nicotine-exposed α6L9S slices was shifted to the left compared with α6L9S slices not exposed to nicotine (EC_{50} = 37 μM; Figure 3.5 F), suggesting an increase in the sensitivity of AMPARs to AMPA.

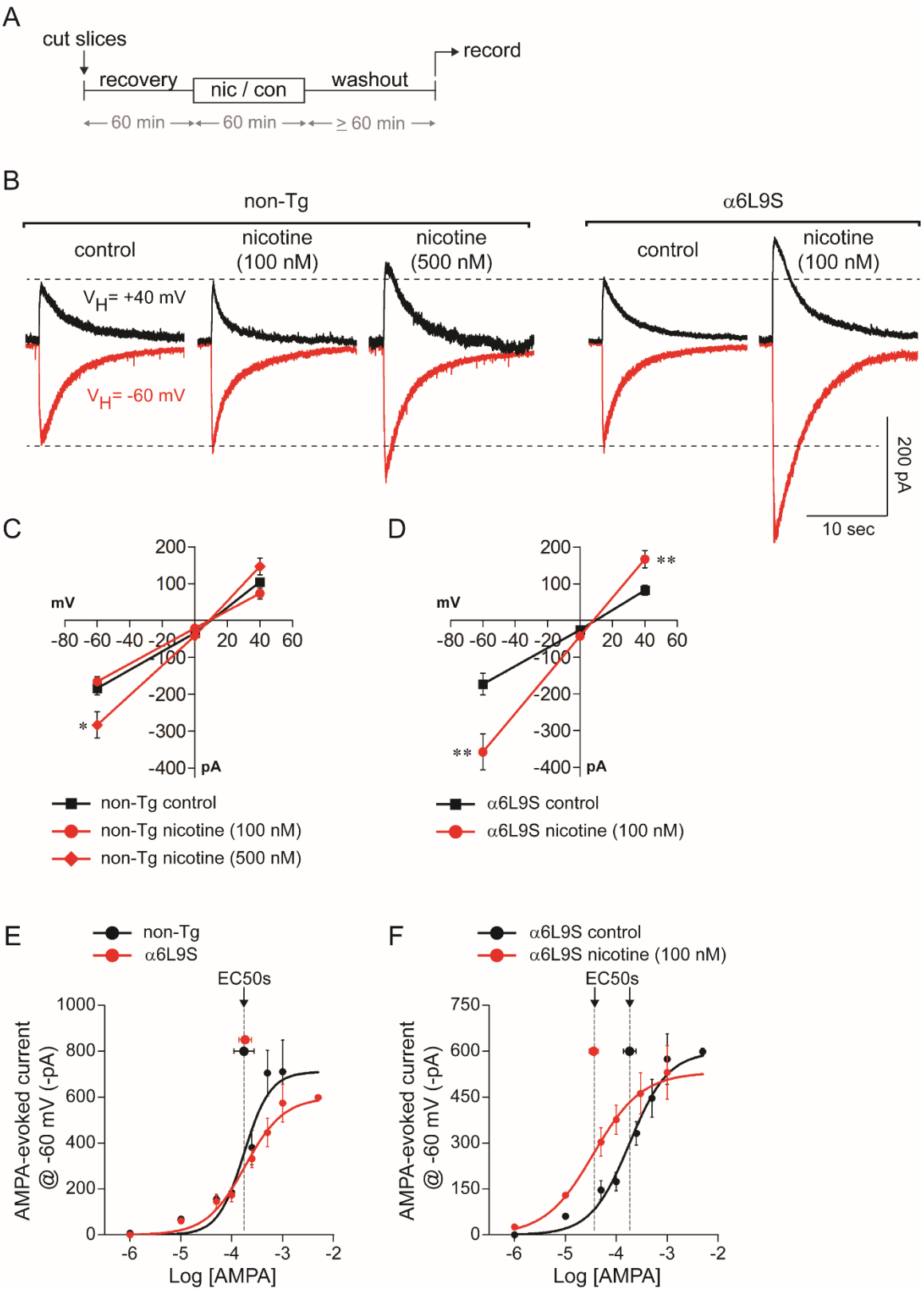
A
cut slices
recovery
nic / con
washout
record
60 min
60 min
≥ 60 min
B
non-Tg
α6L9S
control
nicotine (100 nM)
nicotine (500 nM)
control
nicotine (100 nM)
VH= +40 mV
VH= -60 mV
200 pA
10 sec
C
mV
pA
non-Tg control
non-Tg nicotine (100 nM)
non-Tg nicotine (500 nM)
D
mV
pA
α6L9S control
α6L9S nicotine (100 nM)
E
non-Tg
α6L9S
EC50s
AMPA-evoked current @ -60 mV (-pA)
Log [AMPA]
F
α6L9S control
α6L9S nicotine (100 nM)
EC50s
AMPA-evoked current @ -60 mV (-pA)
Log [AMPA]

Figure 3.5 Activation of α6* nAChRs is sufficient to enhance AMPAR function on the surface of VTA DA neurons. **(A)** Slice treatment procedure. Brain slices from adult α6L9S and non-Tg littermate mice were cut, recovered for 60 minutes, and incubated for 60 minutes in control recording solution or recording solution plus nicotine (100 nM). Nicotine was washed out for ≥60 minutes, and whole-cell recordings were established in VTA DA neurons. **(B)** AMPA currents were evoked by puff-application of AMPA (100 μM) at holding potentials of -60, 0, and +40 mV. Representative recordings from incubation of slices in control and nicotine solutions are shown for α6L9S and non-Tg littermate mice. **(C and D)** Summary showing mean AMPA-evoked currents ([AMPA] = 100 μM) in non-Tg littermate (C) and α6L9S (D) VTA DA neurons in response to control incubation or nicotine incubation at the indicated concentration. The numbers of observations were as follows: non-Tg control (-60 mV, n = 10; 0 mV, n = 7; +40 mV, n = 7); non-Tg 100 nM nicotine (-60 mV, n = 4; 0 mV, n = 4; +40 mV, n = 4), non-Tg 500 nM nicotine (-60 mV, n = 16; 0 mV, n = 12; +40 mV, n = 12), α6L9S control (-60 mV, n = 14; 0 mV, n = 13; +40 mV, n = 13), and α6L9S 100 nM nicotine (-60 mV, n = 11; 0 mV, n = 11; +40 mV, n = 11). **(E)** AMPA concentration-response curve in VTA DA neurons. AMPA-evoked currents were measured in non-Tg and α6L9S neurons. AMPA concentrations and number of observations at each data point are as follows: non-Tg (1 μM, n = 2; 10 μM, n = 6; 50 μM, n = 5; 100 μM, n = 10; 250 μM, n = 5; 500 μM, n = 14; 1000 μM, n = 11), and α6L9S (1 μM, n = 2; 10 μM, n = 4; 50 μM, n = 4; 100 μM, n = 14; 250 μM, n = 5; 500 μM, n = 4; 1000 μM, n = 5; 3000 μM, n = 2). Data (mean ± S.E.M.) were fitted to the Hill equation, and the EC_{50} (±95% confidence interval) for each curve is plotted. **(F)** AMPA concentration-response curve in α6L9S VTA DA neurons. AMPA-evoked currents were measured in α6L9S control slices or slices incubated in 100 nM nicotine for 60 minutes followed by >60 minutes washout prior to recording. Control treated α6L9S data from (E) are replotted here for reference. AMPA concentrations and number of observations at each data point for α6L9S slices treated with nicotine are as follows: α6L9S (1 μM, n = 2; 10 μM, n = 3; 50 μM, n = 2; 100 μM, n = 11; 300 μM, n = 3; 1000 μM, n = 3). Data (mean ± S.E.M.) were fitted to the Hill equation and the EC_{50} (± 95% confidence interval) for each curve is plotted. *$P < 0.05$; **$P < 0.01$.

3.6 Time Dependence For Enhancement of AMPA-Evoked Currents in α6L9S VTA DA Neurons

Next, we studied the time dependence for enhancement of AMPAR function in VTA DA neurons. As with previous experiments, slices were cut and allowed to recover for 60 minutes. We then compared AMPA-evoked current amplitudes from neurons treated in four different ways: 1) incubated for 60 minutes in a control solution without nicotine followed by a washout period of 60–240 minutes prior to recording, 2) incubated for 60 minutes in nicotine (100 nM) followed by a washout period of 60–240 minutes prior to recording, 3) incubated for 10 minutes in nicotine (100 nM) followed by a washout period of 60–240 minutes prior to recording, and 4) incubated for 60 minutes in nicotine (100 nM) followed by a washout period of greater than 240 minutes prior to recording (Figure 3.6 A). Exposure of α6L9S slices to 100 nM nicotine for 10 minutes was insufficient to augment AMPA-evoked currents above control levels (control incubation/washout 60–240 minutes = -173.5 ± 29.4 pA; 10-minute nicotine incubation/washout 60– 240 minutes = -213.5 ± 27.9 pA; Figure 3.6 B and C). However, a 60-minute exposure to nicotine was sufficient to augment AMPA-evoked currents over control (60-minute nicotine incubation/ washout 60–240 minutes = -351.1 ± 64.9 pA; Kruskal–Wallis test, $P < 0.05$; Figure 3.6 B and C). The effect of a 60-minute nicotine exposure was prolonged, as AMPA-evoked currents were still enhanced after a washout period of >240 minutes (60-minute nicotine incubation/washout 60–240 minutes = -411.4 ± 75.5 pA; Kruskal–Wallis test, $P < 0.05$; Figure 3.6 B and C).

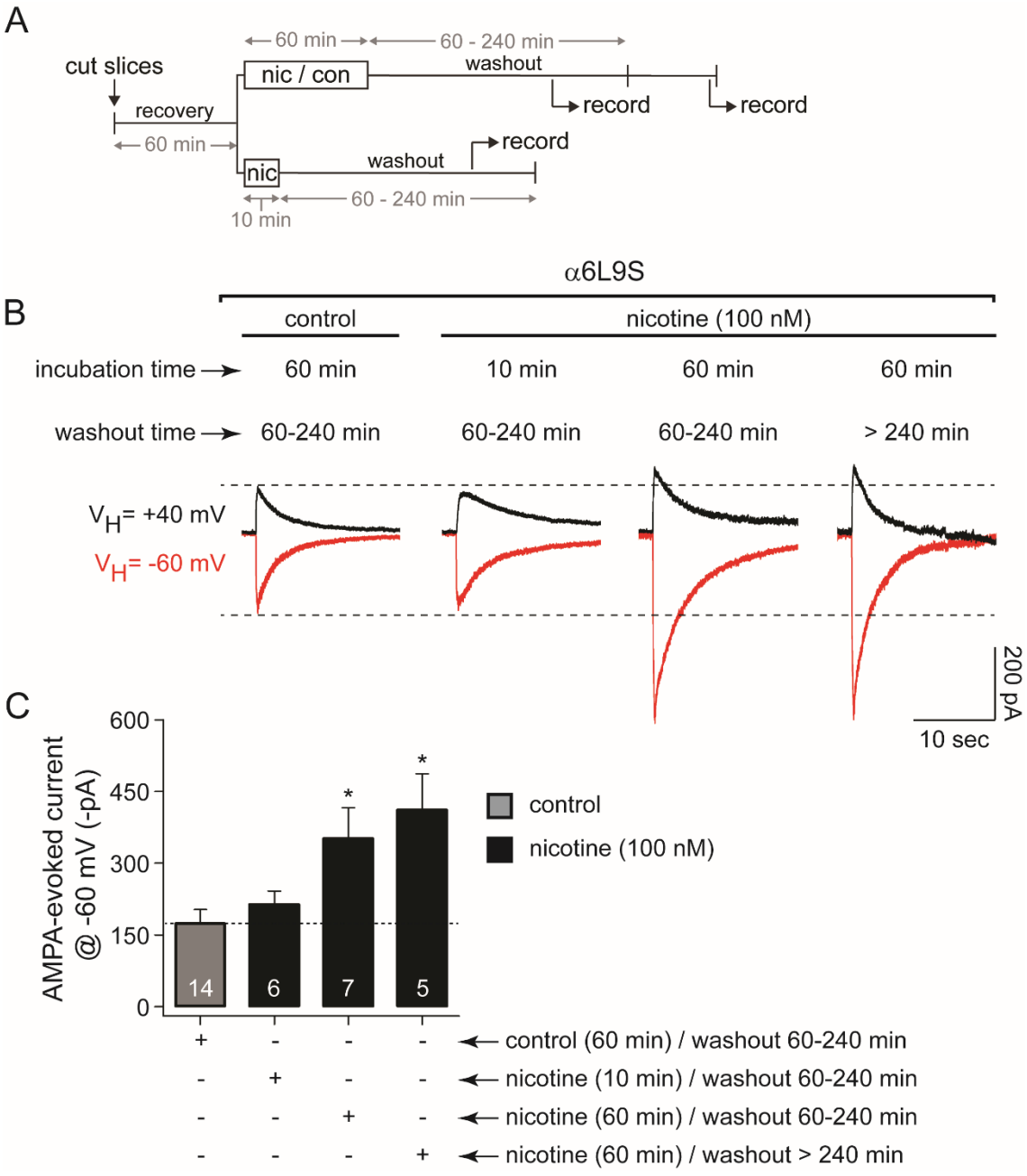

Figure 3.6 Time dependence for enhancement of AMPA-evoked currents in α6L9S VTA DA neurons. **(A)** Slice treatment procedure. Brain slices from α6L9S mice were cut and recovered for 60 minutes. Slices were then incubated in nicotine (100 nM) for either 10 or 60 minutes, followed in either case by a washout period of ≥60 minutes. Some slices treated with nicotine for 60 minutes were allowed >240 minutes of washout prior to recording. **(B)** Representative AMPA-evoked currents ([AMPA] = 100 μM) at +40 and -60 mV in VTA DA neurons in response to treatment detailed in (A). **(C)** Summary showing mean ± S.E.M. AMPA-evoked ([AMPA] = 100 μM) current in α6L9S VTA DA neurons in response to the conditions described in (A). **P* < 0.05 vs control.

3.7 Pharmacology of AMPA-Evoked Current Induction in α6L9S VTA DA Neurons

To better understand the mechanism within VTA DA neurons that leads to enhanced AMPA-evoked currents, we pretreated α6L9S slices for 10 minutes with several pharmacological agents prior to 60 minutes nicotine (100 nM) exposure, washout, and subsequent AMPA-evoked current measurements (Figure 3.7 A). Pretreatment of slices with αCtxMII eliminated the enhanced AMPA-evoked currents seen in α6L9S slices exposed to a control pretreatment prior to nicotine exposure (control = -173.5 ± 29.4 pA, nicotine = -358.4 ± 48.5 pA, and MII = -221.5 ± 45.8 pA; Kruskal– Wallis test, $P < 0.05$; Figure 3.7 B and C). Similarly, blockade of NMDA receptors with AP-5 (10 μM) prior to nicotine treatment eliminated enhanced AMPA-evoked currents (AP-5 = -194.4 ± 32.9 pA; Figure 3.7 B and C). Previous studies indicate that DA D1/ D5 receptors in VTA may play a role in altered synaptic plasticity after exposure to drugs of abuse (Gao & Wolf 2007, Mao et al 2011). Blockade of DA D1/D5 receptors with SCH-23390 (10 μM) did not appear to substantially reduce nicotine-mediated enhancement in AMPA-evoked currents (SCH-23390 = -325.0 ± 44.7 pA; Figure 3.7 B and C), but a Kruskal–Wallis test comparing AMPA-evoked currents from α6L9S SCH-23390-treated slices and untreated control α6L9S slices did not reveal a statistical difference. Several previous reports indicate that homomeric α7 nAChRs play a role in nicotine-elicited AMPAR upregulation (Gao et al 2010, Jin et al 2011). However, pretreatment of slices with MLA (10 nM) did not reduce nicotine-elicited AMPAR upregulation in α6L9S VTA DA neurons (MLA = -497.8 ± 119.8 pA; Kruskal–Wallis test, $P < 0.05$; Figure 3.7 B and C). Previous studies indicate that the activity of CaMKII is

necessary for enhanced AMPAR function after exposure to drugs of abuse (Anderson et al 2008). Inhibiting CaMKII with KN-93 (cell-permeable inhibitor of CaMKII; 5 μM) prior to nicotine treatment eliminated enhanced AMPA-evoked currents (KN-93 = -209.8 ± 37.8 pA; Figure 3.7 C).

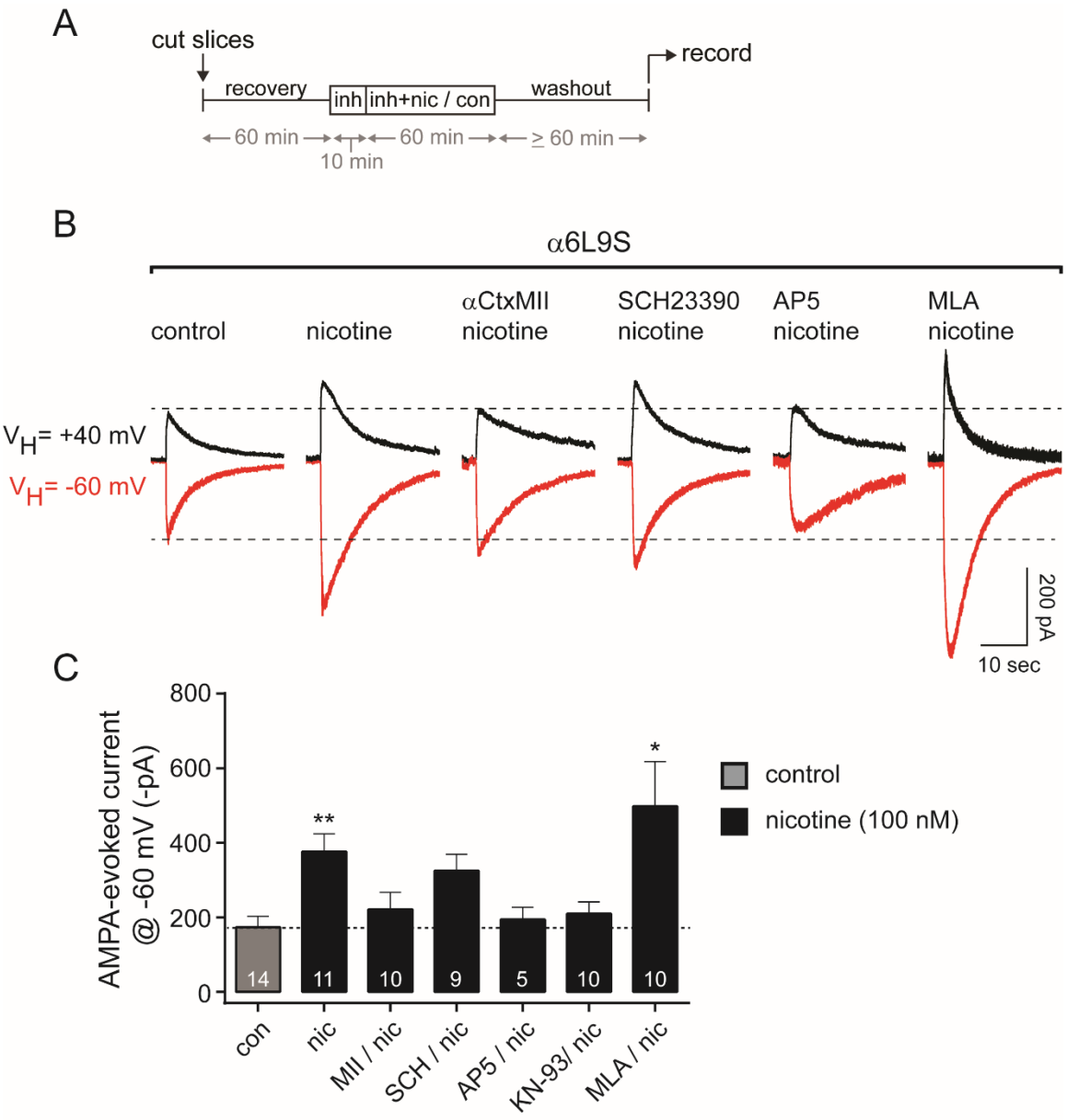

Figure 3.7 Pharmacology of AMPA-evoked current induction in α6L9S VTA DA neurons. **(A)** Slice treatment procedure. α6L9S brain slices were cut and recovered for 60 minutes. Slices were pretreated for 10 minutes with one of the drugs indicated in B, followed by cotreatment with the drug plus nicotine (100 nM) for 60 minutes. Slices were washed out for ≥60 minutes prior to recording. **(B)** Representative AMPA-evoked currents ([AMPA] = 100 μM) at +40 and -60 mV in VTA DA neurons from α6L9S brain slices pre-exposed for 10 minutes to either control recording solution or the following drugs followed by incubation in 100 nM nicotine for 60 minutes: αCtxMII (MII), SCH-23390 (SCH), AP-5, KN-93, and MLA. **(C)** Summary showing mean ± S.E.M. AMPA-evoked currents ([AMPA] = 100 μM) in α6L9S VTA DA neurons in response to the conditions described in (A). **P* < 0.05; ***P* < 0.01 vs control.

3.8 Enhanced AMPA-Evoked Currents in α6L9S VTA DA Neurons Are Mediated by α4 nAChR Subunits

Elimination of α4 nAChR subunits via gene knockout has been shown to significantly reduce α6* nAChR function in synaptosomal DA release experiments (Drenan et al 2010, Salminen et al 2007, Salminen et al 2004), direct assays of striatal nAChR function in brain slices (Drenan et al 2010), and in behavioral experiments (Drenan et al 2010). To test the hypothesis that α4 nAChR subunits are important for α6* nAChR-mediated enhancement of AMPAR function in VTA DA neurons, we crossed α6L9S mice with α4KO animals to eliminate α4 nAChR subunits while still retaining gain-of-function α6 subunits (Drenan et al 2010). Slice treatment in this experiment (Figure 3.8 A) was identical to experiments reported in Figure 3.5. Whereas nicotine (100 nM) treatment of α6L9S slices leads to enhanced AMPAR function, identical treatment of slices from α6L9S mice lacking α4 subunits did not increase AMPA-evoked currents (α6L9S: control = -173.5 ± 29.4 pA, nicotine = -358.4 ± 48.5 pA; α6L9Sα4KO: control = -205.9 ± 23.3 pA, nicotine = -280.3 ± 45.3 pA; Kruskal–Wallis test, $P < 0.05$ for α6L9S control versus nicotine and $P > 0.05$ for α6L9Sα4KO control versus nicotine; Figure 3.8 B and C).

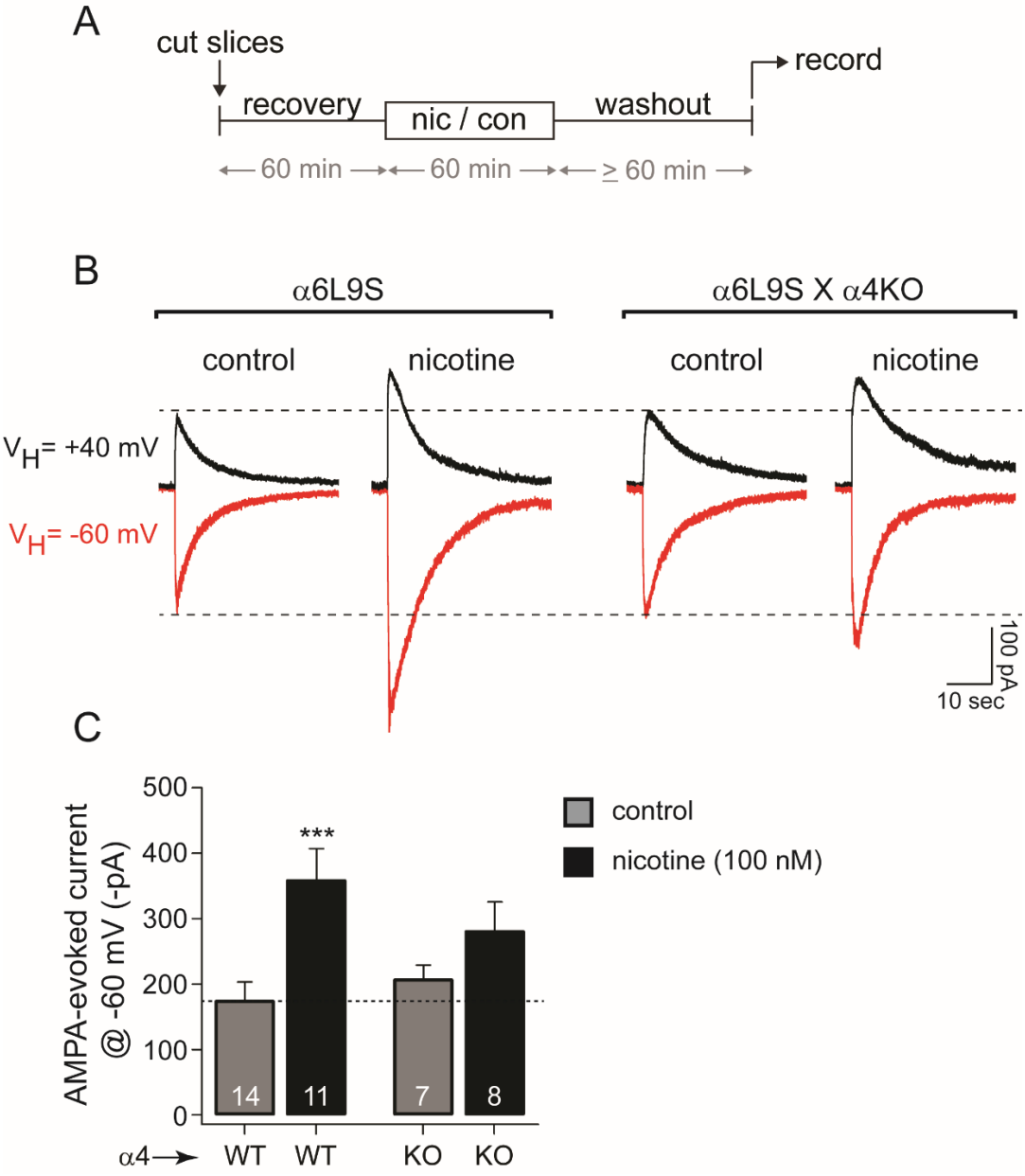

Figure 3.8 Enhanced AMPA-evoked currents in α6L9S VTA DA neurons are mediated, in part, by α4 nAChR subunits. **(A)** Slice treatment procedure. Brain slices from adult α6L9S and α6L9Sα4KO littermate mice were cut, recovered for 60 minutes, and incubated for 60 minutes in control recording solution or recording solution plus nicotine (100 nM). Nicotine was washed out for ≥60 minutes, and whole-cell recordings were established in VTA DA neurons. **(B)** Representative AMPA-evoked currents ([AMPA] = 100 μM) at +40 and -60 mV in VTA DA neurons from α6L9S and α6L9Sα4KO brain slices after incubation in 100 nM nicotine for 60 minutes. **(C)** Summary showing mean ± S.E.M. AMPA-evoked currents ([AMPA] = 100 μM) in α6L9S and α6L9Sα4KO VTA DA neurons in response to the conditions described in A. ***$P < 0.001$ vs control.

3.9 α6* nAChR Function is Reduced in α4KO Mice

To determine whether these results were due to reduced α6 expression and/or function, we performed a series of controls using α4KO animals. First, we crossed α4KO mice with transgenic mice expressing α6 subunits fused with GFP (Figure 3.9 A). This manipulation results in the production of only (non-α4)α6β2* nAChRs (Figure 3.9 B). We used anti-GFP immunohistochemistry and confocal microscopy, as previously described in these mice (Mackey et al 2012), to quantify α6* nAChR expression in VTA neurons in α6GFP mice and α6GFP mice crossed to α4KO mice. We found a small but significant reduction in α6GFP expression in VTA neurons in α6GFP mice lacking α4 subunits compared with α6GFP with intact α4 nAChR subunit expression (α4WT = 17,921 ± 698 arbitrary units, α4KO = 14,507 ± 816 arbitrary units; Mann–Whitney test, *P* = 0.0011; Figure 3.9 C).

Next, we measured α6* nAChR function directly by comparing nicotine- and ACh-evoked currents in α6L9S mice and α6L9S mice lacking α4 subunits (Figure 3.9 D). In contrast to ACh-evoked responses in α6L9S VTA DA neurons with intact α4 subunits, responses from VTA DA neurons in α6L9S slices lacking α4 subunits were smaller (Figure 3.9 E). Inward current amplitudes after puff-application of both 1 and 100 μM ACh were smaller in α6L9Sα4KO neurons relative to α6L9S neurons (α4WT 1 μM ACh = -171 ± 30.3 pA, α4KO 1 μM ACh = -57.8 ± 21.8 pA, and α4KO 100 μM ACh = -77.6 ± 20.2 pA; Figure 3.9 E and F). Similarly, α6L9S VTA DA neurons lacking α4 subunits were less sensitive to nicotine compared with α6L9S cells expressing α4 subunits (Figure 3.9 G). Whereas 1 μM nicotine evoked large inward currents in α6L9S VTA DA neurons that express α4 subunits, 30 μM

nicotine was required to elicit inward currents of the same amplitude in α6L9S slices lacking α4 subunits (α4WT 1 μM nicotine = -198.4 ± 25.8 pA, α4KO 1 μM nicotine = -58.3 ± 11.5 pA, and α4KO 30 μM nicotine = -189.6 ± 45.4 pA; Figure 3.9 G and H). Together, these experiments suggest that activation of α4α6β2* nAChRs are responsible for enhanced AMPA-evoked currents in α6L9S VTA DA neurons.

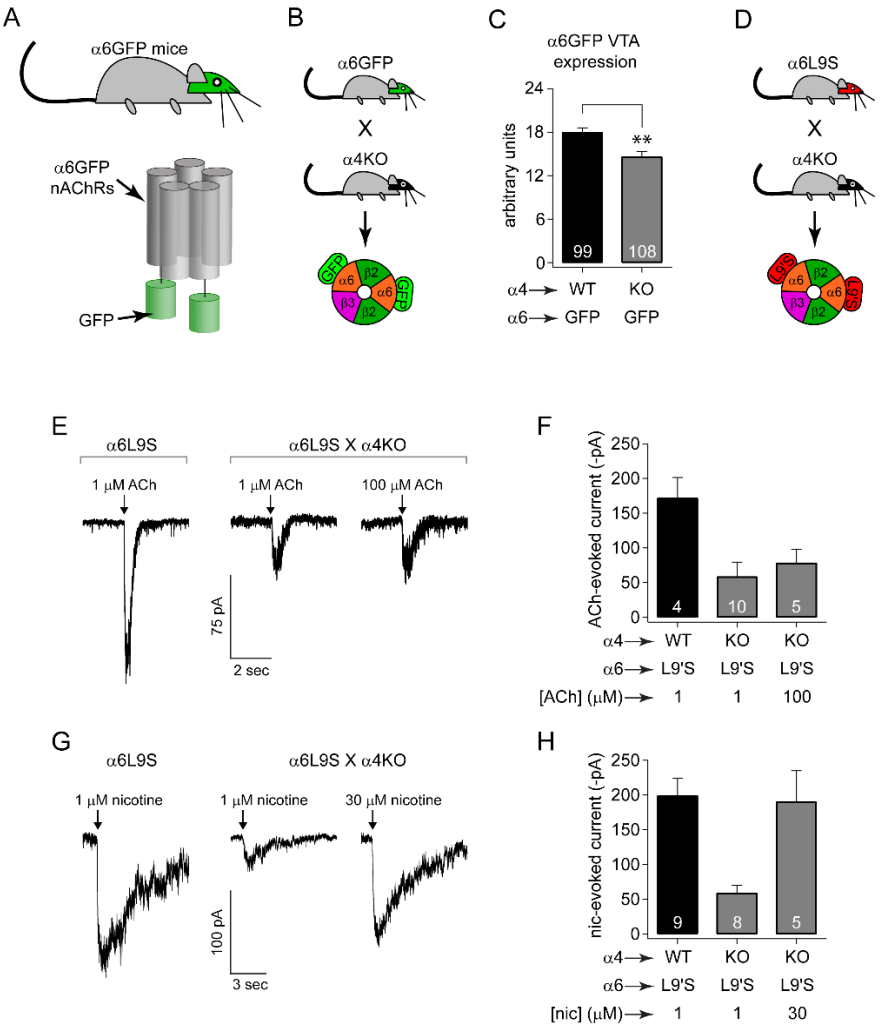

Figure 3.9 α6* nAChR function is reduced in α4KO mice. **(A)** Schematic of α6GFP transgenic mice and α6GFP nAChRs. **(B)** The resulting α6* nAChR that remains after crossing α6GFP mice to α4KO mice is shown. **(C)** α6* nAChRs were quantified in α6GFP and α6GFPα4KO VTA DA neurons using anti-GFP immunohistochemistry and confocal microscopy. Mean per-cell pixel intensity for each genotype is shown. (Done by Hilary Broderick.) **(D)** The resulting α6* nAChR that remains after crossing α6L9S mice to α4KO mice is shown. **(E)** Representative ACh-evoked currents in α6L9S and α6L9Sα4KO VTA DA neurons. VTA DA neurons from both genotypes were patch clamped and ACh was puff-applied (250 milliseconds) at the indicated concentration. **(F)** Summary showing mean ± S.E.M. ACh-evoked current in α6L9S and α6L9Sα4KO VTA DA neurons in response to the indicated concentration of ACh. **(G)** Representative nicotine-evoked currents in α6L9S and α6L9Sα4KO VTA DA neurons. VTA DA neurons in slices from both genotypes were patch clamped and nicotine was puff-applied at the indicated concentration. **(H)** Summary showing mean ± S.E.M. nicotine-evoked current in α6L9S and α6L9Sα4KO VTA DA neurons in response to the indicated concentration of nicotine. $^{**}P < 0.01$.

3.10 NMDA-Evoked Currents Are Not Changed by Nicotine in α6L9S VTA DA Neurons

Next, we tested whether nicotine (100 nM), acting through α6* nAChRs, can increase or decrease NMDA receptor function on the surface of VTA DA neurons (Ungless et al 2001). Whole-cell voltage-clamp recordings were established in VTA DA neurons, and NMDA currents were evoked via puff-application of NMDA at a holding potential of +40 mV. Incubation of α6L9S and non-Tg slices in nicotine (100 nM) for 60 minutes (Figure 3.10 A) did not result in changes in NMDA-evoked currents relative to control treatments (control: non-Tg = 167.8 ± 17.8 pA and α6L9S = 172.8 ± 32.6 pA; nicotine: non-Tg = 185.2 ± 28.5 pA and α6L9S = 167.3 ± 18.7 pA; Kruskal–Wallis test, $P = 0.7893$; Figure 3.10 B and C). These results suggest that although NMDA activation is required for upregulation of AMPAR function on VTA DA neurons (Figure 3.7), activation of nAChRs does not significantly alter NMDA function after 60 minutes of exposure to nicotine.

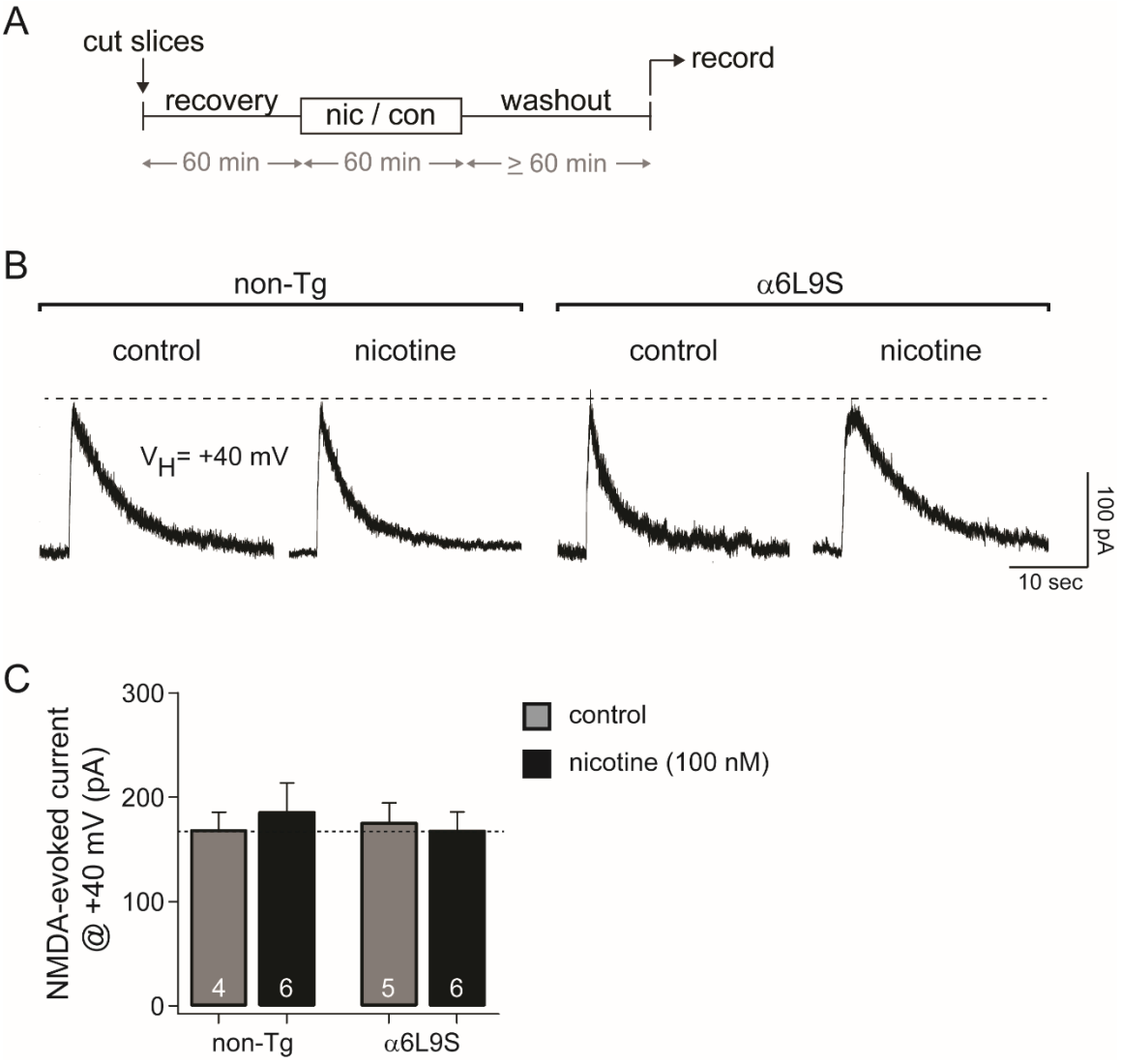

Figure 3.10 NMDA-evoked currents are not changed by nicotine in α6L9S VTA DA neurons. **(A)** Slice treatment procedure. Brain slices from adult α6L9S and non-Tg littermate mice were cut, recovered for 60 minutes, and incubated for 60 minutes in control recording solution or recording solution plus nicotine (100 nM). Nicotine was washed out for ≥60 minutes, and whole-cell recordings were established in VTA DA neurons. **(B)** Representative NMDA-evoked currents ([NMDA] = 100 μM) at +40 mV in VTA DA neurons from α6L9S and non-Tg littermate brain slices in response to control incubation or incubation in 100 nM nicotine for 60 minutes. **(C)** Summary showing mean ± S.E.M. NMDA-evoked currents ([NMDA] = 100 μM) in α6L9S and non-Tg littermate VTA DA neurons in response to the conditions described in A.

3.11 Systemic Nicotine Acts Through α6-Containing nAChRs to Enhance AMPA Receptor Function in VTA DA Neurons

Up to this point we have incubated naïve brain slices in nicotine prior to measuring AMPAR function. We also wanted to determine whether *in vivo* activation of α6* nAChRs is sufficient to support changes in VTA DA neuron synaptic plasticity. We tested the ability of *in vivo* nicotine administration to act selectively through α6* nAChRs to enhance AMPAR function on the surface of these cells. α6L9S and non-Tg control littermate mice were injected (i.p.) with nicotine or vehicle. After 60 min, mice were sacrificed and brain slices were prepared (Figure 3.11 A). Again, AMPAR function was measured using local application of AMPA to the recorded cell. Based on the dose-range found to be sufficient to stimulate locomotor activity in α6L9S mice (0.02 to 0.05 mg/kg)(Berry et al 2015), α6L9S and non-Tg mice were injected with 0.03 mg/kg nicotine or vehicle. This dose was sufficient to enhance AMPA-evoked currents on the surface of VTA DA neurons in α6L9S mice, but was below threshold in non-Tg mice (α6L9S VEH = -214.2 ± 23.1 pA, α6L9S nicotine 0.03 mg/kg = -348.6 ± 42.6 pA, $P = 0.0293$; non-Tg VEH = -203.5 ± 22.2 pA, non-Tg nicotine 0.03 mg/kg = -224.0 ± 36.5, $P = 0.4848$). (Figure 3.11 B and C). A relatively high dose of nicotine (0.17 mg/kg) was needed to increase the amplitude of AMPA-evoked currents on the surface of VTA DA neurons from non-Tg mice (non-Tg nicotine 0.17 mg/kg = -375.7 ± 58.6 pA, $P = 0.019$)(Figure 3.11 B and C). Thus, a single systemic exposure to nicotine can act through α6* nAChRs to enhance glutamatergic transmission in VTA DA neurons.

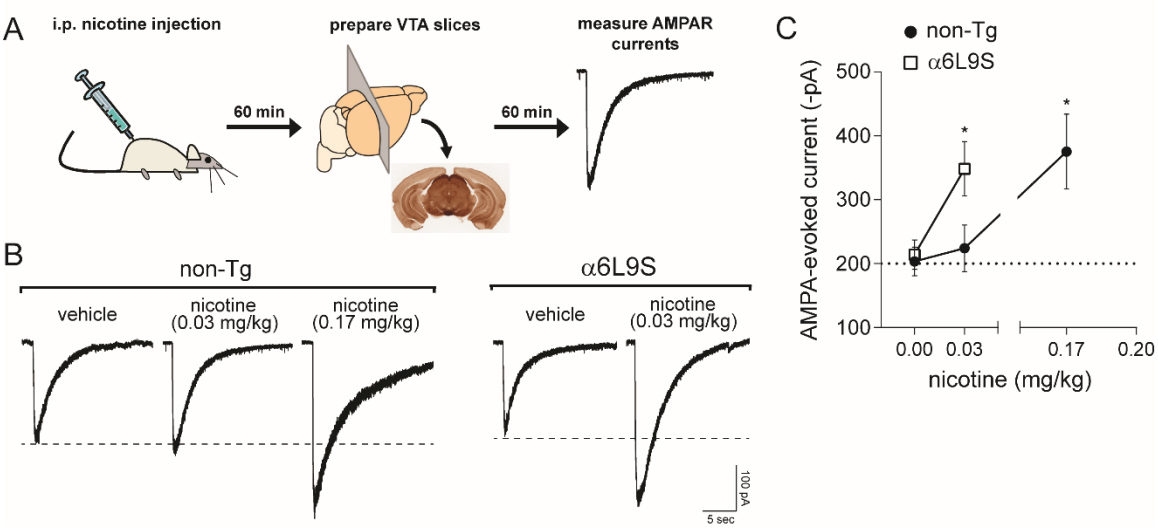

Figure 3.11 Systemic nicotine acts through α6-containing nAChRs to enhance AMPA receptor function in VTA DA neurons. **(A)** Experimental design. α6L9S mice were injected (i.p.) with nicotine at the indicated dose. Sixty minutes after nicotine injection, mice were used to prepare brain slices for patch-clamp recording in VTA DA neurons. AMPAR currents were elicited by locally puffing AMPA onto the cell body of the recorded neuron and recording inward currents in voltage clamp mode. **(B)** A low dose of nicotine (0.03 mg/kg) is sufficient to enhance AMPAR currents in α6L9S VTA DA neurons. Representative AMPA-evoked currents from α6L9S and non-Tg mice injected with the indicated dose of nicotine are shown. **(C)** Quantification of AMPA-evoked current responses in VTA DA neurons from α6L9S and non-Tg mice injected with the indicated dose of nicotine. Mean peak AMPA-evoked currents for each group/treatment are plotted. Mann–Whitney test: $^{*}P < 0.05$ (non-Tg: VEH $n = 4$; nicotine (0.03 mg/kg) $n = 7$; nicotine (0.17 mg/kg) $n = 6$; α6L9S: VEH $n = 6$; nicotine (0.03 mg/kg) $n = 8$).

3.12 Inhibition of α6-containing nAChRs in VTA Blocks AMPAR Enhancement by Systemic Nicotine.

Finally, we tested the hypothesis that systemic, low-dose nicotine administration in α6L9S mice acts through ventral midbrain α6* nAChRs to enhance AMPA-evoked currents. Prior to nicotine (0.03 mg/kg; i.p.) challenge, the VTA of α6L9S mice was infused with αCtxMII (10 pmol) or vehicle (Figure 3.12 A). Brain slices were prepared and AMPA-evoked currents were measured as before. The nicotine-elicited increase in AMPAR function was abolished when αCtxMII was infused into the VTA (α6L9S: VEH/VEH = -246.4 ± 42.1 pA, VEH/nicotine (NIC) = -432.0 ± 40.1 pA, $P = 0.0205$; MII/NIC = -220.0 ± 31.7 pA, $P = 0.0030$)(Figure 3.12 B and C). αCtxMII infusion paired with a vehicle injection did not show any change over baseline (α6L9S: MII/VEH = -204.9 ± 37.2 pA, $P = 0.4738$)(Figure 3.12 B and C). Injection sites in the VTA were verified post-hoc (Figure 3.12 D). These data, along with Figure 3.11, demonstrate that *in vivo* activation of VTA α6* nAChRs is sufficient to drive synaptic plasticity changes in VTA DA neurons that are known to be important for locomotor sensitization and reward behavior.

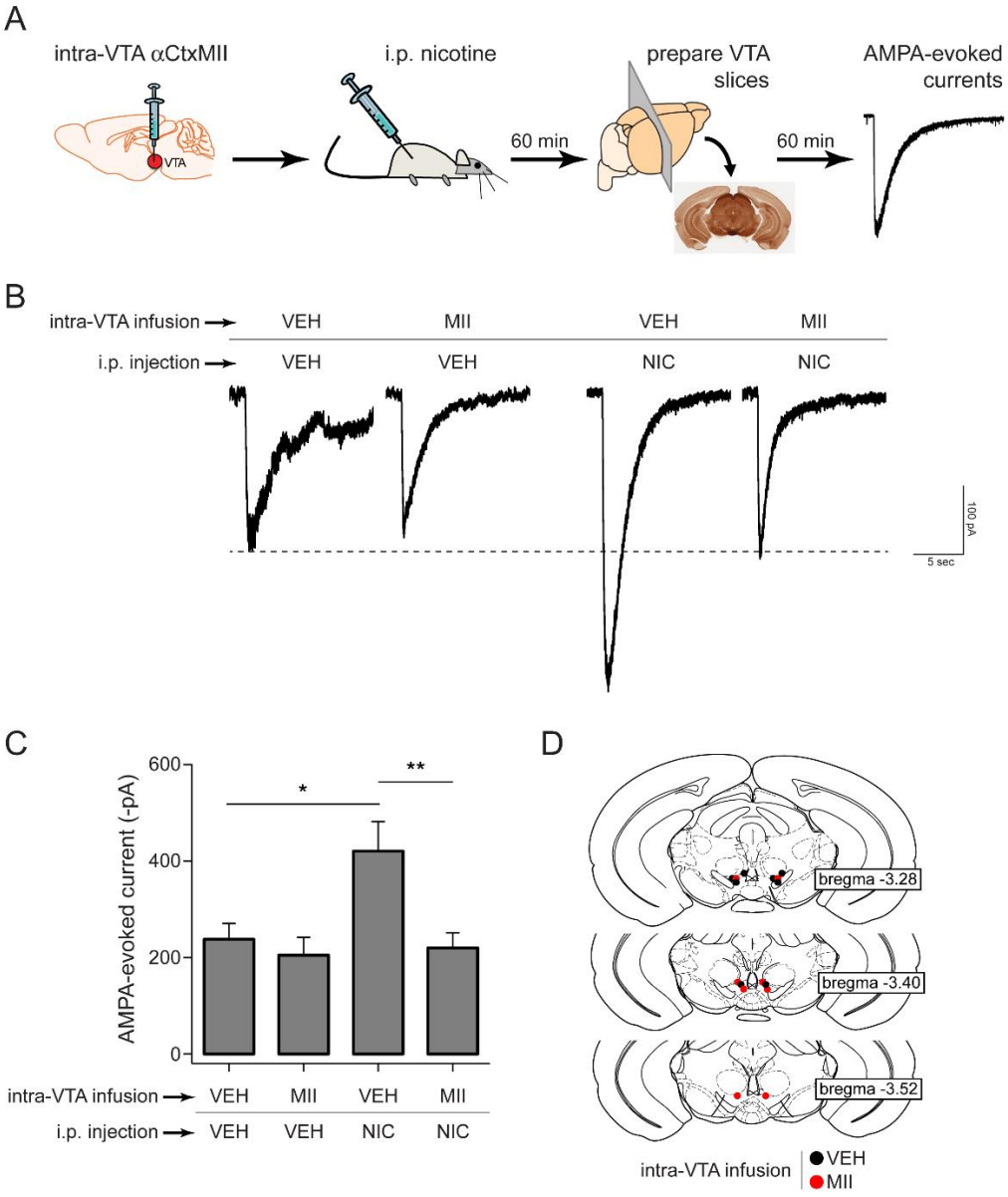

Figure 3.12 Inhibition of α6-containing nAChRs in VTA blocks AMPAR enhancement by systemic nicotine. **(A)** Experimental design. α6L9S mice were cannulated and vehicle or αCtxMII (10 pmol) was infused into the VTA. Following VTA infusion, mice were injected i.p. with saline or nicotine (0.03 mg/kg). Sixty minutes later, brain slices were prepared for recording. AMPA-evoked currents were elicited by locally puffing AMPA onto the cell body of the recorded neuron and recording inward cation currents in voltage clamp mode. **(B)** Representative AMPA-evoked currents from α6L9S mice injected/infused with the indicated drugs are shown. **(C)** Mean peak AMPA-evoked currents for each group shown in (B) are plotted. Mann–Whitney: $^{*}P < 0.05$, $^{**}P < 0.01$. (VEH/VEH: $n = 7$, MII/VEH: $n = 7$, VEH/NIC: $n = 8$, MII/NIC: $n = 8$). **(D)** Cannula location for each mouse in groups indicated in (B) is shown. (Cannulations and infusions done by Dr. Jennifer Berry.)

CHAPTER 4. NICOTINE AND ETHANOL COOPERATE TO ENHANCE VTA AMPA RECEPTOR FUNCTION VIA α6-CONTAINING NICOTINIC RECEPTORS

Portions of this chapter (pgs 70-83) are reprinted from: *Neuropharmacology* 2015 Apr; 91:13-22, doi:10.1016/j.neuropharm.2014.11.014 with permission from Elsevier.

4.1 α6* nAChRs Are Involved in Ethanol-Mediated Increases in AMPAR Function in VTA DA Neurons

α6* nAChRs are crucial for the rewarding properties of ethanol in rodents (Larsson et al 2004, Lof et al 2007, Powers et al 2013). Systemic ethanol exposure is known to enhance AMPAR function on VTA DA neurons (Saal et al 2003, Stuber et al 2008), but α6* nAChR involvement in this process has not yet been studied. We began by testing the hypothesis that exposing slices to drinking-relevant concentrations of ethanol can increase AMPAR function on VTA DA neurons. VTA-containing brain slices were prepared from adult, drug-naïve mice, and slices were allowed to recover for 60 minutes. Slices were then incubated in ethanol or a control recording solution without ethanol for 60 minutes. After a washout period of ≥60 minutes (Figure 4.1 A), stable whole-cell recordings were established in VTA DA neurons. A second, AMPA-filled, micropipette was programmed to move adjacent to the recorded cell, pressure-eject (puff) AMPA (100 μM), and be retracted (as in Figure

3.4). The amplitude of AMPA-evoked currents at a holding potential of −60 mV was measured to assess AMPAR function.

We found that incubating slices from non-Tg mice in ethanol (20 mM) for 60 minutes significantly increased AMPAR function in VTA DA neurons over baseline responses from control slices not exposed to ethanol (control = −187.3 ± 16 pA, 20 mM ethanol = −319.6 ± 43 pA; ANOVA, $P = 0.0034$; *post hoc* test, $P < 0.01$) (Figure 4.1 B, D and E). To examine the role of α6* nAChRs, slices were pre-treated with αCtxMII (100 nM) for 10 minutes prior to ethanol incubation. Pretreatment with αCtxMII blocked ethanol-evoked increases in AMPAR function in VTA DA neurons (αCtxMII = −216.7 ± 44 pA) (Figure 4.1 B and E), suggesting an important role for ongoing α6* nAChR activity in this process. αCtxMII by itself had no effect on AMPA-evoked currents (−182.6 ± 29 pA) (Figure 4.1 E). In a similar fashion, slices were pre-treated in TTX for 10 minutes prior to ethanol incubation to examine whether action potential firing during ethanol exposure is required to evoke an increase in AMPAR function. We found that TTX does not block ethanol-evoked increases in AMPAR function in VTA DA neurons (TTX = −342.3 ± 44 pA; $P < 0.05$) (Figure 4.1 B and E). To corroborate data suggesting that α6* nAChRs play a role in ethanol-mediated enhancement of AMPAR function, we studied changes in AMPAR function in slices from α6L9S mice. Because these mice have enhanced α6* nAChR activity (Drenan et al 2008a), we hypothesized that a lower concentration of ethanol would be able to evoke increases in AMPAR function compared to non-Tg mice if α6* nAChRs are playing a role in this process. Baseline AMPAR function is not altered in α6L9S mice. 5 mM ethanol was insufficient to alter AMPAR function in non-Tg slices (−171.0 ± 24 pA), but

robustly enhanced AMPAR function in α6L9S slices (control = −180.1 ± 22 pA, 5 mM ethanol = −416.1 ± 49 pA; ANOVA, $P < 0.0001$; *post hoc* test, $P < 0.0001$) (Figure 4.1 C, D and F). This enhanced response was also blocked by pretreatment with αCtxMII (−223.0 ± 26 pA) (Figure 4.1 C and F), whereas αCtxMII alone had no effect (−192.3 ± 10 pA) (Figure 4.1 F). As in non-Tg mice, TTX blockade of action potential firing had no effect on ethanol's ability to enhance AMPAR function in α6L9S mice (TTX = −365.9 ± 56 pA; $P < 0.01$) (Figure 4.1 C and F).

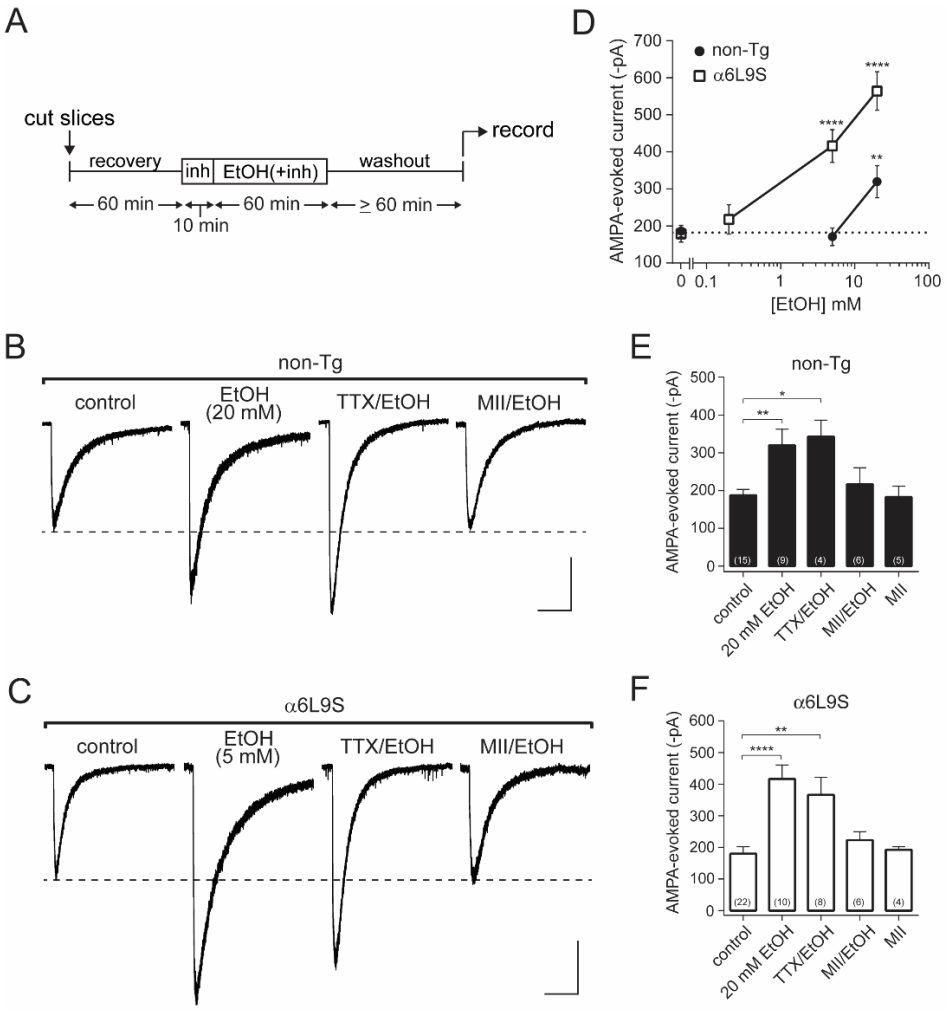

Figure 4.1 α6* nAChRs are involved in ethanol-mediated increases in AMPAR function in VTA DA neurons. **(A)** Schematic illustrating ethanol (EtOH) exposure after cutting brain slices containing the VTA. After a 60 minute recovery period, brain slices were incubated in a control holding solution or an ethanol-containing holding solution for 60 minutes. Slices were transferred out of ethanol for a ≥60 minute washout period before initiating whole-cell recordings from VTA DA neurons. An additional group of brain slices were incubated in an inhibitor (inh), either 100 nM αCtxMII or 0.5 µM TTX, for 10 minutes before starting the 60 minute ethanol incubation. **(B and C)** Representative AMPA-evoked current traces from VTA DA neurons in (B) non-Tg and (C) α6L9S brain slices incubated in control recording solution or ethanol. AMPA (100 µM) was puff-applied while holding VTA DA neurons at −60 mV. Scale 100 pA, 5 sec. **(D)** Summary of AMPA-evoked responses (mean ± SEM) from VTA DA neurons at a holding potential of −60 mV in α6L9S mice and their non-Tg littermates. Dotted line indicates average amplitude of baseline AMPA-evoked responses. **(E and F)** Summary of AMPA-evoked current amplitudes (mean ± SEM) in VTA DA neurons in (E) non-Tg and (F) α6L9S brain slices. **P* < 0.05; ***P* < 0.01; *****P* < 0.0001 (one-way ANOVA, Dunnett post-hoc test comparing drug concentration to no-drug control).

4.2 α6* nAChRs Mediate Enhanced AMPAR Function After *in vivo* Ethanol Administration

Enhanced α6* nAChR activity lowered the concentration of ethanol that is sufficient to enhance AMPAR function using a slice incubation procedure (Figure 4.1 C, D and F). To determine whether the same trend occurred after *in vivo* exposure to ethanol, mice were administered i.p. injections of ethanol. 60 min after this injection, mice were sacrificed and VTA brain slices were prepared. To minimize the possible effect of handling-induced stress, mice were handled once a day for three days, given a mock injection, and given a saline injection on the day immediately prior to the experiment (Figure 4.2 A). As in the previous experiment, AMPA was puff-applied onto a VTA DA neuron while recording inward currents evoked at a holding potential of −60 mV. Relative to a vehicle (saline) injection, ethanol (2.0 g/kg) significantly increased AMPAR function in VTA DA neurons in non-Tg slices (vehicle: −206.5 ± 24 pA, 2.0 g/kg ethanol: −365.2 ± 34 pA; ANOVA, $P = 0.0004$, *post hoc* test, $P < 0.001$) (Figure 4.2 B and D). A dose of 0.5 g/kg ethanol was insufficient to enhance AMPAR function in VTA DA neurons in non-Tg mice (−221.4 ± 17 pA) but did enhance AMPAR function in α6L9S mice (vehicle: −197.5 ± 23 pA, 0.5 g/kg ethanol: −395.1 ± 46 pA; unpaired *t* test, $P = 0.0072$) (Figure 4.2 B–D). Together, these slice incubation and *in vivo* exposure experiments strongly indicate a role for α6* nAChRs in ethanol-mediated enhancement of AMPAR function in VTA.

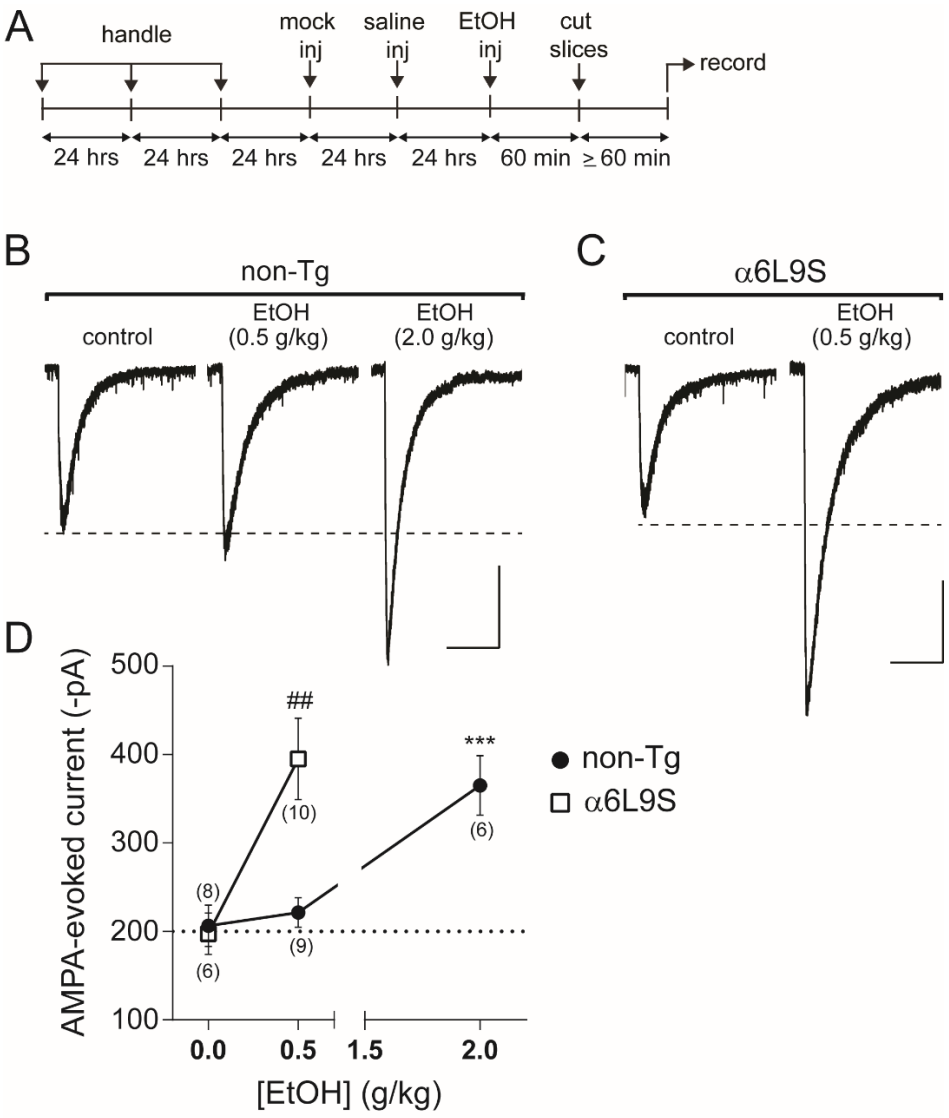

Figure 4.2 α6* nAChRs mediate enhanced AMPAR function after *in vivo* ethanol administration. **(A)** Schematic of experimental procedure. Prior to ethanol injection, mice were habituated to handling by being handled once a day for three days, given a mock injection, and given a saline injection. Mice were given an ethanol or control saline injection 60 minutes prior to cutting brain slices containing the VTA. **(B and C)** Representative AMPA-evoked current traces from VTA DA neurons in (B) non-Tg and (C) α6L9S brain slices cut 60 minutes after a mouse was given a control injection or an ethanol (0.5 g/kg or 2.0 g/kg) injection. AMPA (100 μM) was puff-applied while holding VTA DA neurons at −60 mV. Scale: 100 pA, 5 sec. **(D)** Summary of AMPA-evoked current responses from VTA DA neurons at a holding potential of −60 mV in brain slices from non-Tg and α6L9S mice. The mean ± SEM is plotted while the dotted line indicates amplitude of baseline AMPA-evoked responses. ***$P < 0.001$ (one-way ANOVA, Dunnett post-hoc test comparing drug concentration to no-drug control); $^{\#\#}P < 0.01$ (student's *t*-test comparing control from 0.5 g/kg in α6L9S mice).

4.3 AMPAR Function is Enhanced by Nicotine Exposure in non-Tg and α6L9S Mice

Exposure of naïve brain slices to nicotine also enhances AMPAR function in VTA DA neurons (Jin et al 2011, Mao et al 2011). Although we demonstrated a role for α6* nAChRs in this process (Figure 3.5), we did not identify the nicotine concentration range over which this effect takes place. To examine the action of a combined incubation with nicotine and ethanol (Figure 4.5 and Figure 4.6), we first identified nicotine concentrations that were sufficient and insufficient to enhance AMPA-evoked currents on VTA DA neurons. Brain slices cut from drug-naïve mice were incubated in nicotine for 60 minutes and after a ≥60 minute wash-out period, AMPAR function was measured (Figure 4.3 A). In non-Tg brain slices, 100 nM nicotine was insufficient to increase AMPAR function, but 500 nM nicotine was sufficient (control = −187.3 ± 16 pA, 100 nM nicotine = −166.0 ± 14, 500 nM nicotine = −283.4 ± 36 pA; ANOVA, $P = 0.0288$; *post hoc* test, $P < 0.05$) (Figure 4.3 B). In α6L9S brain slices, nicotine concentrations as low as 10 nM are sufficient to increase AMPAR function (control = −180.1 ± 22 pA, 10 nM nicotine = −320.1 ± 41 pA; ANOVA, $P = 0.0012$; *post hoc* test, $P < 0.05$) (Figure 4.3 B). The highest concentration of nicotine tested that was insufficient to enhance AMPAR function in α6L9S slices is 3 nM (−234.2 ± 36 pA) (Figure 4.3 B).

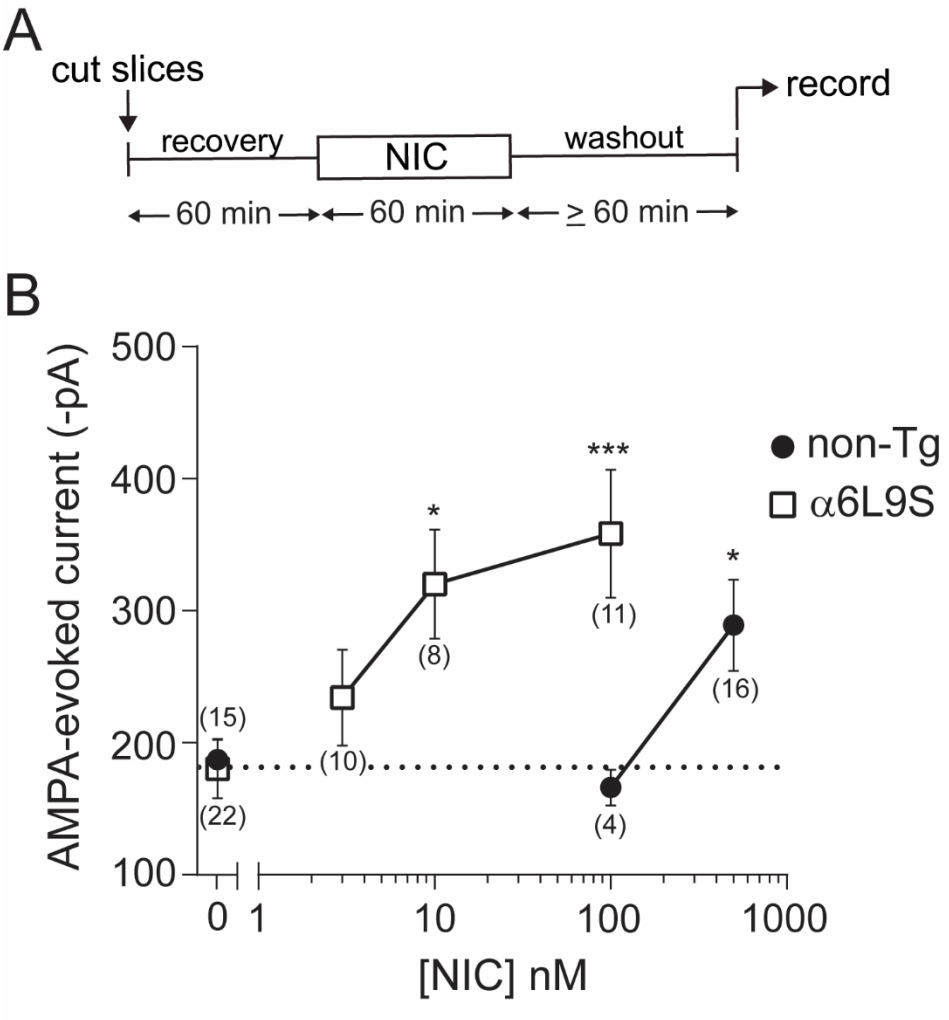

Figure 4.3 AMPAR function is enhanced by nicotine exposure in non-Tg and α6L9S mice. **(A)** Schematic illustrating slice treatment procedure. Brain slices containing the VTA were prepared from non-Tg and α6L9S mice and, after a 60 minute recovery period, incubated in control holding solution or nicotine-containing holding solution for 60 minutes. Whole-cell patch clamp recordings were established in VTA DA neurons ≥60 minutes after slices were removed from nicotine. **(B)** Summary of AMPA-evoked current responses from VTA DA neurons at a holding potential of −60 mV in non-Tg and α6L9S brain slices incubated in nicotine. The mean ± SEM is plotted while the dotted line represents average amplitude of baseline AMPA-evoked responses. **P* < 0.05; ****P* < 0.001 (one-way ANOVA, Dunnett post-hoc test comparing drug concentration to no-drug control).

4.4 Nicotine and Ethanol Exposure Enhance Excitatory Synaptic Transmission in non-Tg and α6L9S Slices

Our AMPA-evoked current approach measures AMPAR function from the total pool of surface-expressed AMPARs, including synaptic and nonsynaptic receptors. Because AMPARs are preferentially localized to synapses, we measured ethanol- and nicotine-elicited changes in AMPA/NMDA ratios in VTA DA neurons using the same conditions we used for AMPA-evoked currents (Figure 4.4 A). AMPA to NMDA ratios were measured as described by McGehee and colleagues (Mao et al 2011). As with AMPA-evoked currents, AMPA/NMDA ratios were significantly enhanced in non-Tg slices following exposure to either 20 mM ethanol or 500 nM nicotine (control = 2.47 ± 0.2, 20 mM ethanol = 3.90 ± 0.1, 500 nM nicotine = 3.41 ± 0.4 pA; ANOVA, $P = 0.0007$) (Figure 4.4 C). Lower concentrations of ethanol (5 mM) or nicotine (100 nM) did not increase AMPA/NMDA ratios (Figure 4.4 C), just as they did not increase AMPA-evoked current responses (Figure 4.1 and Figure 4.3 B). Next, we measured AMPA/NMDA ratios in VTA DA neurons from α6L9S slices incubated with either 5 mM ethanol or 100 nM nicotine – concentrations sufficient to enhance AMPA-evoked currents in these slices. Incubating α6L9S slices for 60 minutes in either 5 mM ethanol or 100 nM nicotine was indeed sufficient to increase AMPA/NMDA ratios (control = 2.30 ± 0.2, 5 mM ethanol = 4.13 ± 0.3, 100 nM nicotine = 3.35 ± 0.2; ANOVA, $P = 0.0013$) (Figure 4.4 D). These results, together with our AMPA-evoked current data, suggest that α6* nAChR activity plays an important role mediating enhanced synaptic plasticity following nicotine and ethanol exposure.

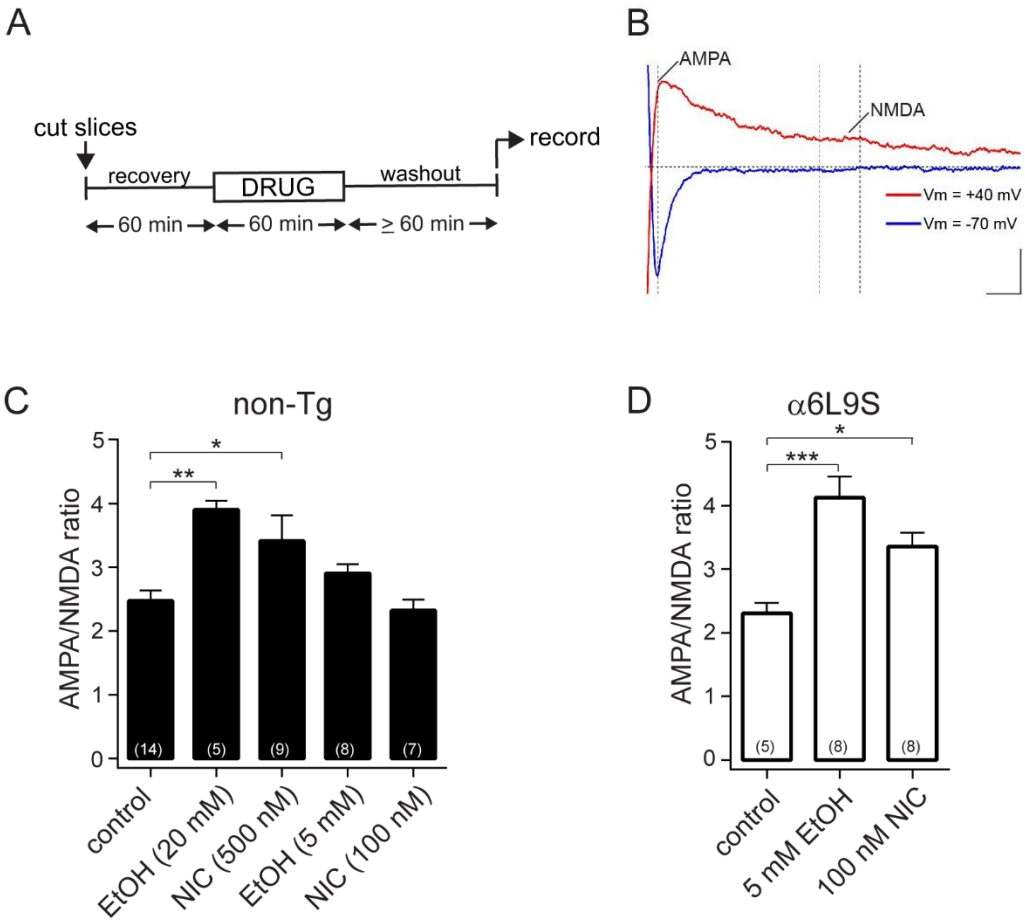

Figure 4.4 Nicotine and ethanol exposure enhance excitatory synaptic transmission in non-Tg and α6L9S slices. **(A)** Schematic illustrating drug (nicotine or ethanol) exposure after cutting brain slices containing the VTA. After a 60 minute recovery period, brain slices were incubated in a control holding solution or a solution containing nicotine or ethanol (concentrations indicated in (C) and (D)) for 60 minutes. Slices were transferred out of ethanol for a ≥60 minute washout period before initiating whole-cell recordings from VTA DA neurons. **(B)** Exemplary synaptic current evoked in a VTA DA neuron, showing AMPAR- and NMDAR-mediated components. AMPA EPSCs were measured at a command voltage of +40 mV (red trace) at the time corresponding to the peak of the AMPA EPSC elicited at a command voltage of −70 mV (blue trace). NMDA EPSCs were measured at +40 mV by averaging the membrane current during a 10 msec window 40 msec after the AMPA EPSC peak (the latter had decayed to baseline by this time, resulting in a current due completely to NMDARs). Scale: 40 pA, 10 msec. **(C and D)** AMPA/NMDA ratios (mean ± SEM) in non-Tg (C) and α6L9S (D) VTA DA neurons after exposure of slices to a control solution or to a solution containing the indicated drug. **P* < 0.05; ***P* < 0.01; ****P* < 0.001 (one-way ANOVA, Dunnett post-hoc test).

4.5 Subthreshold Nicotine and Subthreshold Ethanol Combine to Enhance VTA AMPAR Function in non-Tg Slices

Because both nicotine (Figure 4.3) and ethanol (Figure 4.1) act through α6* nAChRs to enhance AMPAR function in VTA DA neurons, we hypothesized that α6* nAChRs may also play a role in the combined action of nicotine + ethanol. To test this hypothesis, we incubated brain slices in control recording solution containing both nicotine and ethanol for 60 minutes and recorded AMPA-evoked currents after a 60 minute washout period (Figure 4.5 A). Whereas 100 nM nicotine or 5 mM ethanol were insufficient to increase AMPAR function in non-Tg VTA DA neurons when incubated alone, simultaneous co-exposure to these concentrations enhanced AMPAR function (100 nM nicotine = −166.0 ± 14 pA, 5 mM ethanol = −171.0 ± 24 pA, 100 nM nicotine + 5 mM ethanol = −374.3 ± 69 pA; ANOVA, $P = 0.0080$) (Figure 4.5 B and C). To determine whether α6* nAChRs play a role in this response, slices were pre-incubated in αCtxMII (100 nM) for 10 minutes before adding nicotine and ethanol. αCtxMII blocked the combined action of nicotine + ethanol (−254.8 ± 39 pA) (Figure 4.5 B and C). Varenicline, a partial agonist at α4β2* and α6β2* nAChRs (Grady et al 2010), is currently used as a smoking cessation drug. To determine whether varenicline interferes with the combined action of nicotine + ethanol, slices were pre-incubated in varenicline for 10 minutes followed by continuous co-incubation of slices in varenicline (1 μM), nicotine (100 nM), and ethanol (5 mM). Like αCtxMII, varenicline blocked increases in AMPAR function mediated by nicotine + ethanol co-exposure (−227.8 ± 41 pA) (Figure 5.5 B and C). Varenicline by itself had no effect on AMPAR function in non-Tg cells (−204.3 ± 25 pA) (Figure 5.5 C).

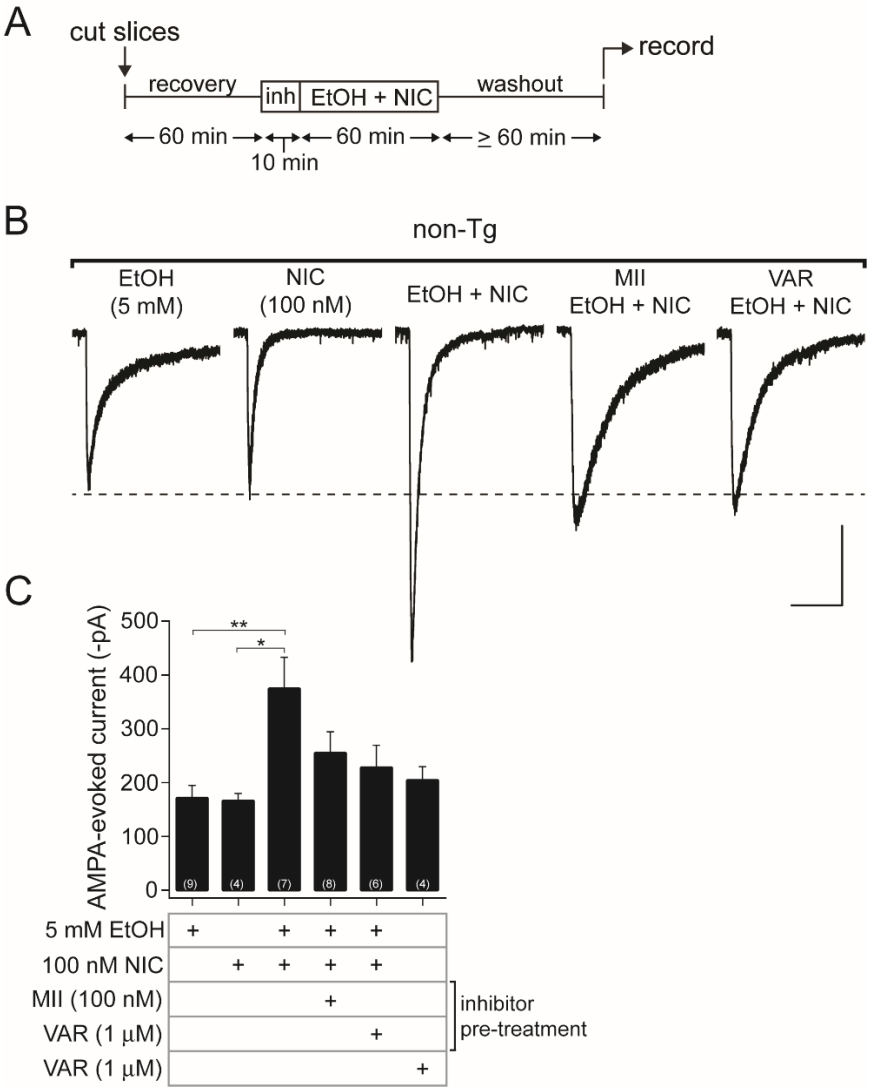

Figure 4.5 Subthreshold nicotine and subthreshold ethanol, when combined, enhance VTA AMPAR function in non-Tg slices. **(A)** Schematic of slice treatment procedure. 60 minutes after preparing brain slices containing the VTA from non-Tg mice, slices were incubated in holding solution containing both nicotine (100 nM) and ethanol (5 mM) for 60 minutes. AMPA-evoked currents were elicited and recorded after a ≥60 minute wash-out period. In some experiments, slices were pre-incubated in either αCtxMII (100 nM) or varenicline (VAR; 1 µM) for 10 minutes before adding nicotine + ethanol for 60 min. Varenicline (1 µM, 70 minutes) alone was also tested, as shown in (C). **(B)** Representative AMPA-evoked currents from non-Tg VTA DA neurons. Slices were treated for 60 minutes with nicotine/ethanol in one of the following ways: 1) 5 mM EtOH only, 2) 100 nM nicotine only, 3) 5 mM EtOH plus 100 nM nicotine. AMPA (100 µM) was puff-applied while holding VTA DA neurons at −60 mV. Scale: 100 pA, 5 sec. **(C)** Summary of AMPA-evoked current amplitudes (mean ± SEM) in VTA DA neurons in non-Tg brain slices. **P* < 0.05; ***P* < 0.01; (one-way ANOVA, Dunnett post-hoc test comparing the 5 mM EtOH group or the 100 nM nicotine group to the EtOH plus nicotine group).

4.6 Subthreshold Nicotine and Subthreshold Ethanol Combine to Enhance VTA AMPAR Function in α6L9S Slices

To further test the idea that α6* nAChRs play a role in AMPAR enhancement following nicotine + ethanol co-exposure, we performed an analogous set of experiments with α6L9S VTA slices (Figure 4.6 A). We previously determined that 3 nM nicotine (Figure 4.3 B) and 200 µM ethanol (Figure 4.1 D) were each insufficient to enhance AMPAR function in α6L9S slices when administered alone. However, when co-administered to α6L9S slices, 3 nM nicotine and 200 µM ethanol enhanced AMPAR function (200 µM ethanol = −217.8 ± 49 pA, 3 nM nicotine = −234.2 ± 36 pA, 200 µM ethanol + 3 nM nicotine = −442.1 ± 72 pA; ANOVA, $P = 0.0065$) (Figure 4.6 B and C). As with non-Tg slices, pre-treatment with either αCtxMII or varenicline blocked the enhancement in AMPAR function seen following nicotine + ethanol co-exposure (MII: −248.0 ± 25 pA, varenicline: −252.0 ± 35 pA) (Figure 4.6 B and C). As in non-Tg slices, varenicline alone did not alter AMPAR function in α6L9S slices (−246.5 ± 28 pA) (Figure 4.6 C).

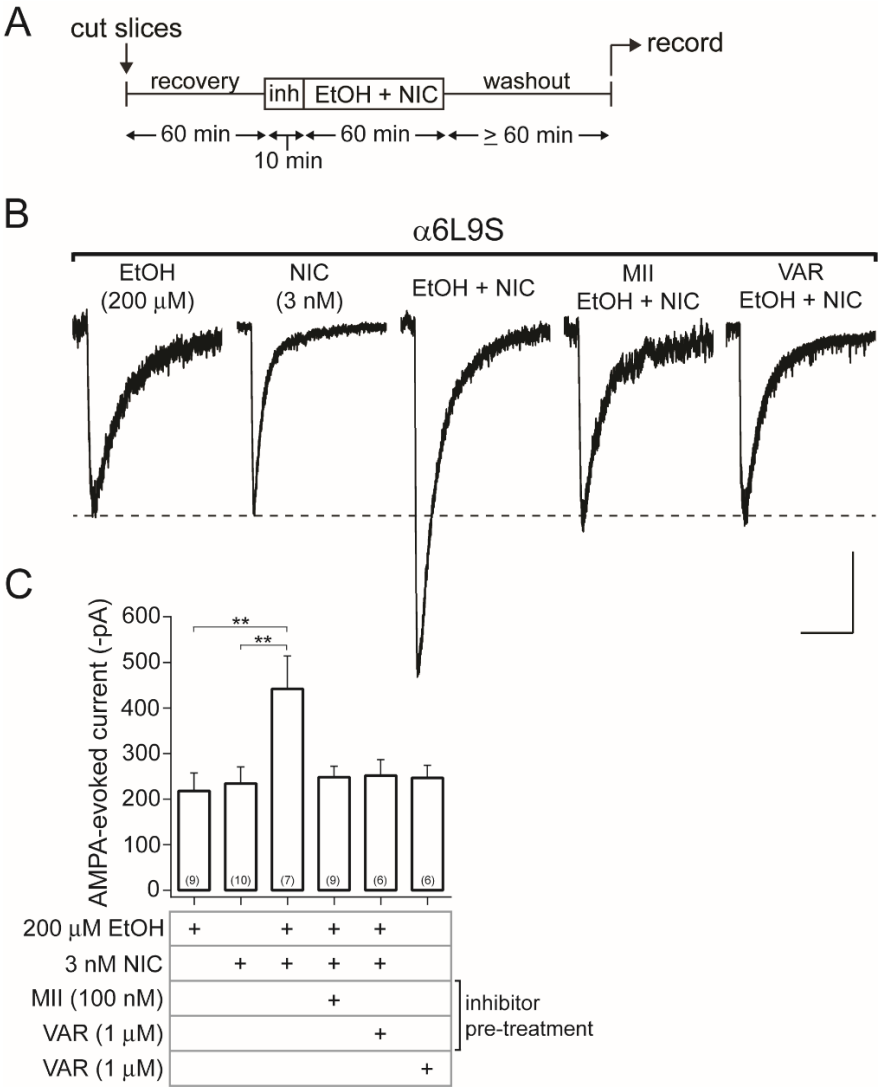

Figure 4.6 Subthreshold nicotine and subthreshold ethanol, when combined, enhance VTA AMPAR function in α6L9S slices. **(A)** Schematic of slice treatment procedure. 60 minutes after preparing brain slices containing the VTA from α6L9S mice, slices were incubated in holding solution containing both nicotine (3 nM) and ethanol (200 μM) for 60 minutes. AMPA-evoked currents were elicited and recorded after a ≥60 minute wash-out period. In some experiments, slices were pre-incubated in either αCtxMII (100 nM) or varenicline (1 μM) for 10 minutes before adding nicotine + ethanol for 60 minutes. Varenicline (1 μM, 70 minutes) alone was also tested, as shown in (C). **(B)** Representative AMPA-evoked currents from α6L9S VTA DA neurons. Slices were treated for 60 minutes with nicotine/ethanol in one of the following ways: 1) 200 μM EtOH only, 2) 3 nM nicotine only, 3) 200 μM EtOH plus 3 nM nicotine. AMPA (100 μM) was puff-applied while holding VTA DA neurons at −60 mV. Scale: 100 pA, 5 sec. **(C)** Summary of AMPA-evoked current amplitudes (mean ± SEM) in VTA DA neurons in α6L9S brain slices. $^{**}P < 0.01$; (one-way ANOVA, Dunnett post-hoc test comparing the 200 μM EtOH group or the 3 nM nicotine group to the EtOH plus nicotine group).

CHAPTER 5. REMOVAL OF α4-CONTAINING nAChRs FROM THE VENTRAL MIDBRAIN ALTERS CIRCUITRY WITHIN THE VTA

5.1 *Chrna*4 vMB cKO Mouse Model

Removal of α4* nAChRs from the VTA leaves (non-α4)α6β2* nAChRs as the primary high sensitivity nAChR subtype (Salminen et al 2007). Therefore, to study the role α6* nAChRs and α4* nAChRs in an additional model to the α6L9S transgenic mouse model, we utilized a ventral midbrain α4 conditional KO mouse model (*Chrna*4 vMB cKO mice). Using mice that have the α4 nAChR subunit gene flanked by loxP sites (*Chrna*4 loxP/loxP mice), we removed α4 nAChR subunits from specific brain regions of adult mice by injecting viral vectors that drive the expression of Cre recombinase (AAV-Cre-GFP). Cre recombinase is an enzyme that catalyzes the deletion of floxed genes (Kaspar et al 2002, McGranahan et al 2011) (Figure 5.1 A). Within the VTA, WT mice express heteromeric nAChRs that can contain α4 nAChR subunits, α6 nAChR subunits, and/or both subunits [(non-α6)α4β2*, (non-α4)α6β2*, and/or α4α6β2* nAChRs, respectively]. In *Chrna*4 loxP/loxP mice, after an injection of AAV-Cre-GFP, only (non-α4)α6β2* nAChRs remain (Figure 5.1 B). The viral vectors used to drive the expression of Cre also drive the expression of GFP so we can visually identify infected cells by fluorescence. For controls, *Chrna*4 loxP/loxP mice were injected with AAV-GFP, a virus driving the expression of GFP but not Cre. We used

immunohistochemistry and confocal microscopy to verify that there is virus expression in the VTA after Cre injections. VTA containing-slices were co-stained with anti-GFP to label the virus and anti-TH to identify DA neurons. We found that the virus was expressed throughout the VTA. We saw that both TH(+) neurons (indicated by one arrow) and TH(-) neurons (indicated by two arrows) express the virus (Figure 5.1 C). TH(-) neurons are presumably GABAergic, as 35% of neurons within the VTA are GABAergic (Nair-Roberts et al 2008).

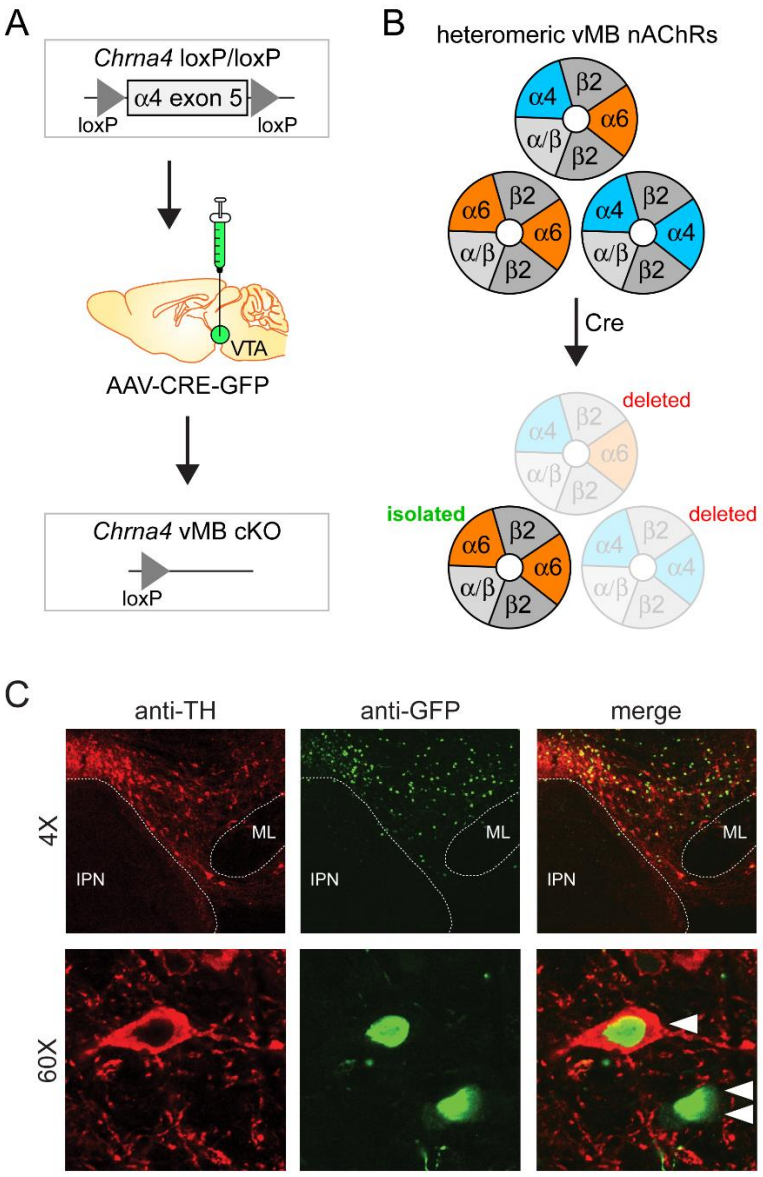

Figure 5.1 *Chrna*4 vMB cKO mice. **(A)** Schematic of the α4 nAChR subunit gene before and after intra-VTA AAV-CRE-GFP injections. *Chrna*4 loxP/loxP mice contain loxP sites flanking exon 5 of the gene encoding the α4 nAChR subunit. To remove α4 nAChR subunits, adult mice were given intra-VTA injections of AAV-CRE-GFP. The resulting *Chrna*4 vMB cKO mice have exon 5 deleted from infected cells and therefore disrupted expression of α4* nAChRs. **(B)** Heteromeric nAChRs expressed in the vMB normally include (non-α6)α4*nAChRs, (non-α4)α6* nAChRs, and α4α6* nAChRs. Following intra-VTA Cre injections, both (non-α6)α4* and α4α6* nAChRs are deleted leaving only (non-α4)α6* nAChRs remaining in the VTA. **(C)** Immunohistochemistry and confocal microscopy images of the VTA in a *Chrna*4 vMB cKO brain slice (green: anti-GFP, red: anti-TH). 60X images showing both a TH(+) and a TH(-) neuron infected by the virus (indicated by one or two white arrows, respectively).

5.2 nAChR Function in *Chrna*4 vMB cKO Mice

To functionally verify the removal of α4 nAChR subunits in *Chrna*4 vMB cKO mice, we measured ACh-evoked currents in VTA DA neurons. VTA DA neurons were held at -60 mV and the response to puff application of ACh was recorded (Figure 5.2 A, top). Cells infected with Cre virus (labeled Cre (+) from here on) were identified by the presence of GFP (Figure 5.2 A, bottom). ACh-evoked currents were significantly decreased in Cre (+) VTA DA neurons in *Chrna*4 vMB cKO brain slices compared to Cre (-) VTA DA neurons in *Chrna*4 loxP/loxP brain slices (Cre (-) = -84.26 ± 5.2 pA, Cre (+) = -28.50 ± 4.1 pA, $P < 0.0001$)(Figure 5.2 B and C). This reduced sensitivity to ACh demonstrates that injecting Cre into the VTA of *Chrna*4 loxP/loxP mice prevents expression of α4* nAChRs. However, while ACh-evoked currents were attenuated in Cre(+) neurons, they were not eliminated. To test the hypothesis that the residual current is mediated by (non-α4)α6* nAChRs, we measured ACh-evoked currents from Cre(+) VTA DA neurons before and after bath application of αCtxMII. A significant proportion of the remaining current was αCtxMII-sensitive (average Cre(+) current in a subpopulation of cells before αCtxMII application = -33.00 ± 4.2 pA, average Cre(+) current after αCtxMII = -12.00 ± 2.3 pA, $P = 0.0286$)(Figure 5.2 D). nAChR removal was also measured in *Chrna*4 loxP/loxP mice crossed with hypersensitive α6L9S mice. A low concentration of 1μM ACh selectively activates hypersensitive α6* nAChRs. When α4* nAChRs are removed in Cre(+) VTA DA neurons, ACh-evoked currents are significantly reduced (Cre (-) = -128.60 ± 14.4 pA, Cre (+) = -13.25 ± 3.3 pA, $P = 0.0016$)(Figure 5.2 E and F). This demonstrates that the majority of ACh-

evoked currents in VTA DA neurons in slices from *Chrna*4 loxP/loxP α6L9S mice are mediated by α4α6* nAChRs and is consistent with our α4KOα6L9S mice results (Figure 3.9).

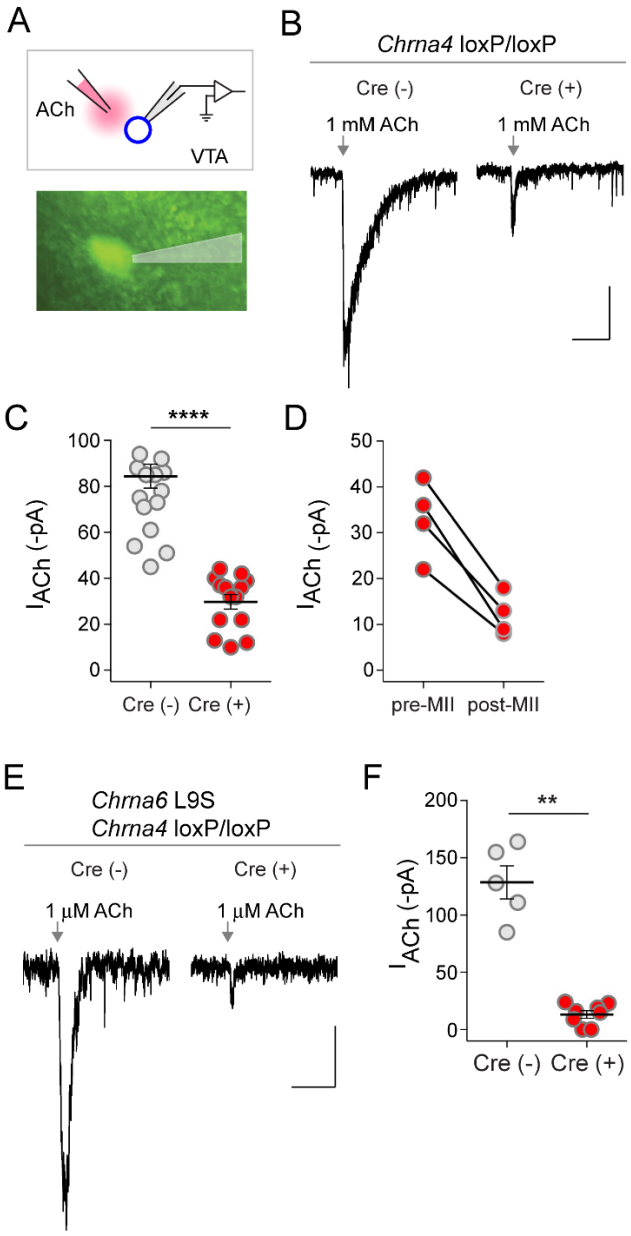

Figure 5.2 nAChR function in *Chrna*4 vMB cKO mice. **(A)** Schematic of experimental approach. VTA DA neurons were voltage clamped at -60 mV during puff application of ACh. VTA DA neurons expressing Cre (Cre +) were identified by the presence of GFP. **(B)** Representative ACh (1 mM)-evoked currents in Cre (-) and Cre (+) VTA DA neurons. Scale: 25 pA, 1 sec. **(C)** Quantification (average ± S.E.M.) of ACh-evoked current amplitude in Cre (-) and Cre (+) VTA DA neurons ****$P < 0.0001$, student's *t*-test. **(D)** Summary of the reduction in ACh (1 mM)-evoked currents following MII (100 nM) bath application for 4 Cre (+) VTA DA neurons. **(E)** Representative ACh (1 µM)-evoked currents in Cre (-) and Cre (+) VTA DA neurons in slices from *Chrna*4loxP/loxP α6L9S and *Chrna*4 vMB cKO α6L9S mice. Scale: 25 pA, 1 sec. **(F)** Quantification (average ± S.E.M.) of ACh-evoked current amplitude in Cre (-) and Cre (+) VTA DA neurons, **$P < 0.01$, Mann-Whitney test.

5.3 Removal of α4 nAChR Subunits Enhances Excitability of VTA DA Neurons

To study the excitability of VTA DA neurons in *Chrna*4 loxP/loxP and *Chrna*4 vMB cKO mice, we injected increasing amounts of current into the cell. Current injection steps lasting 2 seconds were delivered in 20 pA intervals from 0 to +80 pA (Figure 5.3 A). As expected, the firing rate of VTA DA neurons in control *Chrna*4 loxP/loxP brain slices steadily increased with each subsequent current step (Figure 5.3 A and B, gray circles). In α4KO mice, nicotine does not increase the firing rate, as it does in WT mice (Liu et al 2012). However, when we give depolarizing current injection steps, action potential firing still increases in Cre(+) VTA DA neurons in *Chrna*4 vMB cKO slices (Figure 5.3 A and B, red circles). In fact, the firing rate is significantly higher in Cre (+) VTA DA neurons compared to Cre(-) VTA DA neurons at +60 and +80 pA (+60 pA: Cre(-) = 12.30 ± 1.4 Hz, Cre (+) = 20.15 ± 3.8 Hz, $P = 0.0350$; +80 pA: Cre(-) = 13.35 ± 1.6 Hz, Cre (+) = 22.83 ± 4.8 Hz, $P = 0.0435$ (Figure 5.3 B). A similar trend towards enhanced excitability in Cre(+) VTA DA neurons is observed when analyzing the first interspike interval (Figure 5.3 C) with significant differences occurring at the lowest current injection step of +20 pA. Cre(-) and Cre(+) VTA DA neurons have a similar baseline action potential firing rate (Figure 5.3 B, insert) and there is no difference in either the resting membrane potential (Figure 5.3 D) or the input resistance (Figure 5.3 E).

A study using optogenetics to activate VTA GABA neurons found that stimulation decreased the excitability of VTA DA neurons (van Zessen et al 2012). Based on this result, if removal of α4* nAChRs inhibits GABAergic neurons, then we would expect to see the

increases in VTA DA neuron excitability that we do in *Chrna*4 vMB cKO mice. Therefore, we next looked at GABAergic signaling in the VTA of *Chrna*4 vMB cKO mice.

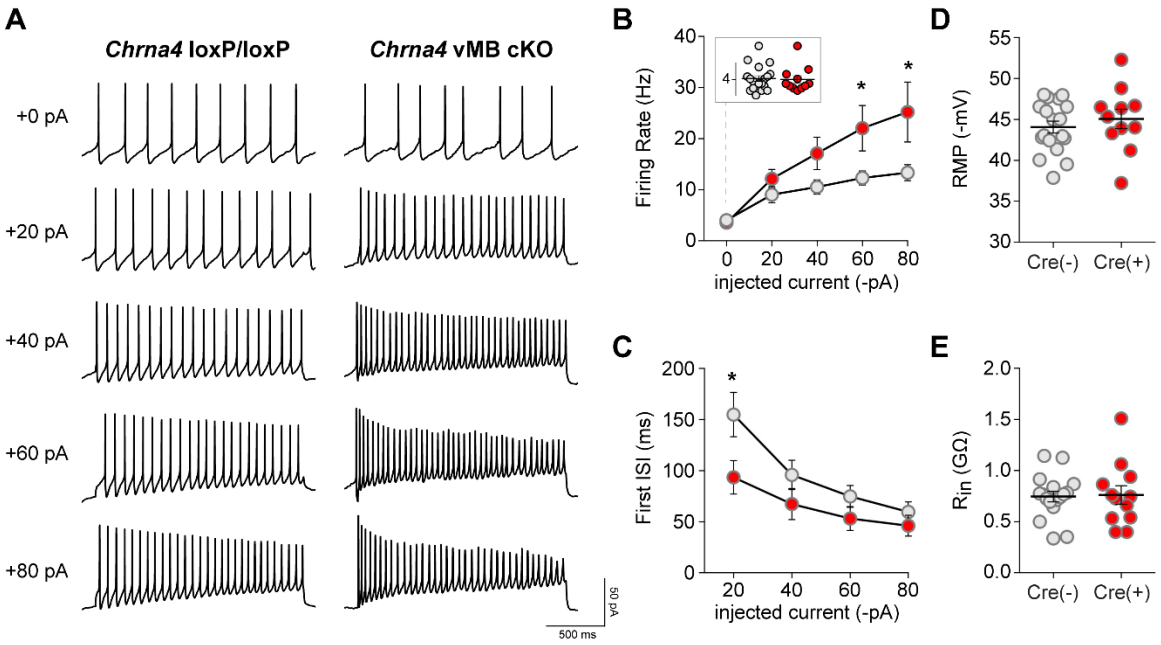

Figure 5.3 Removal of α4 nAChR subunits enhances excitability of VTA DA neurons. **(A)** Representative action potential firing in a Cre (-) VTA DA neuron from a *Chrna*4 loxP/loxP mouse and a Cre(+) VTA DA neuron from a *Chrna*4 vMB cKO mouse. Current was injected at each of the indicated values in 2 second steps. **(B)** Comparison of Cre(-) and Cre(+) VTA DA neuron firing rate during each current injection step (Cre(-) = gray circles, Cre(+) = red circles). **P* < 0.05 **(C)** Comparison of the first interspike interval (ISI) for Cre(-) and Cre(+) VTA DA neurons for each current injection step. **P* < 0.05 **(D)** Resting membrane potential (RPM) of Cre(-) and Cre(+) VTA DA neurons. **(E)** Input resistance (R_{in}) of Cre (-) and Cre(+) VTA DA neurons.

5.4 α4 nAChR Subunit Removal Decreases the Instantaneous Frequency of IPSCs

We next sought to study the mechanism behind the enhanced excitability we see when α4 nAChR subunits are removed from the VTA. The VTA is comprised of around 35% GABAergic neurons that send local collaterals to inhibit DA neurons in the VTA as well as project to forebrain sites such as the NAc (Nair-Roberts et al 2008, Van Bockstaele & Pickel 1995). α4* nAChRs are not only located on DA neurons in the VTA, but also on GABAergic neurons (Klink et al 2001). In *Chrna*4 loxP/loxP mice, the α4 gene is floxed in all cell types. Therefore, when Cre is injected into the VTA, the α4 subunit is removed from both DAergic and GABAergic neurons (Figure 5.1 C). We hypothesize that removal of α4* nAChRs from GABA interneurons results in reduced ACh-mediated GABA release and subsequently reduced inhibition of VTA DA neurons. We measured changes in GABAergic inhibition by recording spontaneous IPSCs in VTA DA neurons of *Chrna*4 loxP/loxP and *Chrna*4 vMB cKO mice (Figure 5.4 A). IPSC instantaneous frequency is significantly reduced in *Chrna*4 vMB cKO mice compared to *Chrna*4 loxP/loxP mice (lox/lox = 12.01 ± 3.0 Hz, vMB cKO = 2.22 ± 1.2 Hz, $P = 0.0047$)(Figure 5.4 B, C, an F). We verified that the currents recorded were GABAergic by showing they can be blocked by bath application of picrotoxin (Figure 5.4 D). The majority of IPSCs were also blocked by TTX suggesting that action potential firing, and presumably GABAergic activity, in the VTA is necessary for a large portion of the IPSCs recorded (Figure 5.4 E). The amplitude of IPSCs was not altered by the removal of α4 nAChR subunits in *Chrna*4 vMB cKO mice compared to *Chrna*4 loxP/loxP mice (lox/lox = 13.79 ± 2.1 pA, vMB cKO = 10.65 ± 2.0 pA, *P* =

0.3337)(Figure 5.4 B, C, and G). This indicates that when α4 nAChR subunits are removed from the VTA of adult mice, GABAergic inhibition of VTA DA neurons is decreased via a presynaptic mechanism.

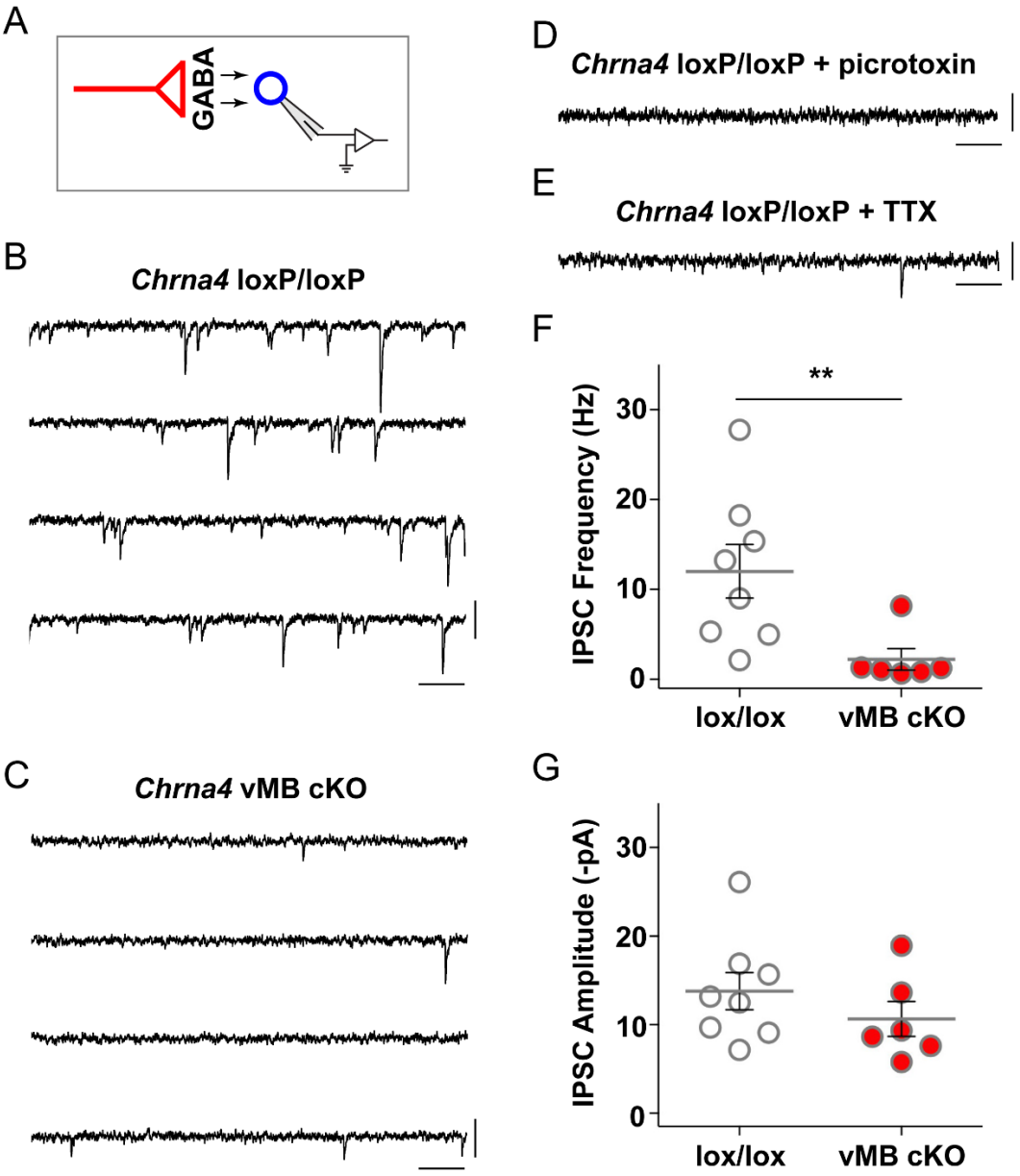

Figure 5.4 α4 nAChR Subunit Removal Decreases the Instantaneous Frequency of IPSCs. **(A)** Schematic illustrating experimental approach. VTA DA neurons were voltage clamped and -60 mV and spontaneous IPSCs were recorded in the presence of CNQX (10 μM). **(B)** A representative trace of spontaneous IPSCs in a VTA DA neuron in a slice from a *Chrna4* loxP/loxP mouse. Scale: 5 pA, 200 msec. **(C)** A representative trace of spontaneous IPSCs in a VTA DA neuron in a slice from a *Chrna4* vMB cKO mouse. Scale: 5 pA, 200 msec. **(D)** Representative trace showing the lack of IPSCs after picrotoxin (100 μM) was bath applied to the slice. Scale: 5 pA, 200 msec. **(E)** Representative trace showing a reduction in IPSCs after TTX (0.5 μM) was bath applied to the slice. Scale: 5 pA, 200 msec. **(F)** Summary (average ± S.E.M.) of IPSC instantaneous frequency. ***P* < 0.01, Mann-Whitney test. **(G)** Summary (average ± S.E.M.) of IPSC amplitude.

5.5 EPSCs are not altered by removal of α4 nAChR subunits from the VTA

To detect if the enhanced excitability of VTA DA neurons is a direct result of increased glutamatergic signaling within the VTA, we measured spontaneous EPSCs (Figure 5.5 A). We found no difference in the instantaneous frequency of spontaneous EPSCs in VTA DA neurons from *Chrna*4 vMB cKO mice compared to *Chrna*4 loxP/loxP mice (lox/lox = 18.20 ± 3.3 Hz, vMB cKO = 16.58 ± 2.6 Hz, $P = 0.6990$)(Figure 5.5 B, C, and E). There was also no difference in the amplitude of spontaneous EPSCS in VTA DA neurons from *Chrna*4 vMB cKO mice compared to *Chrna*4 loxP/loxP mice (lox/lox = 6.01 ± 0.6 pA, vMB cKO = 5.16 ± 0.8 pA, $P = 0.4212$)(Figure 5.5 B, C, and F). Events recorded were confirmed to be glutamatergic EPSCs by blockade with CNQX (Figure 5.5 D). Therefore, we can reasonably conclude that enhanced excitability of Cre (+) VTA DA neurons is attributable to decreased GABAergic signaling and not enhanced glutamatergic signaling within the VTA.

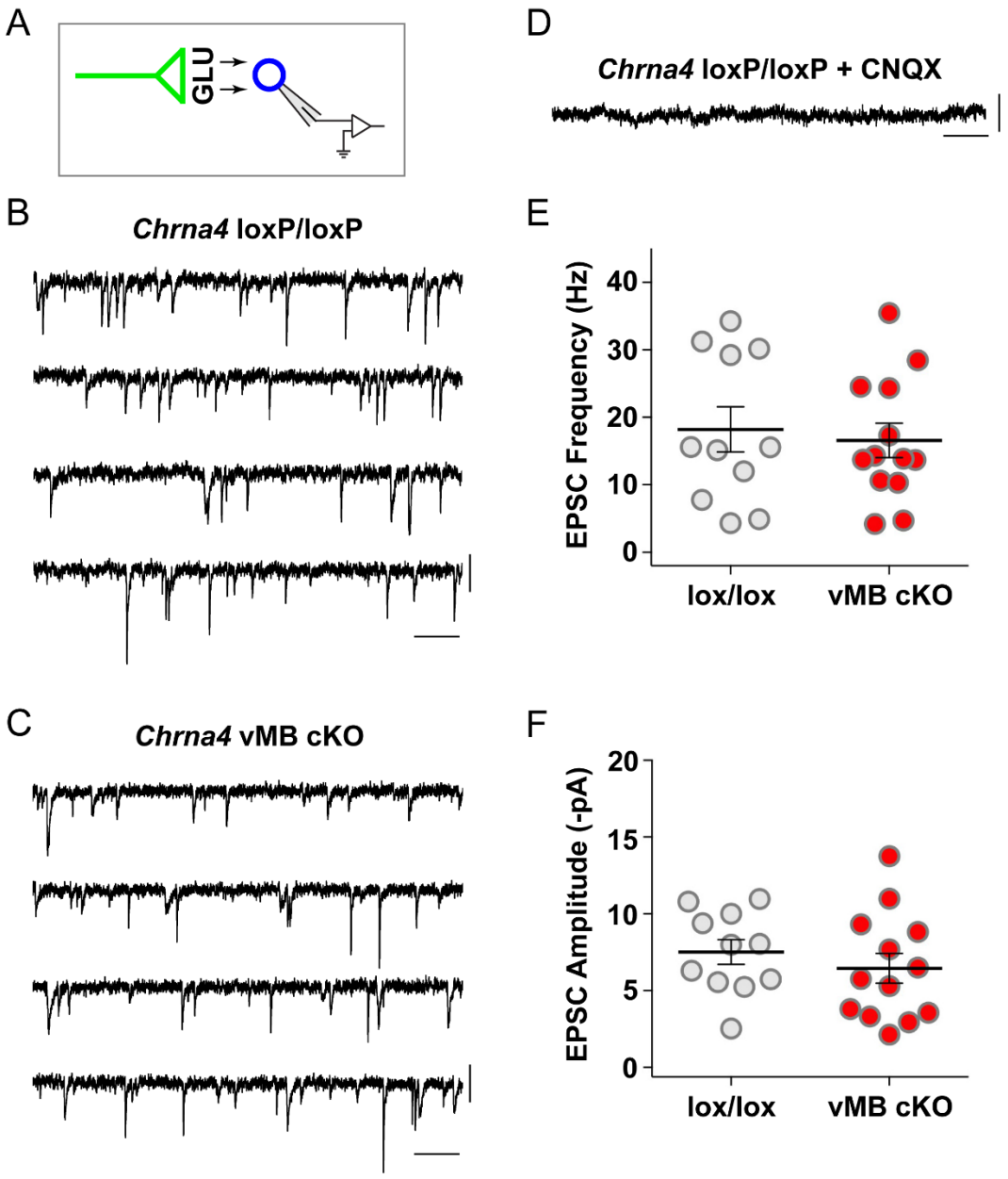

Figure 5.5 EPSCs are not altered by removal of α4 nAChR subunits from the VTA. **(A)** Schematic illustrating experimental approach. VTA DA neurons were voltage clamped and -60 mV and spontaneous EPSCs were recorded in the presence of picrotoxin (100 μM). **(B)** Representative trace of spontaneous EPSCs in a VTA DA neuron in a slice from a *Chrna4* loxP/loxP mouse. Scale: 5 pA, 200 msec. **(C)** Representative trace of spontaneous EPSCs in a VTA DA neuron in a slice from a *Chrna4* vMB cKO mouse. Scale: 5 pA, 200 msec. **(D)** Representative trace showing the lack of EPSCs after CNQX (10 μM) was bath applied to the slice. Scale: 5 pA, 200 msec. **(E)** Summary (average ± S.E.M.) of EPSC instantaneous frequency. **(F)** Summary (average ± S.E.M.) of EPSC amplitude.

5.6 Removal of α4 nAChR Subunits from NAc-Projecting VTA Neurons

To confirm that the reduction in IPSC instantaneous frequency is a result of α4 nAChR subunit removal from neurons within the VTA, we also measured IPSCs after injecting mice with a retrograde HSV-CRE-YFP virus into the NAc (Figure 5.6 A). Because the retrograde virus is taken up by terminals in the NAc and transported back to the VTA, α4* nAChRs are only removed from VTA neurons in the mesolimbic pathway (Figure 5.6 A). Just as with the intra-VTA AAV-CRE-GFP injections, we again see that both TH(+) and TH(-) VTA neurons express the virus (Figure 5.6 B). When recording spontaneous IPSCs we found that IPSC instantaneous frequency is still significantly decreased in VTA DA neurons in *Chrna*4 vMB cKO brain slices compared to VTA DA neurons in *Chrna*4 loxP/loxP control slices (lox/lox = 10.39 ± 1.4 Hz, NAc to VTA cKO = 4.46 ± 1.0 Hz, $P = 0.0031$)(Figure 5.6 C, D, and E) There are no significant change in the spontaneous IPSC amplitude in VTA DA neurons in *Chrna*4 vMB cKO brain slices compared to VTA DA neurons in *Chrna*4 loxP/loxP control slices (lox/lox = 12.06 ± 2.8 pA, NAc to VTA cKO = 11.82 ± 2.0 pA, $P = 0.6241$)(Figure 5.6 C, D and F). Therefore, changes in spontaneous IPSC instantaneous frequency are a result of decreased GABA release from neurons within the VTA and not GABAergic neurons in other nearby brain regions the AAV virus may have spread to, such as the GABA-rich rostromedial tegmental nucleus (RMTg) that sends projections to the VTA but not the NAc (Barrot et al 2012).

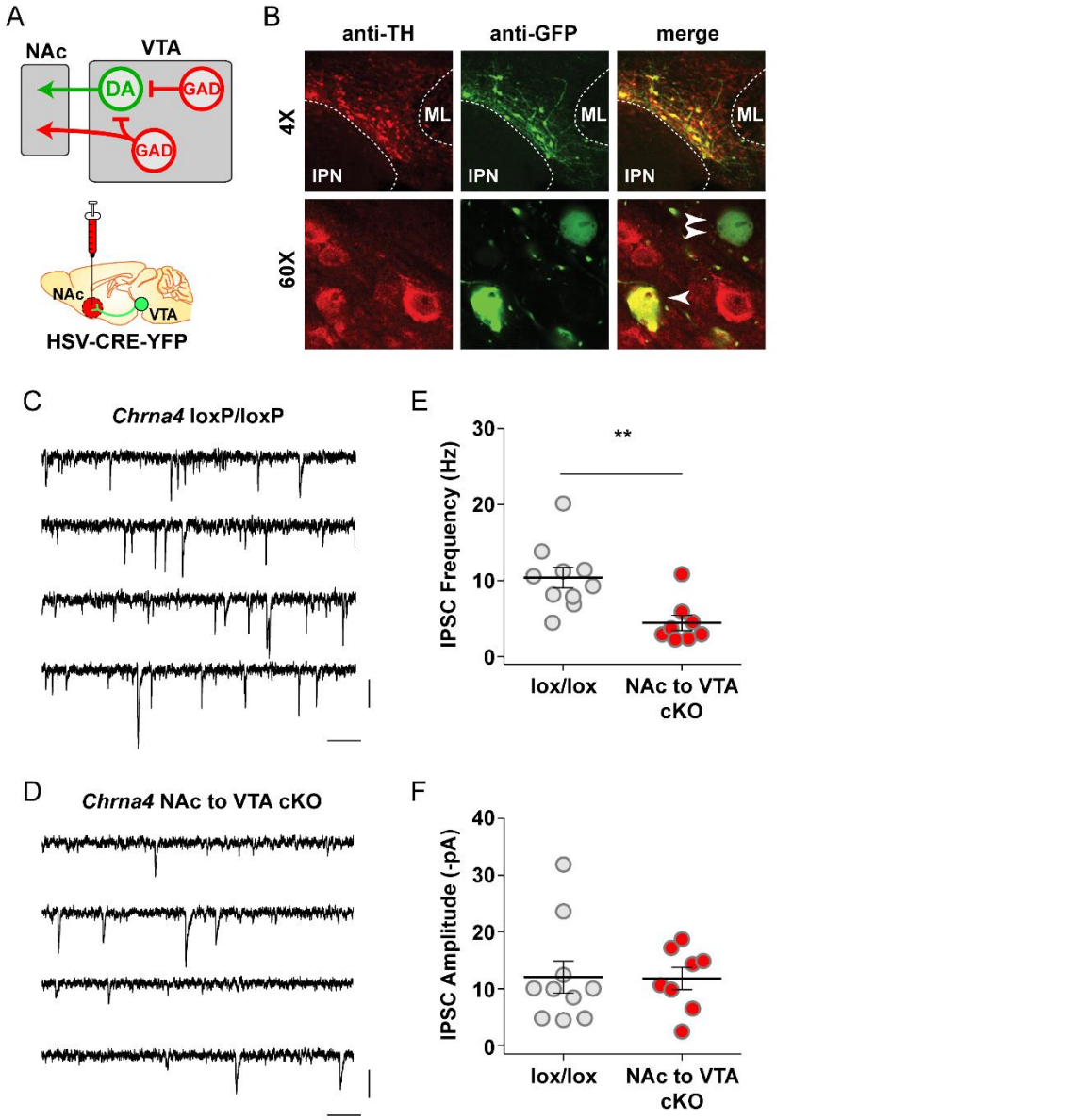

Figure 5.6 Removal of α4 nAChR Subunits from NAc-Projecting VTA Neurons. **(A)** Schematic of retrograde viral injection. When retrograde HSV-CRE-YFP viral vectors are injected into the NAc they are transported to the VTA via terminals of any neurons projecting from the VTA to the NAc. **(B)** Immunohistochemistry and confocal microscopy images of the VTA in a *Chrna*4 vMB cKO brain slice (green: anti-GFP, red: anti-TH). 60X images showing both a TH(+) and a TH(-) neuron infected by the virus (indicated by one or two white arrows, respectively). **(C)** Representative trace of spontaneous IPSCs in a VTA DA neuron in a slice from a *Chrna4* loxP/loxP mouse. Scale: 5 pA, 200 msec. **(D)** Representative trace of spontaneous IPSCs from a VTA DA neuron in a slice from a *Chrna4* vMB cKO mouse. Scale: 5 pA, 200 msec. **(E)** Summary (average ± S.E.M.) of IPSC instantaneous frequency. $^{**}P < 0.01$, Mann-Whitney test. **(F)** Summary (average ± S.E.M.) of IPSC amplitude.

5.7 Nicotine-Mediated Enhancement of Excitatory Synaptic Transmission in VTA DA Neurons Requires α4* nAChRs

In our α4KOα6L9S mouse model, incubating brain slices in nicotine did not significantly enhance AMPAR function on VTA DA neurons (Figure 3.8). Here, we want to see if there is a similar effect when α4* nAChRs are removed selectively from the VTA of adult mice and nicotine is administered systemically. *Chrna*4 loxP/loxP mice were given intra-VTA injections of AAV-GFP or AAV-Cre-GFP viral vectors followed by a two week recovery and handling period before they were given a vehicle or nicotine injection (0.17 mg/kg, i.p.). One hour after the injection, VTA-containing brain slices were prepared for electrophysiology and AMPA/NMDA ratios were measured (Figure 5.7 A). When α4* nAChRs are intact, nicotine significantly enhances AMPA/NMDA ratios in VTA DA neurons (Cre(-)/saline injection: 2.38 ± 0.2 pA, Cre(-)/nicotine injection: 3.85 ± 0.1, $P < 0.01$)(Figure 5.7 B). However, when α4* nAChRs are removed from VTA DA neurons there are no significant changes in AMPA/NMDA ratios following a nicotine injection (Cre(+)/saline injection: 2.20 ± 0.1 pA, Cre(+)/nicotine injection: 2.49 ± 0.2(Figure 5.7 B). This shows that removal of α4* nAChRs from the VTA of adult mice disrupts the ability of acutely delivered nicotine to induce changes in synaptic plasticity. Under these conditions, just as in α4KOα6L9S mice, activation of (non-α4)α6* nAChRs is not sufficient to support induction of plasticity in VTA DA neurons.

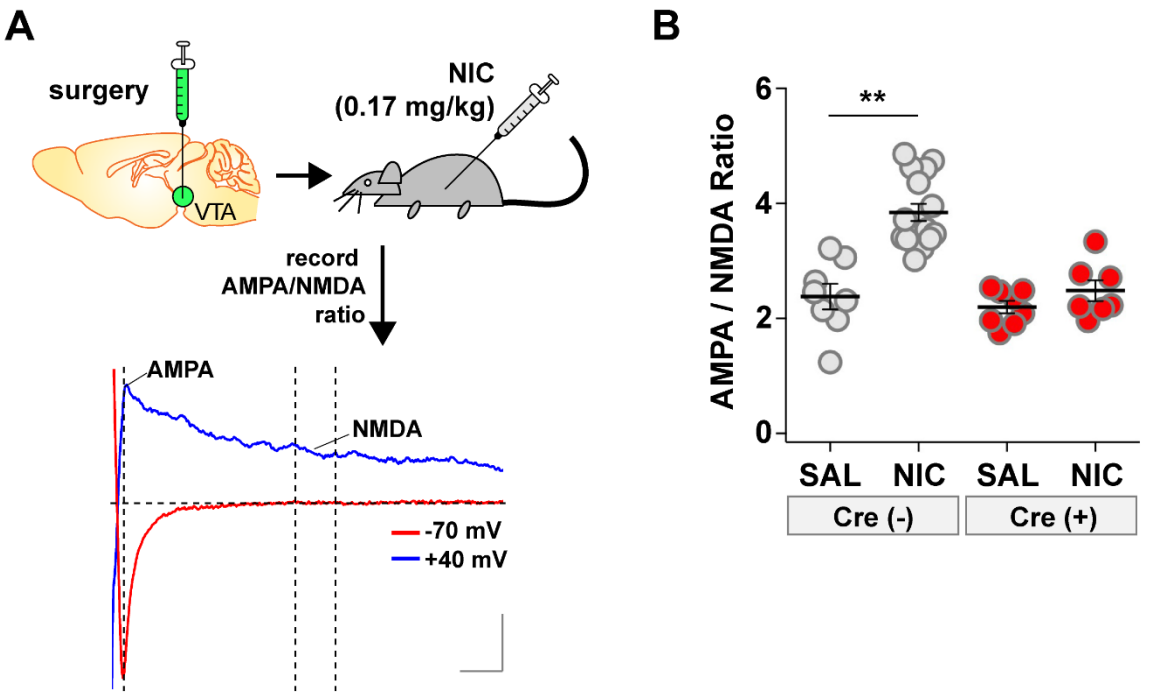

Figure 5.7 Nicotine-mediated enhancement of excitatory synaptic transmission in VTA DA neurons requires α4* nAChRs. **(A)** Schematic illustrating experimental procedure. *Chrna*4 loxP/loxP mice were given intra-VTA AAV-CRE-GFP (or control AAV-GFP) injections at least two weeks prior to a nicotine (0.17 mg/kg, i.p.) injection. 60 minutes after the nicotine injection, VTA brain slices were prepared for electrophysiology to measure AMPA/NMDA ratios. Example evoked synaptic currents recorded from a VTA DA neuron to illustrate AMPAR- and NMDAR-receptor components. The AMPAR-mediated component was measured at a command voltage of +40 mV (blue trace) at the time corresponding to the peak of the AMPA EPSC evoked at a command voltage of -70 mV (red trace). The NMDAR-mediated component was measured on the +40 mV trace by averaging the membrane current during a 10 msec window, 40 msec after the AMPA EPSC peak. Scale: 40 pA, 10 msec. **(B)** Quantification of AMPA/NMDA ratios measured from Cre(-) and Cre(+) VTA DA neurons following a saline or nicotine (0.17 mg/kg, i.p.) injection. **P < 0.01 (Kruskal-Wallis test, followed by Dunn's post hoc test)

5.8 Summary of Proposed Circuitry Changes in the VTA of *Chrna*4 vMB cKO Mice

Based on the results in this chapter, we propose that the increased excitability observed in VTA DA neurons of *Chrna*4 vMB cKO mice when current is injected (Figure 5.3) is a result of disinhibition. We hypothesize that when α4 nAChR subunits are removed from the VTA, cholinergic inputs no longer stimulate GABAergic interneurons, resulting in less GABA release onto VTA DA neurons (Figure 5.8). This reduced inhibition could then in turn cause enhanced excitability of VTA DA neurons.

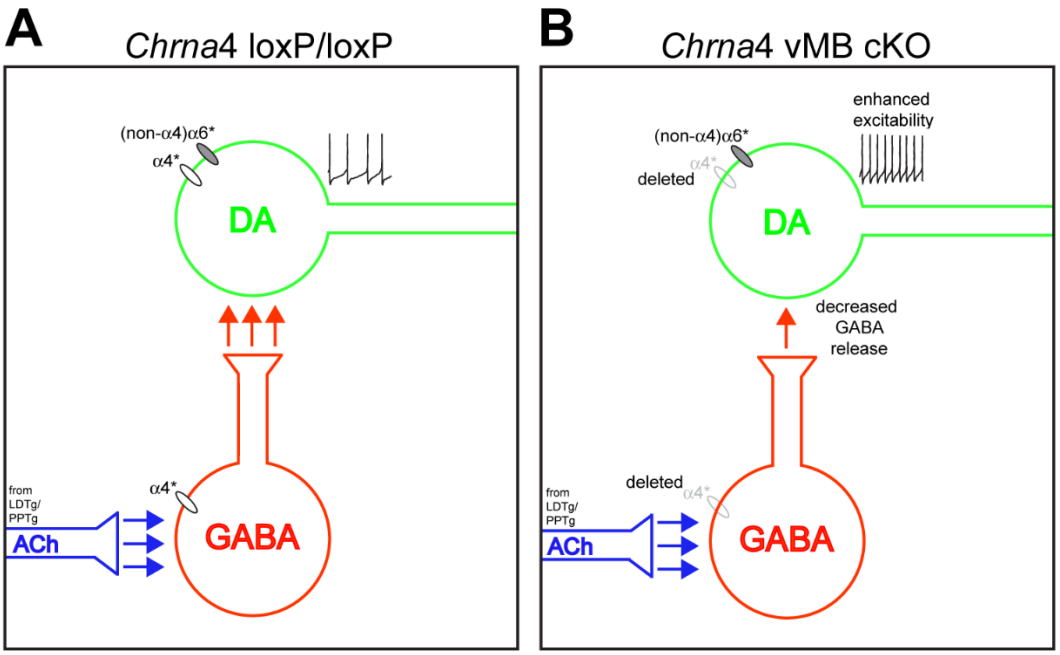

Figure 5.8 Summary of proposed circuitry changes in the VTA of *Chrna*4 vMB cKO mice. **(A)** VTA of control *Chrna*4 loxP/loxP mice with α4* nAChRs intact. **(B)** VTA of *Chrna*4 vMB cKO mice with α4* nAChRs deleted. Without α4* nAChRs, GABAergic neurons are not stimulated by cholinergic inputs from the LDTg/PPTg. Therefore, less GABA is released onto DA neurons. This disinhibition may result in enhanced excitability of VTA DA neurons.

CHAPTER 6. DISCUSSION

6.1 Mouse Models

Mice are an ideal model organism for studying nicotine addiction. Mice and humans have genomes that are roughly 90% identical (Monaco et al 2015) and they share similar brain reward circuitry (Laviolette & van der Kooy 2004). In addition to WT mice, several genetically modified mice were used in these studies, including α6L9S transgenic mice, α4KO mice, and *Chrna*4 loxP/loxP mice. nAChRs containing the α6 subunit have been difficult to study because, as of yet, they have not been robustly and repeatedly expressed *in vitro* in heterologous expression systems without modifications such as chimeric

subunits or concatamers (Letchworth & Whiteaker 2011). Therefore, native α6* nAChRs must be studied *in vivo* or in acute brain slices. Much of the published work on α6 nAChRs reveals information about the necessity of the receptor through the use of α6KO mice or pharmacological inhibitors such as αCtxMII. These approaches have several drawbacks including compensatory changes that may have occurred during development in α6KO mice, and the inability of inhibitors to distinguish between specific receptor subtypes like (non-α4)α6* nAChRs versus α4α6* nAChRs. Our approach using α6L9S mice allows us to complement these approaches by demonstrating sufficiency versus necessity (Drenan & Lester 2012). These mice develop normally and express α6 nAChR subunits in the correct brain regions (Drenan et al 2008a). Although previous work indicates no evidence for overexpression of α6β2* nAChRs (Drenan et al., 2010), the TM2 pore-lining mutation used to sensitize these receptors may alter their pharmacological properties (Labarca et al 1995, Revah et al 1991). Future studies using restricted expression of α4α6L9Sβ2* nAChRs via concatamers (Kuryatov & Lindstrom 2011) will be useful in exploring the latter possibility, whereas development of α6β2*-selective ligands will be useful in addressing the importance of the former possibility.

Crossing α6L9S mice with α4KO mouse models also proved useful in our studies to gain additional information on the role of α6* nAChRs. When α4* nAChRs are removed, the primary high sensitivity receptor remaining in the VTA is the (non-α4)α6* nAChR (Salminen et al 2007). The contribution of α4α6* nAChRs can be studied by comparing results from α6L9S mice to α6L9S mice crossed with α4KO mice as previously done

(Drenan et al 2010). In addition to the traditional α4KO mouse model, we also used a conditional α4KO approach (Figure 5.1). Using *Chrna*4 loxP/loxP mice we have successfully applied Cre-lox technology to remove α4 nAChR subunits from the VTA of adult mice (Figure 5.1). By using adult mice we can overcome any possible compensatory changes that might occur during development. In addition, we can selectively target certain brain regions to study the contributions of α4 subunits in that brain region instead of in a global KO mouse. Thus far, our approach does not distinguish between the role of α4* nAChRs on different cell populations within the VTA (Figure 5.1 C). Future studies by our group will address this.

6.2 VTA DA Neuron Activation by α6β2* nAChRs

Understanding which nAChR subtypes are necessary and sufficient to mediate nicotine's complex action on VTA neurons is a challenge (Drenan and Lester, 2012), and our data provide new information. We show that nicotine-elicited activation of somatodendritic α6β2* nAChRs in VTA DA neurons is sufficient to stimulate an inward conductance that could, under physiologic conditions support prolonged depolarization of these cells (Figure 3.2). β2* nAChRs are absolutely required for nicotine-induced increases in VTA DA neuron firing (Maskos et al 2005, Picciotto et al 1998), and Tapper and colleagues recently reported that activation of α4β2* nAChRs in VTA DA neurons by smoking-relevant concentrations of nicotine can support depolarization and action potential firing (Liu et al 2012). These actions were sensitive to a α6β2* nAChR antagonist, implicating α4α6β2* nAChRs. Additionally, the depolarization measured was long-lived but only

when the α6 nAChR subunit were not inhibited indicating that α4α6β2* nAChRs are desensitization resistant (Liu et al 2012). This report is consistent with our study, which suggests that selective activation of α6β2* nAChRs can increase inward currents in VTA DA neurons (Figure 3.2). Other reports studying the role of VTA α6β2* nAChRs in nicotine self-administration (Gotti et al 2010, Pons et al 2008) and DA release (Gotti et al 2010) support the data we present here. Furthermore, our experiments employing puff-application of nicotine and ACh in α6L9S, α6L9Sα4KO, and *Chrna*4 vMB cKO brain slices (Figures 3.9 and 5.2) provide evidence that α4 subunits play an important role in α6-mediated neuronal activation. In the VTA, α4β2* nAChRs are found in DAergic neurons and in GABAergic neurons and/or terminals (Nashmi et al 2007). Nicotine may act through VTA α4β2* nAChRs via two mechanisms: 1) direct activation at α4β2* nAChRs on DA neurons, and/or 2) desensitization of α4β2* nAChRs in GABAergic neurons leading to DA neuron disinhibition (Mansvelder et al 2002, Nashmi et al 2007). Because α6* nAChRs are restricted to DAergic cells in VTA (Mackey et al 2012), our results suggest that direct action by nicotine on somatodendritic α6* nAChRs may be sufficient to depolarize these cells. In the human brain, there may be redundant mechanisms in the VTA that allow nicotine to activate the mesolimbic DA system.

6.3 Methods of Measuring AMPAR Function

Classically, changes in synaptic plasticity on VTA DA neurons after drug exposure have been assessed by measuring AMPA/NMDA ratios (Saal et al 2003, Ungless et al 2001). However, without additional experiments, it is difficult to pinpoint if differences in the

ratio are due changes in AMPAR function, NMDAR function, or a combination of the two. Our approach involves direct application of AMPA onto the neuron being recorded (Figure 3.4), similar to previous approaches (Kobayashi et al 2009, Sanchez et al 2010). This allows us to directly measure the function of AMPARs expressed on the cell surface. Alternatively, NMDAR function can be measured by locally puff applying NMDA onto the VTA DA neuron during a whole-cell recording (Figure 3.10). Local puff application of drugs using a Picospritzer has been successfully employed in studies of other ligand-gated ion channels as well (Drenan et al 2008a, Eggers & Berger 2004). A fundamental difference in measuring changes in AMPAR function with the ratio method versus the local drug application method is the population of AMPARs being activated. When measuring AMPA/NMDA ratios, an electrode is used to stimulate afferents to release glutamate and activate AMPARs preferentially located at the synapse. When measuring AMPA-evoked currents, the entire surface of the cell is exposed to AMPA and therefore the function of the total population of surface AMPARs, both synaptic and extrasynaptic, is measured. To identify if there are any discrepancies in the two methods, we also began to study AMPA/NMDA ratios. We found that with both nicotine and ethanol exposure, there is no difference in measuring the function of synaptic versus extrasynaptic AMPARs (Figures 3.5, 4.1, and 4.4).

6.4 Nicotine-Induced Changes in AMPAR Function.

Our recordings in isolated brain slices demonstrate that selective activation of $\alpha6\beta2$* nAChRs is sufficient to enhance the function of AMPARs on VTA DA neurons (Figure 3.5).

To our knowledge, this study is the first to implicate α6β2* nAChRs in nicotine-induced changes in glutamatergic synaptic plasticity on VTA DA neurons. A single exposure to nicotine or other drugs of abuse enhances AMPAR-mediated EPSCs in VTA DA neurons (Saal et al 2003) which strongly suggests LTP of excitatory inputs to these cells (Luscher & Malenka 2011, Mansvelder & McGehee 2000, Ungless et al 2001). Subsequent studies addressing which nAChR subtypes mediate this effect are not completely consistent. In slice experiments, McGehee and colleagues report that β2* nAChRs (but not α7 nAChRs) are necessary for increased AMPAR function in synapses after nicotine exposure (Mao et al 2011), whereas in studies with animals injected with nicotine prior to slice preparation, Wu and colleagues suggest that nicotine-elicited increases in AMPAR function can proceed either through β2* or α7 nAChRs (Gao et al 2010, Jin et al 2011). Our results using naïve or nicotine-exposed slices from adult non-Tg or α6L9S mice are more consistent with the former, because we find no necessary role for α7 nAChRs in AMPAR functional enhancement (Figure 3.7). Our results also demonstrate that the contribution of α4 nAChR subunits are necessary. Enhanced AMPAR function does not occur in VTA DA neurons in either α4KOα6L9S (Figure 3.8) or *Chrna*4 vMB cKO (Figure 5.7) brain slices following nicotine exposure. This indicates that activation of (non-α4)α6* nAChRs is not sufficient but rather that activation of α4α6β2* is necessary for nicotine-evoked enhancement of AMPAR function.

Our *in vitro* finding that selective activation α6* nAChRs is sufficient to enhance AMPAR function on VTA DA neurons is confirmed by our *in vivo* results. In α6L9S mice, systemic

administration of α6-selective doses of nicotine (Figure 3.11 B and C) is sufficient to enhance AMPAR function on VTA DA neurons. This result was directly ascribed to α6* nAChRs because αCtxMII infusion into the VTA immediately prior to systemic nicotine administration blocked the enhancement of AMPAR function (Figure 3.12).

In VTA DA neurons, changes in both AMPAR distribution and/or composition are proposed to occur after exposure to nicotine and other drugs of abuse. Several reports suggest that drug exposure (including nicotine) leads to signal transduction events that promote exchange of Ca^{2+} impermeable AMPARs containing GluR2 subunits for high-conductance, Ca^{2+} permeable AMPARs lacking GluR2 subunits (Bellone & Luscher 2006, Luscher & Malenka 2011). This GluR2-lacking receptor pool typically displays inward rectification (Isaac et al 2007, Liu & Zukin 2007), and one study confirms the appearance of this type of AMPAR after a single exposure to nicotine (Gao et al 2010). Another study on nicotine exposure to VTA DA neurons, however, demonstrated increases in AMPA/NMDA ratios but no appearance of an AMPAR pool displaying inward rectification (Baker et al 2013). We find no appearance of inward rectification in AMPA-evoked currents (Figure 3.5 B and D), which is more consistent with enhancement in numbers of GluR2-containing AMPARs rather than production of a significant amount of GluR2-lacking AMPARs. However, our data showing an increase in AMPAR sensitivity in response to α6β2* activation (Figure 3.5 F) support a number of possible mechanisms, including increased AMPAR conductance—a hallmark of GluR2-lacking AMPARs. Future

pharmacological studies in α6L9S and WT slices exposed to nicotine are needed to characterize AMPAR sensitivity changes.

It is also important to understand what circuit and/or molecular signal transduction events are necessary and/or sufficient to enhance AMPAR function in VTA DA neurons after nicotine exposure. At the circuit level, an approach utilizing optogenetics demonstrated conclusively that *in vivo* activation of VTA DA neurons was sufficient to promote AMPAR redistribution (Brown et al 2010). Because α6β2* nAChRs are selectively expressed in DA neurons in the VTA (Drenan et al 2008a, Mackey et al 2012), our results lead us to favor a similar conclusion for nicotine: activation of α6β2* nAChRs on VTA DA neurons is sufficient to promote enhanced AMPAR function. Two other molecular events have been shown to be important for induction of synaptic plasticity in VTA DA neurons: D1/D5 DA receptor activation (Brown et al 2010, Mao et al 2011, Schilstrom et al 2006), and NMDA receptor activation (Saal et al 2003, Ungless et al 2001). Although our SCH-23390 results are inconclusive, NMDA receptor activation is necessary for α6β2* nAChR-mediated increases in AMPAR function (Figure 3.7 C). Although NMDAR activity is necessary, the mechanism of enhanced AMPAR function does not require enhanced NMDAR function (Figure 3.10). While the involvement of kinase activity has not been extensively studied with regards to nicotine-evoked increases in glutamatergic synaptic plasticity, CaMKII is required for increased AMPA/NMDA ratios after cocaine exposure (Anderson et al 2008, Liu et al 2014). Cocaine results in the phosphorylation of S831 on GluR1 subunits by CaMKII, leading to their increased expression at the synapse (Anderson

et al 2008, White et al 2013). Our results using KN-93 indicate CaMKII activity is necessary for α6β2* nAChR-mediated increases in AMPAR function as well (Figure 3.7 C). Further experiments probing what target sites CaMKII phosphorylates will help determine if changes in AMPAR composition or distribution lead to enhanced AMPAR function. Together with previous studies on nicotine and other drugs of abuse, our data studying α6β2* nAChRs support the contention that there may be multiple mechanisms in place that nicotine can use to enhance the responsiveness of VTA DA neurons, ultimately leading to a heightened behavioral response to nicotine.

6.5 Ethanol-Mediated Enhancement of AMPAR Function

Our results indicate that α6* nAChR activity is important in ethanol-mediated enhancement of AMPAR function both *in vitro* by incubating naïve VTA-containing brain slices in ethanol (Figures 4.1 and 4.4) and *in vivo* by giving mice ethanol injections (Figure 4.2). We demonstrated α6* nAChR involvement with a genetic approach using selective α6* nAChR activation in α6L9S mice and a pharmacological approach by showing that a α6* nAChR antagonist (αCtxMII) blocks ethanol-mediated enhancement of AMPAR function (Figure 4.1). This suggests that endogenous ACh and ethanol combine at α6* nAChRs to produce sufficient nAChR activity to initiate signaling events ultimately resulting in AMPAR functional enhancement. ACh, presumably released from LDTg and/or PPTg axon terminals, is present in VTA slices and contributes to baseline α6* nAChR activity in VTA DA neurons (Drenan et al 2008a). Our findings with nicotine in α6L9Sα4KO mice (Figure 3.8) and previous reports on α4α6* nAChRs (Drenan et al 2010,

Liu et al 2012), suggest that α4 nAChR subunits are incorporated into α6* nAChRs that mediate these effects. Thus, most VTA α6* nAChRs contain α4 and β2 subunits and α4α6β2* nAChRs could thus be subject to ethanol's nAChR potentiating properties.

Ethanol is known to alter DA neuron activity and accumbal DA release via indirect, activity-dependent mechanisms. For example, ethanol increases ACh release in the VTA (Larsson et al 2005), and ACh-induced firing in VTA DA neurons can be potentiated by ethanol (Liu et al 2013a). The increased concentration of ACh in the VTA could activate α6* nAChRs, leading to the α6* nAChR-mediated increases in AMPAR function we report. Another indirect, activity-dependent mechanism through which ethanol may contribute to reward is by reducing GABAergic inhibition to VTA DA neurons (Di Chiara et al 1996, Spanagel et al 1992). Although it is possible that ethanol and nAChR activation collaborate to enhance AMPAR function via either of these mechanisms, we wanted to test the hypothesis that ethanol increases AMPAR function by acting directly on DA neurons in an activity-independent manner. Therefore, we blocked action potential firing by pre-incubating slices in TTX prior to and during the ethanol incubation. Our data shows that neuronal activity is not required to enhance AMPAR function after ethanol exposure (Figure 4.1 E and F). This strongly supports a direct mechanism of action on DA neurons rather than the indirect, activity-dependent mechanisms discussed above. Prior studies support that a direct activity-independent mechanism is possible. ACh that is released in VTA slices and which contributes to baseline α6* nAChR activity is insensitive to TTX (Drenan et al 2008a). Recently, Berg and colleagues reported a novel, cell-autonomous mechanism by which

nicotine elicits enhanced AMPAR trafficking to the surface of hippocampal neurons (Halff et al 2014). Our data showing that AMPAR function is enhanced even in the presence of TTX (Figure 4.1 E and F) suggest that a similar cell-autonomous, α6-mediated effect could also occur in VTA DA neurons.

6.6 The Combined Activity of Nicotine and Ethanol in Enhancement of AMPAR Function

Our data demonstrating that subthreshold concentrations of nicotine and ethanol can combine to enhance AMPAR function on the surface of VTA DA neurons (Figures 4.5 and 4.6) is consistent with previous reports showing simultaneous nicotine + ethanol co-exposure is synergistic or additive (Clark & Little 2004, Liu et al 2013a, Liu et al 2013b, Tizabi et al 2007, Tizabi et al 2002). Our demonstration that 100 nM nicotine plus 5 mM ethanol combine to enhance VTA AMPAR function (Figure 4.5) is relevant to human consumption of these drugs. A blood alcohol concentration of approximately 25 mg/dL (0.025% or 5 mM) is achievable with one drink and would not be expected to produce behavioral changes in humans other than mild euphoria and/or slight social disinhibition. A nicotine plasma level of 100 nM is easily achievable by one cigarette in a person naïve to nicotine (Henningfield 1995). In a daily smoker, this level of nicotine in plasma would be attainable by afternoon or evening simply due to accumulation of the drug from cigarettes smoked throughout the day (DHHS 1988). These properties of nicotine and ethanol, taken together with our data suggest that, in humans, one drink plus one cigarette may be sufficient to produce synaptic plasticity changes in VTA DA neurons that

are relevant to the addiction process. Genetic evidence points to a prominent role for α6-containing nAChRs in alcohol consumption as well as nicotine addiction (Hoft et al 2009a, Hoft et al 2009b). Our data suggest that α6-containing nAChRs play a central role in the response to subthreshold, co-applied concentrations of nicotine and ethanol via αCtxMII inhibition in non-Tg mice (Figure 4.5 B and C) and via selective activation in α6L9S mice (Figure 4.6). In experiments involving DA release from striatal synaptosomes, αCtxMII-sensitive (α6-dependent) nAChRs are the most sensitive to nicotine (Salminen et al 2007), supporting the notion that they are capable of responding meaningfully to subthreshold nicotine when ethanol is present to enhance receptor activity. In further support of the idea that α6-containing nAChRs confer the ability to respond to very low concentrations of nicotine, α6KO mice have reduced tendency to self-administer low (10 ng) concentrations of nicotine (Exley et al 2011).

Varenicline is a partial agonist with similar efficacy and potency at both αCtxMII-sensitive (α6-containing) and αCtxMII-resistant (non-α6) nAChRs (Grady et al 2010). Varenicline is thought to promote abstinence from smoking via a dual mechanism: 1) varenicline substitutes for nicotine in activating nAChRs, and 2) varenicline competes with and blunts the full action of nicotine in activating nAChRs (Rollema et al 2007). Our results suggest that varenicline, similar to αCtxMII, may interfere with the ability of nicotine and/or ethanol to enhance AMPAR function in VTA neurons (Figures 4.5 and 4.6). This is consistent with varenicline's action in preclinical and clinical studies. For example, varenicline reduces ethanol intake in mice (Hendrickson et al 2010) and rats (Steensland

et al 2007). Varenicline also reduces alcohol consumption in heavy drinking smokers (Fucito et al 2011, McKee et al 2009, Mitchell et al 2012). Together, this suggests that patients taking varenicline may be afforded some protection from the addictive properties of subthreshold concentrations of nicotine + alcohol. Varenicline, or other compounds with partial agonist properties at α4* and/or α6* nAChRs but a better side effect profile, could be useful in attenuating nicotine/alcohol co-addiction.

6.7 Role of α4 nAChR Subunits in VTA DA Neuron Excitability

In addition to studying changes in glutamatergic synaptic plasticity in *Chrna*4 vMB cKO mice (Figure 5.7), we also identified circuitry changes within the VTA. In our *Chrna*4 vMB cKO mouse model, we interestingly saw enhanced excitability of VTA DA neurons (Figure 5.3). This may be counterintuitive based off previously published studies in α4KO mice. One study found that activation of VTA DA neurons by nicotine is dependent upon α4* nAChRs (Zhao-Shea et al 2011) and another study showed that while the baseline action potential firing rate is the same in WT and α4KO mice, nicotine does not result in an increase in the firing rate of VTA DA neurons in α4KO mice (Liu et al 2012). Likewise, we saw no difference in the baseline firing rate (Figure 5.3). However, during current injection steps we saw that, compared to Cre(-) VTA DA neurons from control *Chrna*4 loxP/loxP mice, Cre(+) VTA DA neurons from *Chrna*4 vMB cKO mice have a decreased first interspike interval at lower current injections and increased firing rate over the whole two second current injection step at higher current injections (Figure 5.3). We reasoned that because in our model, α4 nAChR subunits can be removed from any cell type that

expresses α4 nAChR subunits (Figure 5.1), that the enhanced excitability of DA neurons was due to removal of α4 nAChR subunits on GABA neurons. Within the VTA, GABA interneurons highly express α4β2* nAChRs (Klink et al 2001, Mansvelder et al 2002). These GABAergic neurons also fire spontaneously (Steffensen et al 1998) and therefore may tonically inhibit VTA DA neurons. Interestingly, picrotoxin administered into the VTA results in increased DA release in the NAc (Ikemoto et al 1997a), suggesting that removal of GABAergic signaling in the VTA excites DA neurons. Moreover, rats will self-administer picrotoxin into the VTA (Ikemoto et al 1997b). Therefore, we looked at spontaneous IPSCs in VTA DA neurons as a way to analyze changes in GABA release after removal of α4 nAChR subunits. We indeed did see a decrease in the instantaneous frequency of spontaneous IPSCS in VTA DA neurons in *Chrna*4 vMB cKO mice compared to control *Chrna*4 loxP/loxP mice that still have α4 nAChR subunit expression intact (Figure 5.4). Spontaneous IPSC instantaneous frequency was also dramatically reduced in control *Chrna*4 loxP/loxP mice in the presence of TTX, indicating activity of GABAergic neurons within the VTA is important for GABA release (Figure 5.4 E).

Our results showing that removal of α4* nAChRs from the VTA decreases IPSC instantaneous frequency implies GABAergic neurons are controlled by cholinergic signaling. We hypothesize that ACh released onto GABAergic neurons acts on α4β2* nAChRs and stimulates GABA release. This is plausible as the VTA receives cholinergic input from the PPTg and LDTg (Mao & McGehee 2010) and endogenous ACh has previously been shown to contribute to IPSCs in VTA DA neurons (Mansvelder et al 2002).

Future experiments measuring the firing rate of VTA GABAergic interneurons in *Chrna*4 vMB cKO mice will provide further insight into cholinergic control of GABAergic neurons within the VTA.

Therefore, our proposed mechanism for increased VTA DA neuron excitability is a disinhibition mechanism as illustrated in Figure 5.8. We hypothesize that in control *Chrna*4 loxP/loxP mice, afferents from the PPTg and LDTg release ACh in the VTA, which activates $\alpha4\beta2$* nAChRs located on GABAergic interneurons, and stimulates GABA release. In *Chrna*4 vMB cKO mice, removal of $\alpha4\beta2$* nAChRs from the VTA results in less GABA released onto VTA DA neurons and removal of this source of tonic inhibition results in enhanced VTA DA neuron excitability. In mice with hypersensitive $\alpha4$* nAChRs selectively expressed on GABAergic neurons, low doses of nicotine resulted in reward-like behavior (Ngolab et al 2015). Because $\alpha4\beta2$* nAChRs have been shown to rapidly desensitize (Mansvelder et al 2002) this could be explained by a disinhibition mechanism similar to what we propose is occurring in our study. However, the authors concluded that desensitization is not responsible for reward due to their finding that DHβE (a moderately selective α4* nAChR antagonist) does not similarly lead to a nicotine conditioned place preference (Ngolab et al 2015).

The VTA also receives GABAergic input from the nearby RMTg, also referred to as the tail of the VTA (Barrot et al 2012). While we took measures to try to contain the virus to the VTA and limit the spread to nearby regions through small injection volumes and the use of the AAV2 serotype which diffuses less (Passini et al 2004), it is possible that $\alpha4$ nAChR

subunits may be removed from the RMTg as well. Therefore, we repeated our IPSC recordings in *Chrna*4 loxP/loxP mice given injections of a retrograde Cre virus into the NAc (Figure 5.6 A) and saw similar decreases in IPSC instantaneous frequency but not amplitude (Figure 5.6 C-F). We still saw viral expression in both DA and non-DA neurons within the VTA (Figure 5.6 B), indicating that both DA and GABA VTA neurons send projections to the NAc. Furthermore, the recorded DA neuron itself does not have to express the Cre virus in order to exhibit decreased IPSC instantaneous frequency in *Chrna*4 vMB cKO mice, as long as the virus was indeed expressed in the VTA. This indicates that some VTA GABA neurons send projections to both the NAc and VTA DA neurons.

Further, we wanted to rule out the possibility that the enhanced excitability we see in VTA DA neurons is due to increased glutamatergic signaling. Therefore we measured spontaneous EPSCs (Figure 5.5). We saw no differences in either the instantaneous frequency nor the amplitude in *Chrna*4 vMB cKO mice compared to control *Chrna*4 loxP/loxP mice with α4 nAChR subunits intact. This is consistent with a previous study indicating that α7 nAChRs, not α4* nAChRs, are the primary nAChR subtype responsible for glutamatergic release in the VTA (Mansvelder & McGehee 2000).

Our electrophysiology results showing enhanced excitability of VTA DA neurons is consistent with locomotor data collected by a colleague also working with this mouse model in our lab. Baseline locomotor activity of *Chrna*4 vMB cKO mice is significantly higher compared to *Chrna*4 loxP/loxP control mice (unpublished result). DA levels in the

NAc have not been measured in *Chrna*4 vMB cKO mice. However, our data showing enhanced VTA DA neuron excitability and increased locomotor activity in *Chrna*4 vMB cKO mice, is consistent with data showing that α4KO mice have increased basal levels of DA in the NAc (Marubio et al 2003).

Our data highlights the importance of α4 nAChR subunit expression in the adult mouse VTA in controlling the activity of VTA DA neurons. Developing mouse models where removal of α4 nAChR subunits is targeted to specific cell types, DAergic neurons versus GABAergic neurons, will provide further insight into the role of α4* nAChRs within the VTA.

6.8 Future Directions

While we demonstrated the involvement of α6* nAChRs in nicotine-mediated AMPAR enhancement on VTA DA neurons, more work still needs to be done to better understand the downstream mechanism of AMPAR insertion. Our results showing no inward rectification suggest an increase in the number of AMPARs expressed on the cell surface. On the other hand, when constructing concentration-response curves, we saw increased AMPAR sensitivity. Rather than an increase in the number of AMPARs expressed on the cell surface, an increase in AMPAR sensitivity suggests an exchange of AMPARs for those with an increased conductance. Future studies should be done to better understand which mechanism of AMPAR insertion occurs in VTA DA neurons following nicotine exposure. Experiments with pharmacological inhibitors that distinguish between different AMPAR subtypes, such as philanthotoxin, could be performed to address this

issue. Alternatively, looking at the kinases involved in AMPAR insertion could provide insight into this mechanism. We show that CaMKII activity is necessary for increased AMPAR function. Future experiments can be done to determine which AMPAR subunits are phosphorylated and at what site following nicotine exposure.

When doing experiments with *Chrna*4 vMB cKO mice, we found that VTA DA neurons in these mice are more excitable in response to depolarizing current injections than VTA DA neurons in *Chrna*4 loxP/loxP control mice. Our method of removing α4 nAChR subunits from *Chrna*4 loxP/loxP mice via Cre viral injections has the advantage of removing α4* nAChRs from adult mice as well as from specific brain regions. However, α4 nAChR subunits are removed from both dopaminergic neurons and non-dopaminergic neurons within the VTA. Therefore, we cannot tell if α4 nAChR subunit removal from dopaminergic neurons, GABAergic neurons, or a combination of the two is primarily responsible for the enhanced excitability of VTA DA neurons in *Chrna*4 vMB cKO mice. Future studies selectively removing α4 nAChR subunits from specific cell types will be useful to further understand the circuitry within the VTA. Such experiments could be accomplished by crossing mice that express Cre under the control of specific promoters with *Chrna*4 loxP/loxP mice. Drawbacks to this approach include the removal of α4* nAChRs globally and during development.

We hypothesized that removal of α4* nAChRs decreased cholinergic excitation of GABAergic neurons, resulting in decreased GABA release. Additional experiments recording the firing rate of GABAergic neurons could provide further support of our

hypothesis in addition to our IPSC recordings from DA neurons. If our hypothesis is correct, there will be a decrease in the spontaneous firing rate of GABAergic neurons in *Chrna*4 vMB cKO mice. Finally, it would be of interest to see if α4* nAChR selective antagonists, such as DHβE could recapitulate the results we obtained with *Chrna*4 vMB cKO mice.

While our results indicate that α6* nAChRs may play a crucial role in the development of nicotine dependence, there are currently no drugs available to selectively target these receptors without also acting on (non-α6)α4* nAChRs. Improvements in the ability to stably, robustly express α6* nAChRs in heterologous systems would allow high throughput screening to help identify selective molecules. Our results suggest such drugs may be useful not only for tobacco cessation but also for treating alcoholism or tobacco and alcohol co-abuse.

6.9 Conclusions

Overall, these studies highlight the importance of α4α6* nAChRs in the initiation of cellular changes that play a role in addiction. Our data show for the first time that activation of α4α6β2* nAChRs by nicotine is sufficient to stimulate a depolarizing conductance in VTA DA neurons as well as enhance AMPAR function on the cell surface. We also show involvement of α6β2* nAChRs in ethanol-mediated enhancement of AMPAR function and demonstrate that ethanol and nicotine can combine to enhance excitatory transmission in the mesolimbic DA pathway. While α6* nAChRs are expressed solely on DA neurons in the VTA, α4* nAChRs are also expressed on GABA neurons where

we find they play an important role in controlling GABA release and therefore DA neuron excitability. Together, our data show that $\alpha4\alpha6\beta2$* nAChRs are emerging as a key target for smoking and alcohol cessation pharmacotherapies.

REFERENCES

REFERENCES

Addy NA, Fornasiero EF, Stevens TR, Taylor JR, Picciotto MR. 2007. Role of calcineurin in nicotine-mediated locomotor sensitization. *The Journal of neuroscience : the official journal of the Society for Neuroscience* 27: 8571-80

Aistrup GL, Marszalec W, Narahashi T. 1999. Ethanol modulation of nicotinic acetylcholine receptor currents in cultured cortical neurons. *Molecular pharmacology* 55: 39-49

Anderson SM, Famous KR, Sadri-Vakili G, Kumaresan V, Schmidt HD, et al. 2008. CaMKII: a biochemical bridge linking accumbens dopamine and glutamate systems in cocaine seeking. *Nat Neurosci* 11: 344-53

Azam L, Chen Y, Leslie FM. 2007. Developmental regulation of nicotinic acetylcholine receptors within midbrain dopamine neurons. *Neuroscience* 144: 1347-60

Azam L, Maskos U, Changeux JP, Dowell CD, Christensen S, et al. 2010. α-Conotoxin BuIA[T5A;P6O]: a novel ligand that discriminates between $\alpha6\beta4$ and $\alpha6\beta2$ nicotinic acetylcholine receptors and blocks nicotine-stimulated norepinephrine release. *FASEB J* 24: 5113-23

Azam L, Winzer-Serhan UH, Chen Y, Leslie FM. 2002. Expression of neuronal nicotinic acetylcholine receptor subunit mRNAs within midbrain dopamine neurons. *J Comp Neurol* 444: 260-74

Baker LK, Mao D, Chi H, Govind AP, Vallejo YF, et al. 2013. Intermittent nicotine exposure upregulates nAChRs in VTA dopamine neurons and sensitises locomotor responding to the drug. *The European journal of neuroscience*

Barrett SP, Tichauer M, Leyton M, Pihl RO. 2006. Nicotine increases alcohol self-administration in non-dependent male smokers. *Drug and alcohol dependence* 81: 197-204

Barrot M, Sesack SR, Georges F, Pistis M, Hong S, Jhou TC. 2012. Braking dopamine systems: a new GABA master structure for mesolimbic and nigrostriatal functions. *The Journal of neuroscience : the official journal of the Society for Neuroscience* 32: 14094-101

Bellone C, Luscher C. 2006. Cocaine triggered AMPA receptor redistribution is reversed in vivo by mGluR-dependent long-term depression. *Nat Neurosci* 9: 636-41

Berry JN, Engle SE, McIntosh JM, Drenan RM. 2015. alpha6-Containing nicotinic acetylcholine receptors in midbrain dopamine neurons are poised to govern dopamine-mediated behaviors and synaptic plasticity. *Neuroscience* 304: 161-75

Bhutada P, Mundhada Y, Ghodki Y, Dixit P, Umathe S, Jain K. 2012. Acquisition, expression, and reinstatement of ethanol-induced conditioned place preference in mice: effects of exposure to stress and modulation by mecamylamine. *Journal of psychopharmacology (Oxford, England)* 26: 315-23

Blomqvist O, Ericson M, Johnson DH, Engel JA, Soderpalm B. 1996. Voluntary ethanol intake in the rat: effects of nicotinic acetylcholine receptor blockade or subchronic nicotine treatment. *European journal of pharmacology* 314: 257-67

Bobo JK. 1992. Nicotine dependence and alcoholism epidemiology and treatment. *Journal of psychoactive drugs* 24: 123-9

Bonci A, Malenka RC. 1999. Properties and plasticity of excitatory synapses on dopaminergic and GABAergic cells in the ventral tegmental area. *The Journal of neuroscience : the official journal of the Society for Neuroscience* 19: 3723-30

Borgland SL, Malenka RC, Bonci A. 2004. Acute and chronic cocaine-induced potentiation of synaptic strength in the ventral tegmental area: electrophysiological and behavioral correlates in individual rats. *The Journal of neuroscience : the official journal of the Society for Neuroscience* 24: 7482-90

Brown MT, Bellone C, Mameli M, Labouebe G, Bocklisch C, et al. 2010. Drug-driven AMPA receptor redistribution mimicked by selective dopamine neuron stimulation. *PLoS One* 5: e15870

Calabresi P, Lacey MG, North RA. 1989. Nicotinic excitation of rat ventral tegmental neurones in vitro studied by intracellular recording. *Br J Pharmacol* 98: 135-40

Cardoso RA, Brozowski SJ, Chavez-Noriega LE, Harpold M, Valenzuela CF, Harris RA. 1999. Effects of ethanol on recombinant human neuronal nicotinic acetylcholine receptors expressed in Xenopus oocytes. *The Journal of pharmacology and experimental therapeutics* 289: 774-80

Cartier GE, Yoshikami D, Gray WR, Luo S, Olivera BM, McIntosh JM. 1996. A new α-conotoxin which targets $\alpha3\beta2$ nicotinic acetylcholine receptors. *J Biol Chem* 271: 7522-8

CDC. 1993. Smoking cessation during previous year among adults--United States, 1990 and 1991. *MMWR. Morbidity and mortality weekly report* 42: 504-7

CDC. 2002. Cigarette smoking among adults--United States, 2000. *MMWR. Morbidity and mortality weekly report* 51: 642-5

Champtiaux N, Gotti C, Cordero-Erausquin M, David DJ, Przybylski C, et al. 2003. Subunit composition of functional nicotinic receptors in dopaminergic neurons investigated with knock-out mice. *The Journal of neuroscience : the official journal of the Society for Neuroscience* 23: 7820-9

Champtiaux N, Han ZY, Bessis A, Rossi FM, Zoli M, et al. 2002. Distribution and pharmacology of $\alpha6$-containing nicotinic acetylcholine receptors analyzed with mutant mice. *The Journal of neuroscience : the official journal of the Society for Neuroscience* 22: 1208-17

Chandler LJ, Norwood D, Sutton G. 1999. Chronic ethanol upregulates NMDA and AMPA, but not kainate receptor subunit proteins in rat primary cortical cultures. *Alcoholism, clinical and experimental research* 23: 363-70

Chen BT, Bowers MS, Martin M, Hopf FW, Guillory AM, et al. 2008. Cocaine but not natural reward self-administration nor passive cocaine infusion produces persistent LTP in the VTA. *Neuron* 59: 288-97

Clark A, Little HJ. 2004. Interactions between low concentrations of ethanol and nicotine on firing rate of ventral tegmental dopamine neurones. *Drug and alcohol dependence* 75: 199-206

Cohen BN, Mackey ED, Grady SR, McKinney S, Patzlaff NE, et al. 2012. Nicotinic cholinergic mechanisms causing elevated dopamine release and abnormal locomotor behavior. *Neuroscience* 200: 31-41

Corrigall WA, Coen KM. 1991. Selective dopamine antagonists reduce nicotine self-administration. *Psychopharmacology* 104: 171-6

Corrigall WA, Coen KM, Adamson KL. 1994. Self-administered nicotine activates the mesolimbic dopamine system through the ventral tegmental area. *Brain research* 653: 278-84

Corrigall WA, Franklin KB, Coen KM, Clarke PB. 1992. The mesolimbic dopaminergic system is implicated in the reinforcing effects of nicotine. *Psychopharmacology* 107: 285-9

Corringer PJ, Le Novere N, Changeux JP. 2000. Nicotinic receptors at the amino acid level. *Annual review of pharmacology and toxicology* 40: 431-58

Cox BC, Marritt AM, Perry DC, Kellar KJ. 2008. Transport of multiple nicotinic acetylcholine receptors in the rat optic nerve: high densities of receptors containing α6 and β3 subunits. *Journal of neurochemistry* 105: 1924-38

Cui C, Booker TK, Allen RS, Grady SR, Whiteaker P, et al. 2003. The β3 nicotinic receptor subunit: a component of α-Conotoxin MII-binding nicotinic acetylcholine receptors that modulate dopamine release and related behaviors. *The Journal of neuroscience : the official journal of the Society for Neuroscience* 23: 11045-53

Cull-Candy S, Brickley S, Farrant M. 2001. NMDA receptor subunits: diversity, development and disease. *Current Opinion in Neurobiology* 11: 327-35

Dani JA, Bertrand D. 2007. Nicotinic acetylcholine receptors and nicotinic cholinergic mechanisms of the central nervous system. *Annual review of pharmacology and toxicology* 47: 699-729

DHHS. 1988. The Health Consequences of Smoking: Nicotine Addiction: a Report of the Surgeon General. Washington, D.C.

Di Chiara G, Acquas E, Tanda G. 1996. Ethanol as a neurochemical surrogate of conventional reinforcers: the dopamine-opioid link. *Alcohol (Fayetteville, N.Y.)* 13: 13-7

Di Chiara G, Imperato A. 1988. Drugs abused by humans preferentially increase synaptic dopamine concentrations in the mesolimbic system of freely moving rats. *Proc Natl Acad Sci U S A* 85: 5274-8

DiFranza JR, Guerrera MP. 1990. Alcoholism and smoking. *Journal of studies on alcohol* 51: 130-5

Dong Y, Saal D, Thomas M, Faust R, Bonci A, et al. 2004. Cocaine-induced potentiation of synaptic strength in dopamine neurons: behavioral correlates in GluRA(-/-) mice. *Proc Natl Acad Sci U S A* 101: 14282-7

Dopico AM, Lovinger DM. 2009. Acute Alcohol Action and Desensitization of Ligand-Gated Ion Channels. *Pharmacological reviews* 61: 98-114

Drenan RM, Engle SE, Lester HA, McIntosh JM, Brunzell DH. *2012 Neuroscience Meeting Planner, New Orleans, LA, 2012,* Program number 455.03/P19.

Drenan RM, Grady SR, Steele AD, McKinney S, Patzlaff NE, et al. 2010. Cholinergic modulation of locomotion and striatal dopamine release is mediated by $\alpha 6\alpha 4$* nicotinic acetylcholine receptors. *The Journal of neuroscience : the official journal of the Society for Neuroscience* 30: 9877-89

Drenan RM, Grady SR, Whiteaker P, McClure-Begley T, McKinney S, et al. 2008a. *In vivo* activation of midbrain dopamine neurons via sensitized, high-affinity $\alpha 6$* nicotinic acetylcholine receptors. *Neuron* 60: 123-36

Drenan RM, Lester HA. 2012. Insights into the Neurobiology of the Nicotinic Cholinergic System and Nicotine Addiction from Mice Expressing Nicotinic Receptors Harboring Gain-of-Function Mutations. *Pharmacological reviews*

Drenan RM, Nashmi R, Imoukhuede P, Just H, McKinney S, Lester HA. 2008b. Subcellular trafficking, pentameric assembly, and subunit stoichiometry of neuronal nicotinic acetylcholine receptors containing fluorescently labeled α6 and β3 subunits. *Molecular pharmacology* 73: 27-41

Ebbert JO, Wyatt KD, Hays JT, Klee EW, Hurt RD. 2010. Varenicline for smoking cessation: efficacy, safety, and treatment recommendations. *Patient preference and adherence* 4: 355-62

Eggers ED, Berger AJ. 2004. Mechanisms for the modulation of native glycine receptor channels by ethanol. *Journal of neurophysiology* 91: 2685-95

Etherton MR, Tabuchi K, Sharma M, Ko J, Sudhof TC. 2011. An autism-associated point mutation in the neuroligin cytoplasmic tail selectively impairs AMPA receptor-mediated synaptic transmission in hippocampus. *The EMBO journal* 30: 2908-19

Exley R, Maubourguet N, David V, Eddine R, Evrard A, et al. 2011. Distinct contributions of nicotinic acetylcholine receptor subunit α4 and subunit α6 to the reinforcing effects of nicotine. *Proc Natl Acad Sci U S A* 108: 7577-82

Falk DE, Yi HY, Hiller-Sturmhofel S. 2006. An epidemiologic analysis of co-occurring alcohol and tobacco use and disorders: findings from the National Epidemiologic Survey on Alcohol and Related Conditions. *Alcohol research & health : the journal of the National Institute on Alcohol Abuse and Alcoholism* 29: 162-71

Fowler CD, Lu Q, Johnson PM, Marks MJ, Kenny PJ. 2011. Habenular α5 nicotinic receptor subunit signalling controls nicotine intake. *Nature* 471: 597-601

Friedman GD, Tekawa I, Klatsky AL, Sidney S, Armstrong MA. 1991. Alcohol drinking and cigarette smoking: an exploration of the association in middle-aged men and women. *Drug and alcohol dependence* 27: 283-90

Fucito LM, Toll BA, Wu R, Romano DM, Tek E, O'Malley SS. 2011. A preliminary investigation of varenicline for heavy drinking smokers. *Psychopharmacology* 215: 655-63

Gao C, Wolf ME. 2007. Dopamine alters AMPA receptor synaptic expression and subunit composition in dopamine neurons of the ventral tegmental area cultured with prefrontal cortex neurons. *The Journal of neuroscience : the official journal of the Society for Neuroscience* 27: 14275-85

Gao M, Jin Y, Yang K, Zhang D, Lukas RJ, Wu J. 2010. Mechanisms involved in systemic nicotine-induced glutamatergic synaptic plasticity on dopamine neurons in the ventral tegmental area. *The Journal of neuroscience : the official journal of the Society for Neuroscience* 30: 13814-25

Gotti C, Guiducci S, Tedesco V, Corbioli S, Zanetti L, et al. 2010. Nicotinic acetylcholine receptors in the mesolimbic pathway: primary role of ventral tegmental area $\alpha6\beta2$* receptors in mediating systemic nicotine effects on dopamine release, locomotion, and reinforcement. *The Journal of neuroscience : the official journal of the Society for Neuroscience* 30: 5311-25

Gotti C, Moretti M, Clementi F, Riganti L, McIntosh JM, et al. 2005. Expression of nigrostriatal $\alpha6$-containing nicotinic acetylcholine receptors is selectively reduced, but not eliminated, by $\beta3$ subunit gene deletion. *Molecular pharmacology* 67: 2007-15

Grady SR, Drenan RM, Breining SR, Yohannes D, Wageman CR, et al. 2010. Structural differences determine the relative selectivity of nicotinic compounds for native $\alpha4\beta2$*-, $\alpha6\beta2$*-, $\alpha3\beta4$*- and $\alpha7$-nicotine acetylcholine receptors. *Neuropharmacology* 58: 1054-66

Grant BF, Hasin DS, Chou SP, Stinson FS, Dawson DA. 2004. Nicotine dependence and psychiatric disorders in the United States: results from the national epidemiologic survey on alcohol and related conditions. *Arch Gen Psychiatry* 61: 1107-15

Halff AW, Gomez-Varela D, John D, Berg DK. 2014. A novel mechanism for nicotinic potentiation of glutamatergic synapses. *The Journal of neuroscience : the official journal of the Society for Neuroscience* 34: 2051-64

Harrison EL, Hinson RE, McKee SA. 2009. Experimenting and daily smokers: episodic patterns of alcohol and cigarette use. *Addictive behaviors* 34: 484-6

Harvey SC, Maddox FN, Luetje CW. 1996. Multiple determinants of dihydro-beta-erythroidine sensitivity on rat neuronal nicotinic receptor alpha subunits. *Journal of neurochemistry* 67: 1953-9

Hays JT, Ebbert JO, Sood A. 2008. Efficacy and safety of varenicline for smoking cessation. *Am J Med* 121: S32-42

Heikkinen AE, Moykkynen TP, Korpi ER. 2009. Long-lasting modulation of glutamatergic transmission in VTA dopamine neurons after a single dose of benzodiazepine agonists. *Neuropsychopharmacology : official publication of the American College of Neuropsychopharmacology* 34: 290-8

Hendrickson LM, Zhao-Shea R, Pang X, Gardner PD, Tapper AR. 2010. Activation of α4* nAChRs is necessary and sufficient for varenicline-induced reduction of alcohol consumption. *The Journal of neuroscience : the official journal of the Society for Neuroscience* 30: 10169-76

Henningfield JE. 1995. Nicotine Medications for Smoking Cessation. *New England Journal of Medicine* 333: 1196-203

Hill JA, Jr., Zoli M, Bourgeois JP, Changeux JP. 1993. Immunocytochemical localization of a neuronal nicotinic receptor: the beta 2-subunit. *The Journal of neuroscience : the official journal of the Society for Neuroscience* 13: 1551-68

Hoft NR, Corley RP, McQueen MB, Huizinga D, Menard S, Ehringer MA. 2009a. SNPs in CHRNA6 and CHRNB3 are associated with alcohol consumption in a nationally representative sample. *Genes, brain, and behavior* 8: 631-7

Hoft NR, Corley RP, McQueen MB, Schlaepfer IR, Huizinga D, Ehringer MA. 2009b. Genetic association of the CHRNA6 and CHRNB3 genes with tobacco dependence in a nationally representative sample. *Neuropsychopharmacology : official publication of the American College of Neuropsychopharmacology* 34: 698-706

Ikemoto S, Kohl RR, McBride WJ. 1997a. GABA(A) receptor blockade in the anterior ventral tegmental area increases extracellular levels of dopamine in the nucleus accumbens of rats. *Journal of neurochemistry* 69: 137-43

Ikemoto S, Murphy JM, McBride WJ. 1997b. Self-infusion of GABA(A) antagonists directly into the ventral tegmental area and adjacent regions. *Behavioral neuroscience* 111: 369-80

Isaac JT, Ashby MC, McBain CJ. 2007. The role of the GluR2 subunit in AMPA receptor function and synaptic plasticity. *Neuron* 54: 859-71

Itier V, Bertrand D. 2001. Neuronal nicotinic receptors: from protein structure to function. *FEBS Lett* 504: 118-25

Jin Y, Yang K, Wang H, Wu J. 2011. Exposure of nicotine to ventral tegmental area slices induces glutamatergic synaptic plasticity on dopamine neurons. *Synapse (New York, N.Y.)* 65: 332-8

Jones IW, Wonnacott S. 2004. Precise localization of alpha7 nicotinic acetylcholine receptors on glutamatergic axon terminals in the rat ventral tegmental area. *The Journal of neuroscience : the official journal of the Society for Neuroscience* 24: 11244-52

Kaspar BK, Vissel B, Bengoechea T, Crone S, Randolph-Moore L, et al. 2002. Adeno-associated virus effectively mediates conditional gene modification in the brain. *Proceedings of the National Academy of Sciences* 99: 2320-25

Kauer JA, Malenka RC. 2007. Synaptic plasticity and addiction. *Nat Rev Neurosci* 8: 844-58

Klink R, de Kerchove d'Exaerde A, Zoli M, Changeux JP. 2001. Molecular and physiological diversity of nicotinic acetylcholine receptors in the midbrain dopaminergic nuclei. *The Journal of neuroscience : the official journal of the Society for Neuroscience* 21: 1452-63

Knight C, Howard P, Baker CL, Marton JP. 2010. The cost-effectiveness of an extended course (12+12 weeks) of varenicline compared with other available smoking cessation strategies in the United States: an extension and update to the BENESCO model. *Value in health : the journal of the International Society for Pharmacoeconomics and Outcomes Research* 13: 209-14

Kobayashi M, Kojima M, Koyanagi Y, Adachi K, Imamura K, Koshikawa N. 2009. Presynaptic and postsynaptic modulation of glutamatergic synaptic transmission by activation of α1- and β-adrenoceptors in layer V pyramidal neurons of rat cerebral cortex. *Synapse (New York, N.Y.)* 63: 269-81

Kuryatov A, Lindstrom J. 2011. Expression of functional human α6β2β3* acetylcholine receptors in *Xenopus laevis* oocytes achieved through subunit chimeras and concatamers. *Molecular pharmacology* 79: 126-40

Labarca C, Nowak MW, Zhang H, Tang L, Deshpande P, Lester HA. 1995. Channel gating governed symmetrically by conserved leucine residues in the M2 domain of nicotinic receptors. *Nature* 376: 514-6

Lammel S, Hetzel A, Hackel O, Jones I, Liss B, Roeper J. 2008. Unique properties of mesoprefrontal neurons within a dual mesocorticolimbic dopamine system. *Neuron* 57: 760-73

Lammel S, Ion DI, Roeper J, Malenka RC. 2011. Projection-specific modulation of dopamine neuron synapses by aversive and rewarding stimuli. *Neuron* 70: 855-62

Lammel S, Lim BK, Malenka RC. 2014. Reward and aversion in a heterogeneous midbrain dopamine system. *Neuropharmacology* 76 Pt B: 351-9

Lanca AJ, Adamson KL, Coen KM, Chow BL, Corrigall WA. 2000. The pedunculopontine tegmental nucleus and the role of cholinergic neurons in nicotine self-administration in the rat: a correlative neuroanatomical and behavioral study. *Neuroscience* 96: 735-42

Larsson A, Edstrom L, Svensson L, Soderpalm B, Engel JA. 2005. Voluntary ethanol intake increases extracellular acetylcholine levels in the ventral tegmental area in the rat. *Alcohol and alcoholism (Oxford, Oxfordshire)* 40: 349-58

Larsson A, Jerlhag E, Svensson L, Soderpalm B, Engel JA. 2004. Is an alpha-conotoxin MII-sensitive mechanism involved in the neurochemical, stimulatory, and rewarding effects of ethanol? *Alcohol (Fayetteville, N.Y.)* 34: 239-50

Laviolette SR, van der Kooy D. 2004. The neurobiology of nicotine addiction: bridging the gap from molecules to behaviour. *Nat Rev Neurosci* 5: 55-65

Le Novere N, Corringer PJ, Changeux JP. 2002. The diversity of subunit composition in nAChRs: evolutionary origins, physiologic and pharmacologic consequences. *Journal of neurobiology* 53: 447-56

Le Novere N, Zoli M, Changeux JP. 1996. Neuronal nicotinic receptor α6 subunit mRNA is selectively concentrated in catecholaminergic nuclei of the rat brain. *The European journal of neuroscience* 8: 2428-39

Lena C, de Kerchove D'Exaerde A, Cordero-Erausquin M, Le Novere N, del Mar Arroyo-Jimenez M, Changeux JP. 1999. Diversity and distribution of nicotinic acetylcholine receptors in the locus ceruleus neurons. *Proc Natl Acad Sci U S A* 96: 12126-31

Letchworth SR, Whiteaker P. 2011. Progress and Challenges in the Study of α6-Containing Nicotinic Acetylcholine Receptors. *Biochemical pharmacology* 82: 862-72

Li DP, Yang Q, Pan HM, Pan HL. 2008. Pre- and postsynaptic plasticity underlying augmented glutamatergic inputs to hypothalamic presympathetic neurons in spontaneously hypertensive rats. *The Journal of physiology* 586: 1637-47

Liu L, Hendrickson LM, Guildford MJ, Zhao-Shea R, Gardner PD, Tapper AR. 2013a. Nicotinic acetylcholine receptors containing the alpha4 subunit modulate alcohol reward. *Biological psychiatry* 73: 738-46

Liu L, Zhao-Shea R, McIntosh JM, Gardner P, Tapper A. 2012. Nicotine Persistently Activates Ventral Tegmental Area Dopaminergic Neurons Via Nicotinic Acetylcholine Receptors Containing α4 and α6 subunits. *Molecular pharmacology*

Liu L, Zhao-Shea R, McIntosh JM, Tapper AR. 2013b. Nicotinic acetylcholine receptors containing the alpha6 subunit contribute to ethanol activation of ventral tegmental area dopaminergic neurons. *Biochemical pharmacology* 86: 1194-200

Liu SJ, Zukin RS. 2007. Ca^{2+}-permeable AMPA receptors in synaptic plasticity and neuronal death. *Trends in neurosciences* 30: 126-34

Liu X, Liu Y, Zhong P, Wilkinson B, Qi J, et al. 2014. CaMKII activity in the ventral tegmental area gates cocaine-induced synaptic plasticity in the nucleus accumbens. *Neuropsychopharmacology : official publication of the American College of Neuropsychopharmacology* 39: 989-99

Lof E, Olausson P, deBejczy A, Stomberg R, McIntosh JM, et al. 2007. Nicotinic acetylcholine receptors in the ventral tegmental area mediate the dopamine activating and reinforcing properties of ethanol cues. *Psychopharmacology* 195: 333-43

Luscher C, Malenka RC. 2011. Drug-evoked synaptic plasticity in addiction: from molecular changes to circuit remodeling. *Neuron* 69: 650-63

Mackey ED, Engle SE, Kim MR, O'Neill HC, Wageman CR, et al. 2012. α6* Nicotinic Acetylcholine Receptor Expression and Function in a Visual Salience Circuit. *The Journal of neuroscience : the official journal of the Society for Neuroscience* 32: 10226-37

Malenka RC, Bear MF. 2004. LTP and LTD: an embarrassment of riches. *Neuron* 44: 5-21

Mansvelder HD, Keath JR, McGehee DS. 2002. Synaptic mechanisms underlie nicotine-induced excitability of brain reward areas. *Neuron* 33: 905-19

Mansvelder HD, McGehee DS. 2000. Long-term potentiation of excitatory inputs to brain reward areas by nicotine. *Neuron* 27: 349-57

Mao D, Gallagher K, McGehee DS. 2011. Nicotine potentiation of excitatory inputs to ventral tegmental area dopamine neurons. *The Journal of neuroscience : the official journal of the Society for Neuroscience* 31: 6710-20

Mao D, McGehee DS. 2010. Nicotine and behavioral sensitization. *Journal of molecular neuroscience : MN* 40: 154-63

Mark GP, Shabani S, Dobbs LK, Hansen ST. 2011. Cholinergic modulation of mesolimbic dopamine function and reward. *Physiology & behavior* 104: 76-81

Marubio LM, Gardier AM, Durier S, David D, Klink R, et al. 2003. Effects of nicotine in the dopaminergic system of mice lacking the α4 subunit of neuronal nicotinic acetylcholine receptors. *The European journal of neuroscience* 17: 1329-37

Maskos U, Molles BE, Pons S, Besson M, Guiard BP, et al. 2005. Nicotine reinforcement and cognition restored by targeted expression of nicotinic receptors. *Nature* 436: 103-7

Mathers CD, Loncar D. 2006. Projections of global mortality and burden of disease from 2002 to 2030. *PLoS medicine* 3: e442

McGranahan TM, Patzlaff NE, Grady SR, Heinemann SF, Booker TK. 2011. alpha4beta2 nicotinic acetylcholine receptors on dopaminergic neurons mediate nicotine reward and anxiety relief. *The Journal of neuroscience : the official journal of the Society for Neuroscience* 31: 10891-902

McKee SA, Harrison EL, O'Malley SS, Krishnan-Sarin S, Shi J, et al. 2009. Varenicline reduces alcohol self-administration in heavy-drinking smokers. *Biological psychiatry* 66: 185-90

McKee SA, Sinha R, Weinberger AH, Sofuoglu M, Harrison EL, et al. 2011. Stress decreases the ability to resist smoking and potentiates smoking intensity and reward. *Journal of psychopharmacology (Oxford, England)* 25: 490-502

McKinney M, Jacksonville MC. 2005. Brain cholinergic vulnerability: Relevance to behavior and disease. *Biochemical pharmacology* 70: 1115-24

Millar NS, Gotti C. 2009. Diversity of vertebrate nicotinic acetylcholine receptors. *Neuropharmacology* 56: 237-46

Miller NS, Gold MS. 1998. Comorbid cigarette and alcohol addiction: epidemiology and treatment. *Journal of addictive diseases* 17: 55-66

Mineur YS, Abizaid A, Rao Y, Salas R, DiLeone RJ, et al. 2011. Nicotine decreases food intake through activation of POMC neurons. *Science* 332: 1330-2

Mitchell JM, Teague CH, Kayser AS, Bartlett SE, Fields HL. 2012. Varenicline decreases alcohol consumption in heavy-drinking smokers. *Psychopharmacology* 223: 299-306

Mitchell SH, de Wit H, Zacny JP. 1995. Effects of varying ethanol dose on cigarette consumption in healthy normal volunteers. *Behavioural pharmacology* 6: 359-65

Monaco G, van Dam S, Casal Novo Ribeiro JL, Larbi A, de Magalhaes JP. 2015. A comparison of human and mouse gene co-expression networks reveals conservation and divergence at the tissue, pathway and disease levels. *BMC evolutionary biology* 15: 259

Murase S, Grenhoff J, Chouvet G, Gonon FG, Svensson TH. 1993. Prefrontal cortex regulates burst firing and transmitter release in rat mesolimbic dopamine neurons studied in vivo. *Neuroscience letters* 157: 53-6

Nair-Roberts RG, Chatelain-Badie SD, Benson E, White-Cooper H, Bolam JP, Ungless MA. 2008. Stereological estimates of dopaminergic, GABAergic and glutamatergic neurons in the ventral tegmental area, substantia nigra and retrorubral field in the rat. *Neuroscience* 152: 1024-31

Nashmi R, Xiao C, Deshpande P, McKinney S, Grady SR, et al. 2007. Chronic nicotine cell specifically upregulates functional α4* nicotinic receptors: basis for both tolerance in midbrain and enhanced long-term potentiation in perforant path. *The Journal of neuroscience : the official journal of the Society for Neuroscience* 27: 8202-18

NCCD. 2014. The Health Consequences of Smoking-50 Years of Progress: A Report of the Surgeon General. Atlanta (GA): U.S. Deartment of Health and Human Services, Centers for Disease Control and Prevention, National Center for Chronic Disease Prevention and Health Promotion, Office on Smoking and Health

Ngolab J, Liu L, Zhao-Shea R, Gao G, Gardner PD, Tapper AR. 2015. Functional Upregulation of alpha4* Nicotinic Acetylcholine Receptors in VTA GABAergic Neurons Increases Sensitivity to Nicotine Reward. *The Journal of neuroscience : the official journal of the Society for Neuroscience* 35: 8570-8

Passini MA, Watson DJ, Wolfe JH. 2004. Gene delivery to the mouse brain with adeno-associated virus. *Methods in molecular biology (Clifton, N.J.)* 246: 225-36

Picciotto MR, Addy NA, Mineur YS, Brunzell DH. 2008. It is not "either/or": activation and desensitization of nicotinic acetylcholine receptors both contribute to behaviors related to nicotine addiction and mood. *Prog Neurobiol* 84: 329-42

Picciotto MR, Zoli M, Lena C, Bessis A, Lallemand Y, et al. 1995. Abnormal avoidance learning in mice lacking functional high-affinity nicotine receptor in the brain. *Nature* 374: 65-7

Picciotto MR, Zoli M, Rimondini R, Lena C, Marubio LM, et al. 1998. Acetylcholine receptors containing the β2 subunit are involved in the reinforcing properties of nicotine. *Nature* 391: 173-7

Pidoplichko VI, DeBiasi M, Williams JT, Dani JA. 1997. Nicotine activates and desensitizes midbrain dopamine neurons. *Nature* 390: 401-4

Placzek AN, Zhang TA, Dani JA. 2009. Age Dependent Nicotinic Influences over Dopamine Neuron Synaptic Plasticity. *Biochemical pharmacology* 78: 686-92

Pons S, Fattore L, Cossu G, Tolu S, Porcu E, et al. 2008. Crucial role of α4 and α6 nicotinic acetylcholine receptor subunits from ventral tegmental area in systemic nicotine self-administration. *The Journal of neuroscience : the official journal of the Society for Neuroscience* 28: 12318-27

Powers MS, Broderick HJ, Drenan RM, Chester JA. 2013. Nicotinic acetylcholine receptors containing alpha6 subunits contribute to alcohol reward-related behaviours. *Genes, brain, and behavior* 12: 543-53

Pratt LA, Brody DJ. 2010. Depression and smoking in the U.S. household population aged 20 and over, 2005-2008. *NCHS data brief*: 1-8

Rahman S, Zhang J, Corrigall WA. 2003. Effects of acute and chronic nicotine on somatodendritic dopamine release of the rat ventral tegmental area: in vivo microdialysis study. *Neuroscience letters* 348: 61-4

Revah F, Bertrand D, Galzi JL, Devillers-Thiery A, Mulle C, et al. 1991. Mutations in the channel domain alter desensitization of a neuronal nicotinic receptor. *Nature* 353: 846-9

Rollema H, Chambers LK, Coe JW, Glowa J, Hurst RS, et al. 2007. Pharmacological profile of the α4β2 nicotinic acetylcholine receptor partial agonist varenicline, an effective smoking cessation aid. *Neuropharmacology* 52: 985-94

Rose JE, Brauer LH, Behm FM, Cramblett M, Calkins K, Lawhon D. 2004. Psychopharmacological interactions between nicotine and ethanol. *Nicotine & tobacco research : official journal of the Society for Research on Nicotine and Tobacco* 6: 133-44

Ross SA, Wong JY, Clifford JJ, Kinsella A, Massalas JS, et al. 2000. Phenotypic characterization of an α4 neuronal nicotinic acetylcholine receptor subunit knock-out mouse. *The Journal of neuroscience : the official journal of the Society for Neuroscience* 20: 6431-41

Saal D, Dong Y, Bonci A, Malenka RC. 2003. Drugs of abuse and stress trigger a common synaptic adaptation in dopamine neurons. *Neuron* 37: 577-82

Sagud M, Mihaljevic-Peles A, Muck-Seler D, Pivac N, Vuksan-Cusa B, et al. 2009. Smoking and schizophrenia. *Psychiatria Danubina* 21: 371-5

Salminen O, Drapeau JA, McIntosh JM, Collins AC, Marks MJ, Grady SR. 2007. Pharmacology of α-Conotoxin MII-Sensitive Subtypes of Nicotinic Acetylcholine Receptors Isolated by Breeding of Null Mutant Mice. *Molecular pharmacology* 71: 1563-71

Salminen O, Murphy KL, McIntosh JM, Drago J, Marks MJ, et al. 2004. Subunit composition and pharmacology of two classes of striatal presynaptic nicotinic acetylcholine receptors mediating dopamine release in mice. *Molecular pharmacology* 65: 1526-35

Sanchez JT, Wang Y, Rubel EW, Barria A. 2010. Development of glutamatergic synaptic transmission in binaural auditory neurons. *Journal of neurophysiology* 104: 1774-89

Sanjakdar SS, Maldoon PP, Marks MJ, Brunzell DH, Maskos U, et al. 2015. Differential Roles of a6b2* and a4b2* Neuronal Nicotinic Receptors in Nicotine- and Cocaine-Conditioned Reward in Mice. *Neuropsychopharmacology : official publication of the American College of Neuropsychopharmacology* 40: 350-60

Schilström B, Nomikos GG, Nisell M, Hertel P, Svensson TH. 1997. N-methyl-d-aspartate receptor antagonism in the ventral tegmental area diminishes the systemic nicotine-induced dopamine release in the nucleus accumbens. *Neuroscience* 82: 781-89

Schilstrom B, Yaka R, Argilli E, Suvarna N, Schumann J, et al. 2006. Cocaine enhances NMDA receptor-mediated currents in ventral tegmental area cells via dopamine D5 receptor-dependent redistribution of NMDA receptors. *The Journal of neuroscience : the official journal of the Society for Neuroscience* 26: 8549-58

Spanagel R, Herz A, Shippenberg TS. 1992. Opposing tonically active endogenous opioid systems modulate the mesolimbic dopaminergic pathway. *Proceedings of the National Academy of Sciences* 89: 2046-50

Steensland P, Simms JA, Holgate J, Richards JK, Bartlett SE. 2007. Varenicline, an $\alpha 4\beta 2$ nicotinic acetylcholine receptor partial agonist, selectively decreases ethanol consumption and seeking. *Proc Natl Acad Sci U S A* 104: 12518-23

Steffensen SC, Svingos AL, Pickel VM, Henriksen SJ. 1998. Electrophysiological characterization of GABAergic neurons in the ventral tegmental area. *The Journal of neuroscience : the official journal of the Society for Neuroscience* 18: 8003-15

Stuber GD, Hopf FW, Hahn J, Cho SL, Guillory A, Bonci A. 2008. Voluntary ethanol intake enhances excitatory synaptic strength in the ventral tegmental area. *Alcoholism, clinical and experimental research* 32: 1714-20

Tapper AR, McKinney SL, Nashmi R, Schwarz J, Deshpande P, et al. 2004. Nicotine activation of $\alpha 4$* receptors: sufficient for reward, tolerance, and sensitization. *Science* 306: 1029-32

Thomas MJ, Malenka RC, Bonci A. 2000. Modulation of long-term depression by dopamine in the mesolimbic system. *The Journal of neuroscience : the official journal of the Society for Neuroscience* 20: 5581-6

Tizabi Y, Bai L, Copeland RL, Jr., Taylor RE. 2007. Combined effects of systemic alcohol and nicotine on dopamine release in the nucleus accumbens shell. *Alcohol and alcoholism (Oxford, Oxfordshire)* 42: 413-6

Tizabi Y, Copeland RL, Jr., Louis VA, Taylor RE. 2002. Effects of combined systemic alcohol and central nicotine administration into ventral tegmental area on dopamine release in the nucleus accumbens. *Alcoholism, clinical and experimental research* 26: 394-9

Ungless MA, Whistler JL, Malenka RC, Bonci A. 2001. Single cocaine exposure in vivo induces long-term potentiation in dopamine neurons. *Nature* 411: 583-7

Van Bockstaele EJ, Pickel VM. 1995. GABA-containing neurons in the ventral tegmental area project to the nucleus accumbens in rat brain. *Brain research* 682: 215-21

van Zessen R, Phillips JL, Budygin EA, Stuber GD. 2012. Activation of VTA GABA neurons disrupts reward consumption. *Neuron* 73: 1184-94

West R, Ussher M, Evans M, Rashid M. 2006. Assessing DSM-IV nicotine withdrawal symptoms: a comparison and evaluation of five different scales. *Psychopharmacology* 184: 619-27

White SL, Schmidt HD, Vassoler FM, Pierce RC. 2013. Acute cocaine increases phosphorylation of CaMKII and GluA1 in the dorsolateral striatum of drug naïve rats, but not cocaine-experienced rats. *Neuroscience letters* 537: 71-76

Whiteaker P, McIntosh JM, Luo S, Collins AC, Marks MJ. 2000. [^{125}I]-α-Conotoxin MII identifies a novel nicotinic acetylcholine receptor population in mouse brain. *Molecular pharmacology* 57: 913-25

Wolf ME, Sun X, Mangiavacchi S, Chao SZ. 2004. Psychomotor stimulants and neuronal plasticity. *Neuropharmacology* 47 Suppl 1: 61-79

Wooltorton JR, Pidoplichko VI, Broide RS, Dani JA. 2003. Differential desensitization and distribution of nicotinic acetylcholine receptor subtypes in midbrain dopamine areas. *The Journal of neuroscience : the official journal of the Society for Neuroscience* 23: 3176-85

Zhang TA, Placzek AN, Dani JA. 2010. In vitro identification and electrophysiological characterization of dopamine neurons in the ventral tegmental area. *Neuropharmacology* 59: 431-6

Zhao-Shea R, Liu L, Soll LG, Improgo MR, Meyers EE, et al. 2011. Nicotine-mediated activation of dopaminergic neurons in distinct regions of the ventral tegmental area. *Neuropsychopharmacology : official publication of the American College of Neuropsychopharmacology* 36: 1021-32

Zoli M, Lena C, Picciotto MR, Changeux JP. 1998. Identification of four classes of brain nicotinic receptors using beta2 mutant mice. *The Journal of neuroscience : the official journal of the Society for Neuroscience* 18: 4461-72

VITA

VITA

STACI ENGLE
sengle@purdue.edu

EDUCATION

Doctor of Philosophy
Medicinal Chemistry and Molecular Pharmacology
Purdue University, May 2016

Bachelor of Science
Major: Biochemistry/Molecular Biology
Second Major: Chemistry; Minor: Biology
Illinois State University, May 2011

RESEARCH EXPERIENCE

- **Graduate Research Assistant** – Fall 2011-Spring 2016
  - Purdue University, Department of Medicinal Chemistry and Molecular Pharmacology, Dr. Ryan Drenan
- **Summer Research Intern** – Summer 2010
  - Summer Undergraduate Research Program, Case Western Reserve University, Department of Pharmacology, Dr. Youwei Zhang
- **Undergraduate Research Student** – Spring 2008-2011
  - Illinois State University, Biological Sciences Department, Dr. Laura Vogel

TEACHING EXPERIENCE

- **Teaching Assistant** – Purdue University
  - Laboratory for Organic Chemistry I, Spring 2014
  - Integrated Pharmacotherapy II, Fall 2013
- **Tutor** – Visor Academic Center, Illinois State University, Fall 2009-Spring 2011
  - General Chemistry, Anatomy and Physiology I and II

FELLOWSHIPS and AWARDS

- Jenkins-Knevel Award for Outstanding Graduate Research (2015)
- Bilsland Dissertation Fellowship (2015)
- John Davisson Endowment Research Award (2014)
- Paget Travel Award (2013)
- Frederick N. Andrews Fellowship (2011-2013)

PUBLICATIONS

1. Berry, J.N., **Engle, S.E.**, McIntosh, J.M., and Drenan, R.M. (2015) α6-containing nicotinic acetylcholine receptors in midbrain dopamine neurons are poised to govern dopamine-mediated behaviors and synaptic plasticity. *Neuroscience* 304:161-175.
2. **Engle, S.E.**, McIntosh, J.M., and Drenan, R.M. (2015) Nicotine and ethanol cooperate to enhance ventral tegmental area AMPA receptor function via α6-containing nicotinic receptors. *Neuropharmacology* 91:13-22.
3. Shih, P.Y., **Engle, S.E.**, Oh, G., Deshpande, P., Puskar, N., Lester, H.A., and Drenan, R.M. (2014) Differential expression and function of nicotinic acetylcholine receptors in subdivisions of medial habenula. *J. Neurosci*. 34(29): 9789-802.
4. **Engle, S.E.**, Shih, P.Y., McIntosh, J.M., and Drenan, R.M. (2013) α4α6β2* nAChR activation on VTA DA neurons is sufficient to stimulate a depolarizing conductance and enhance surface AMPA receptor function. *Mol. Pharmacol*. 84(3): 393-406.
5. **Engle, S.E.**, Broderick, H.J., and Drenan, R.M. (2012) Local application of drugs to study nicotinic acetylcholine receptor function in mouse brain slices. *J. Vis. Exp.* (68), e50034, DOI: 10.3791/50034.
6. Mackey, E.D.W., **Engle, S.E**., Kim, M., O'Neill, H.C., Wageman, C.R., Patzlaff, N.E., Wang, Y., Grady, S.R., McIntosh, J.M., Marks, M.J., Lester, H.A., and Drenan, R.M. (2012) α6* nicotinic acetylcholine receptor expression and function in a visual salience circuit. *J. Neurosci*. 32(30): 10226-10237.
7. Wang, J., **Engle, S.**, and Zhang, Y. (2011) A new in vitro system for activating the cell cycle checkpoint. *Cell Cycle* 10(3): 500-506.

POSTER PRESENTATIONS

1. **Engle, S.E.**, Berry, J.N., Arvin, M.C., McIntosh, J.M., and Drenan, R.M. Removal of α4 nAChR subunits from adult VTA neurons alters VTA DA neuron excitability and locomotor activity. Society for Neuroscience Annual Meeting, 2015.
2. **Engle, S.E.**, McIntosh, J.M., and Drenan, R.M. Nicotine and ethanol cooperate to enhance ventral tegmental area AMPA receptor function via α6-containing nicotinic receptors. Health and Disease: Science, Culture and Policy Research Poster Session, Purdue University, 2015.

3. **Engle, S.E.**, McIntosh, J.M., and Drenan, R.M. Combinations of nicotine and ethanol enhance AMPA receptor function in VTA DA neurons through activation of α6β2* nAChRs. Society for Neuroscience Annual Meeting, 2014.
4. **Engle, S.E.** McIntosh, J.M., and Drenan, R.M. Activation of α4α6β2* nAChRs on VTA DA neurons by nicotine and ethanol is sufficient for enhancement of AMPA receptor function on the cell surface. Health and Disease: Science, Culture and Policy Research Poster Session, 2014.
5. **Engle, S.E.**, McIntosh, J.M., and Drenan, R.M. Activation of α4α6β2* nAChRs on VTA DA neurons is sufficient for depolarization and enhanced function of AMPA receptors on the cell surface. Society for Neuroscience Annual Meeting, 2013.
6. **Engle, S.E.**, Stafford, A., Brunzell, D.H., and Drenan, R.M. Selective activation of α6* nAChRs is sufficient for activation of VTA DA neurons, the induction of synaptic plasticity, and nicotine reward behavior. Chronic Disease Research Poster Session, Purdue College of Health and Human Sciences, 2013.
7. **Engle, S.E.** and Vogel, L.A. Measuring intestinal secretory IgA to track changes in the mucosal immune response with age. Illinois State University Phi Sigma Research Symposium, 2011.
8. **Engle, S.**, Thies, M., Jones, M., Kim, J., and Baur, J. Development of a new fundraising initiative to support student travel and research grants at Illinois State University. 241st ACS National Meeting, Fall 2011.
9. **Engle, S.**, Wang, J. and Zhang, Y. Establishing a new *in vitro* system for studying the DNA damage checkpoint response. Case Western Reserve University Department of Pharmacology Summer Undergraduate Research Program Symposium, 2010.

PROFESSIONAL ASSOCIATIONS/SERVICE ACTIVITIES

- Search Committee for the Head of the Department of Medicinal Chemistry and Molecular Pharmacology (student representative, 2014)
- Association for Women in Science (collegiate member, 2014-present)
- Society for Neuroscience (student member, 2012-present)
- American Society for Pharmacology and Experimental Therapeutics (student member, 2010-present)
- American Chemical Society (student member, 2010-2012)